SPECTROSCOPIC DETERMINATION OF INDUSTRIAL OIL BLENDS USING MULTIVARIATE CALIBRATON

A Thesis Submitted to

the Graduate School of Engineering and Sciences of

İzmir Institute of Technology

in Partial Fulfillment of the Requirements for the Degree of

MASTER OF SCIENCE

in Chemistry

by

Ayşegül YALÇIN

December 2009

İZMİR

We approve the thesis of **Ayşegül YALÇIN**

Assoc.Prof. Dr. Durmuş ÖZDEMİR
Supervisor

Prof. Dr. Ahmet E. EROĞLU
Committee Member

Assoc.Prof. Dr. Figen TOKATLI
Committee Member

17 December 2009

Prof. Dr. Levent ARTOK
Head of the Department of Chemistry

Assoc.Prof. Dr. Talat YALÇIN
Dean of the Graduate School of
Engineering and Sciences

ACKNOWLEDGEMENTS

This thesis could not have been written without the guidance of Assoc. Dr. Durmuş ÖZDEMİR who is not only my supervisor but also encouraged and challenged me throughout my academic program. He patiently guided me through the evaluation period of the thesis, never accepting less than my best efforts. I thank him so much.

I would like to thank Betül ÖZTÜRK and Ibrahim KARAMAN for their constructive comments on this thesis and for being exceptional collaborators. Also thanks to Müşerref YERSEL for being supportive and patient labmate.

Special thanks to Prof. Dr. Ahmet E. EROGLU and Assoc. Prof. Dr. Figen TOKATLI for participating as committee members.

I am pleased to pay my thanks to Technological Research Council of Turkey (TÜBİTAK) for funding the TEYDEB project and to ASSAN Aluminum Corporation for giving chance to work on this project, and supplying the samples.

Additionally, I would like to acknowledge all my colleagues in İYTE, Chemistry Department for their friendship over two years period of my academic life.

Thanks to my dearest friend Didem ŞEN who supported and encouraged me through the thesis studies.

Finally, I would like to express grateful thanks to my lovely family for their motivation, continuous support and patience. My father, Öcal, and my mother, Ferhan, are the persons who always supported me for my educational decisions since I was a child and who raised me with their endless love. My sister, Müge, thanks to you for being supportive and caring. I owe them all so much.

ABSTRACT

SPECTROSCOPIC DETERMINATION OF INDUSTRIAL OIL BLENDS USING MULTIVARIATE CALIBRATION

This study focuses on the development of multivariate calibration models for the aluminum rolling oil additives and contaminants using Fourier Transform Infrared (FTIR) spectroscopy and a genetic algorithm based inverse least squares (GILS) method. Multivariate calibration models were generated for both synthetic mixtures and real process samples taken from an industrial aluminum production plant. Two different additives and six different suspected contaminants were investigated in the base oil lubricant. Gas chromatography (GC) was used for the analysis of real process samples in order to establish reference values of additives and contaminants in the base rolling oil. FTIR spectra of real samples together with the reference values established with GC analysis were used to generate multivariate calibration models. GC analysis revealed that most of the contaminants gave overlapped chromatograms and therefore only the total contamination was determined with reference GC analysis. On the other hand, FTIR spectroscopy coupled with multivariate calibration was able to resolve overlapping components with synthetic samples. The reference values for both additives and contaminants obtained by GC were compared with the results of the spectroscopic analysis. The multivariate calibration models based on spectroscopic data validated with the real process samples in a period of twelve months, however only a set of 3-month data is given in this thesis. The R^2 values between GC and multivariate spectroscopic determinations were around 0.99 indicating a good correlation between the two methods.

ÖZET

ENDÜSTRİYEL YAĞ KARIŞIMLARININ ÇOK DEĞİŞKENLİ KALİBRASYON KULLANILARAK SPEKTROSKOPİK TAYİNİ

Bu çalışmada, alüminyum levha ve folyo üretiminde kontrolü ürün kalitesi açısından büyük önem taşıyan, hadde yağlarındaki kirlilik ve katkı yağlarının tayini için fourier dönüşümlü infrared spektroskopi (FTIR) ve bir genetik algoritmaya dayalı ters en küçük kareler metodu kullanılarak çok değişkenli kalibrasyon modellerinin geliştirilmesi amaçlanmıştır. İki farklı katkı yağı ve altı farklı kontaminant için, hem sentetik örnekler hem de işletmeden alınan gerçek örneklerle çok değişkenli kalibrasyon modelleri kurulmuştur. Gaz kromatografi (GC) yöntemi, bu çoklu karışımlardaki bileşenlerin referans değerlerini belirlemek amacıyla kullanılmıştır. Genetik algoritmaya dayalı ters en küçük kareler (GILS) yöntemi, FTIR ile ölçümleri alınan aluminyum hadde yağı karışımlarındaki katkı ve kirlilik miktarlarının tayininde kullanılmıştır. GC sonuçları kirlilik diye tanımlanan yağların çakışan kromatogramlar verdiğini göstermiş, bu sebeple de bu yöntemle yapılan analizlerde, kirlilik tayini 'toplam kirlilik' olarak yapılmıştır. Öte yandan sentetik örneklerin spektroskopik analiz verileri ve GILS birlikte kullanıldığında çakışan bileşenlerin de tayin edilmesi mümkün olmuştur. Böylelikle GILS ile kurulan modeller ile işletmeden alınan gerçek örneklerdeki katkı ve kirlilik miktarlarının tahmini değerleri hesaplanmıştır. Katkı ve kirlilik miktarlarının kromatografik analizlerden elde edilen referans değerleri, spektroskopik analiz sonuçlarıyla karşılaştırılmıştır. Modellerin korelasyon katsayıları 0.99 olarak belirlenmiş, modellerin oldukça başarılı olduğu görülmüştür.

TABLE OF CONTENTS

LIST OF TABLES

LIST OF FIGURES

CHAPTER 1

INTRODUCTION

1.1. Aluminum Industry

During the past several decades, aluminum producers have been successful in developing new products and taking market share from competitors like steel. Aluminum is strong, lightweight, and eminently recyclable. Thus it had come to dominate the beverage can market and had become one of the most consumable materials in automobile manufacturing (Answers 2009).

1.2. Aluminum Products

Aluminum sheet, plate, and foil represent the aluminum industry's major product group and aluminum is first produced in the form of sheet ingot. These ingots are flat rolled and rerolled until the desired thickness is achieved. Plate is a quarter-inch (0.635 cm) thick or more; sheet is 0.006 inch (0.015 cm) to 0.249 inch (0.632 cm); and foil is less than 0.006 inch (less than 0.015 cm). Sheet is the most widely used form of aluminum and is found in all of the industry's major markets, including containers and packaging (most notably beverage cans) and transportation (i.e. panels for automobile bodies) (The Aluminum Association 2009). Plate is used for the skins of jetliners and to make storage tanks, among other heavy-duty applications (Figure 1.1).

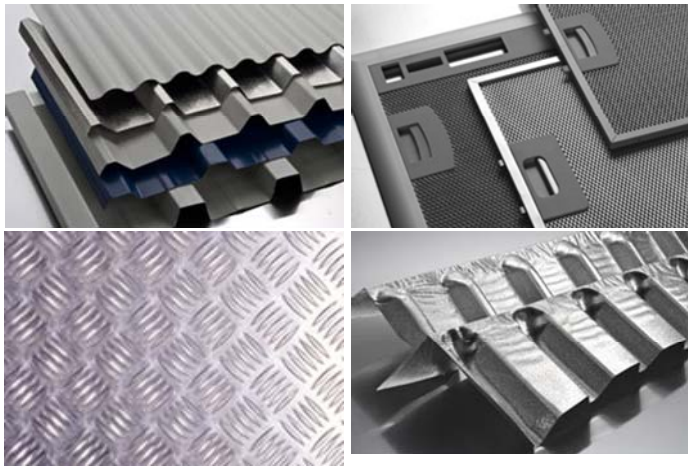

Figure 1.1. Aluminum sheet and plate products
(Source: ASSAN 2009)

Foil is used to wrap the foods, but is also utilized in building insulation and electrical capacitors, pharmaceutical closures as well as a wide variety of packaging applications (ASSAN 2009). Figure 1.2 shows a number of foil products.

Figure 1.2. Aluminum foil products
(Source: ASSAN 2009).

1.3. Aluminum Sheet and Foil Production

Aluminum is melted at fairly high temperatures (≈650°C). The molten aluminum is poured in a mould (usually called a closed die) and shape casting procedure is applied. The next step is the extrusion step in which the metal is squeezed in a closed cavity tool (known as die) either by a mechanical or hydraulic process. Aluminum can be hot or cold extruded. If it is hot extruded it is heated to 300 to 600 °C (European Aluminium Association 2009 and eFunda 2009). Figure 1.3 shows representative drawings of extrusion press.

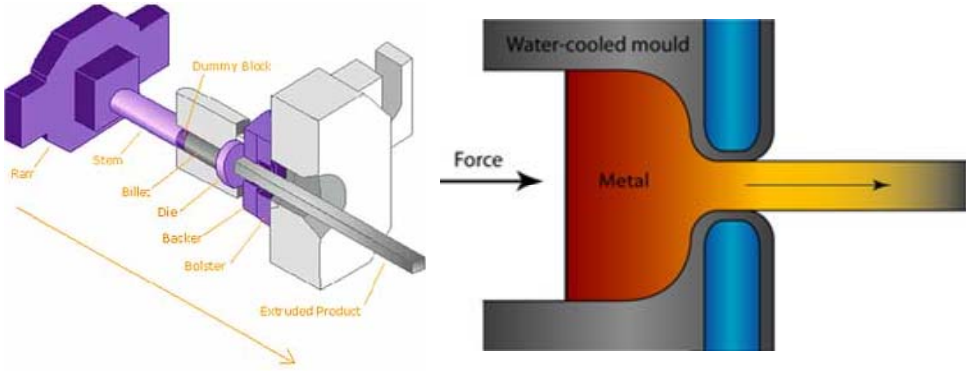

Figure 1.3. Aluminum extrusion press
(Source: Extruded Profile 2009)

The last step is the rolling step in which the metal is passed between two roller using the proper lubricants, and the thickness is reduced (Figure 1.4) (eFunda 2009).

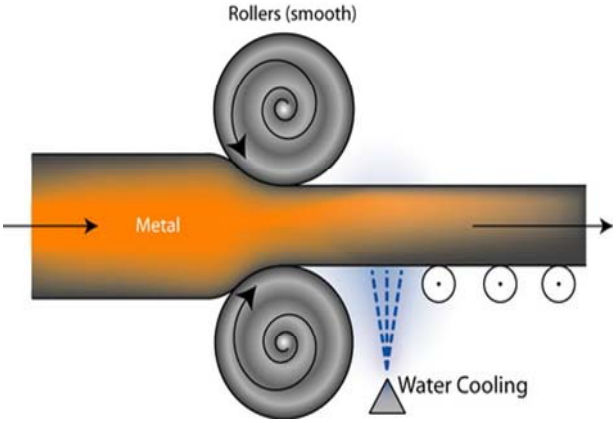

Figure 1.4. Rolling process.
(Source: Extruded Profile 2009)

Rolling can be either hot or cold (Figure 1.5). Hot rolling process helps the initial breakdown of ingots. Porosity is reduced while mechanical strength is improved. Cold rolling is often used at the final stages of production in which the dimensional accuracy and high quality surfaces is achieved (Suranaree University of Technology 2009).

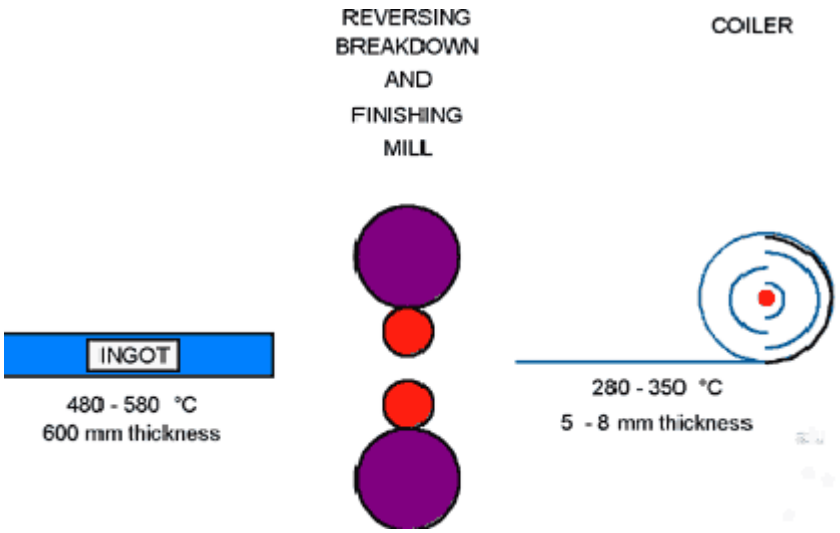

(a)

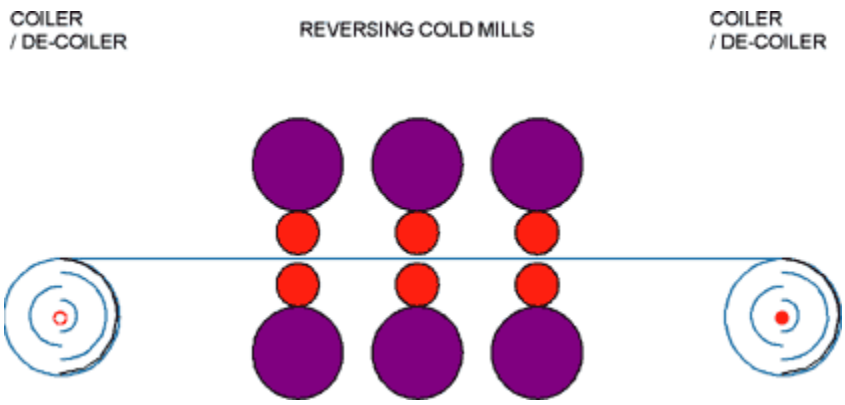

(b)

Figure 1.5. Rolling types, (a) hot rolling, and (b) cold rolling (Source:European Aluminium Association 2009).

1.4. Problems That Arise in Aluminum Sheet and Foil Production

In flat product production, aluminum metal is squeezed between two rolling mills and deformed. This process occurs at high speeds and high deformation conditions, which are the special conditions for rolling. Therefore, a special condition must be maintained by an 'agent' in between the interface (Guthrie 2005). The proper

frictional conditions are achieved and the abnormal warming of the plate is prevented by this manner. This agent is so-called 'the lubricants' which are used for minimizing the friction and reducing the heat of friction (Gale 2004).

The rolling process is continuous since the rolled aluminum is opened up from one coil while it is wrapped in another. So maintaining the continuity of interface conditions is important. The necessary conditions of the interface is maintained by adding certain and appropriate amounts of lubricating additives which are the mixtures of fatty acids, fatty alcohols, and antioxidants, and have low viscosity with reliable flashing points (Guthrie 2005).

Another important criterion for effective rolling is not only the purity of oil but also the stability of the additive balance. If the balance between the frictional and lubricating factor is distorted, the aluminum surface quality is affected unfavorably. During their usage, those rolling lubricants are polluted by the oils which are used for the other parts (gear and hydraulic) of the rolling system. The leaks from the machinery oils cause contamination in those additive lubricants resulting in serious staining problems on the surface of the product (Sprissler, et al. 1985). Therefore it is important to control these leaks to improve the product quality.

1.5. Literature Background

Aluminum rolling process is continuous since the rolled aluminum is opened up from one coil while it is wrapped in another. Therefore additives are used for maintaining the continuous lubrication. During the rolling process, mechanical cooling lubricants leaking from the mill equipments cause contamination resulting in serious staining problems which reduce the product quality. The control of these leaks is very important for product quality. In other words, the level of these contaminants should be reduced in order to enhance good quality products.

The product quality is enhanced by the addition of lubricant additives. As indicated above, additives are used for minimizing the friction between the mills. The amount of additives should be controlled since the additive balance is important for product quality. The determination of additives in base oils which are used in machines is possible by using gas chromatographic techniques. The antioxidants and anti-wear

additives can be identified by gas chromatography-mass spectrometry (GC-MS), using MS detector in selected ions monitoring (Bernabei, et al. 2000).

The lubricating performance may be affected by the free fatty acid content, the degree of esterification, etc. so those effects should be monitored. Monitoring these effects is possible by HPLC, GC and Gel Permeation Chromatography (GPC) (Heenan, et al. 1993).

During aluminum rolling, the rolling mill oils become contaminated with mechanical lubricants leaking from the mill equipment such as gear and hydraulic systems. Those leaks must be detected before the staining problems arise. Slow leaks can be controlled by High Performance Liquid chromatography (HPLC). However, the use of this technique in rolling mill plants results in long analysis times which is not practical (Sprissler, et al. 1985).

Chromatographic techniques, especially Gas Chromatography (GC) find widespread use in the determination of the contaminants as well as the additives. Quantitative analysis is possible by using these techniques. Chromatographic separations are employed to quantify specific compounds that may be included in the oil, and to detect the additives or less expensive oil components used as diluents (Jennings 1997).

However, for the continuous monitoring of several rolling mills, these chromatographic techniques may not be practical for the routine analysis, having long analysis times these techniques are not very practical for routine analysis. Spectroscopic techniques which are more accurate and fast are widely used for the characterization of organic compounds just as the mechanical lubricants.

The structure of machinery oils is organic so that the identification of their structure, understanding the molecular interactions and inspection of the impurities is possible by using Fourier Transform Infrared spectroscopy. The monolayers of the lubricant oil residues retained on the surface of aluminum sheets can be characterized by FTIR (Hirani, et al. 2007).

The machinery oils containing fatty acid esters and alcohols are not only identified qualitatively but also determined quantitatively, using the spectroscopic techniques. Another quantitative study for the determination of the fatty alcohols and fatty acid esters in machinery oils by using FTIR spectrometry (Vahaoja, et al. 2005).

Furthermore spectroscopic techniques having complex data are usually coupled with the multivariate calibration techniques, since univariate techniques fail to give

efficient results for the complex data sets. Near infrared spectra was coupled with partial least squares (PLS) for the analysis of the contaminant in a number of lubricating oils (Paschoal, et al. 2003).

Gasoline, ethylene glycol and water contamination in automotive engine lubricating oils were determined using attenuated total reflectance (ATR) mid infrared spectroscopy and PLS (Borin, et al. 2005)

Fourier transform infrared (FTIR) spectroscopy combined with multivariate calibration was used to monitor lubricating oil degradation and analysis of possible contaminants in aluminum cold rolling systems (Wiseman and Ahsue 1992).

CHAPTER 2

GAS CHROMATOGRAPHY

2.1. The Principle

The basic principle of gas chromatography is the separation of volatile compounds in mixtures which provides both qualitative and quantitative information about the analytes of interest. Chromatographic separations are based on the partitioning of the compounds to be analyzed between two phases by the carrier gas flow. One of the phases is the 'stationary' phase which can be either liquid or a solid. The other phase is the 'mobile' phase which is a gas. The carrier gas flows through the separation column as the mobile phase (Schomburg 1990).

2.2. The Instrumentation: Elements of a Gas Chromatograph

A gas chromatograph basically consists of a flowing mobile phase, an injection port (serves to introduce the sample into the flowing mobile phase), and a separation column containing the stationary phase, a detector, and a data recording system (Figure 2.1). The sample is carried by the flowing mobile phase which is so-called 'carrier gas'. The carrier gas can be hydrogen (H_2), helium (He), nitrogen (N_2) or argon (Ar). The lightest gas, H_2, is preferably used where short retention times with high efficiency are achieved. Heavier gases such as N_2 or Ar can also be used but the separation times last longer and the optimization of the efficiency becomes difficult (Schomburg 1990).

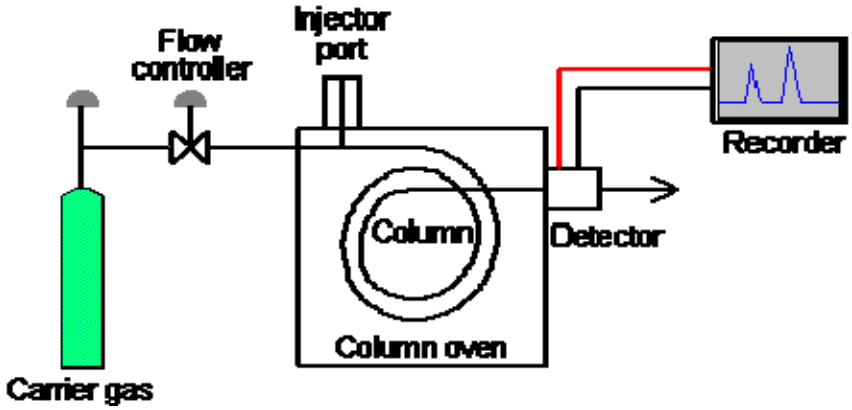

Figure 2.1. Schematic representation of a gas chromatograph
(Source: Sheffield Hallam University 2009)

2.2.1. Columns

The most widely used separation columns are the type of packed columns and capillary columns. Packed columns are 1.5 - 10 m in length having an internal diameter of 2 - 4 mm. The tubing is usually made of stainless steel or glass and contains a packing of finely divided, inert, solid support material that is coated with a liquid or solid stationary phase. The nature of the coating material determines what type of materials will be most strongly adsorbed. Thus numerous columns are available that are designed to separate specific types of compounds (Figure 2.2).

Nowadays capillary columns are becoming very popular because of their high efficiency (which is characterized by the number of theoretical plates per unit length) and temperature stability (Schomburg 1990). This type of column is usually made up of fused silica tubing with an inner diameter of about 30-500 µm, and a length of 10, 30, 60 meters are available. The stationary phase which only covers the inner surface is usually a thin film of thermally stable immobilized methylpolysiloxane (OV-1, DB 1, CP-Sil 5, SE-54 etc) (Schomburg 1990) and it is used for general purposes, capable of separating most of the organic compounds. The stationary phase material changes due to the different objective (Schomburg 1990).

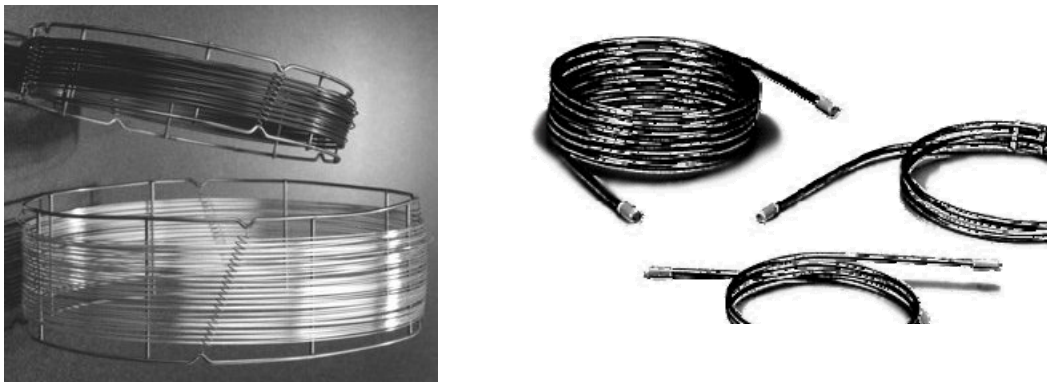

(a) (b)

Figure 2.2. Column types (a) Capillary columns (Source: Quadrex Corporation), (b) Packed columns, (Source: Cobert Associates 2009).

2.2.2. Detectors

In gas chromatography an electrical signal is continuously generated by the detector. This signal can be enhanced by measuring a physical property of the sample component. (Schomburg 1990). The most widely used detectors are the 'flame ionization detector (FID)' and 'thermal conductivity detector (TCD)' (Figure 2.3). If a TCD is used, the generated signal is proportional to the concentration of the component in the carrier gas. If an FID is applied, the generated signal is then proportional to the mass flow of the solute. For FID, the signal is generated by the ionization of the molecules of the eluted sample; the detector signal is not affected by the carrier gas. However, TCDs are concentration dependent response detectors. Therefore 'thermal conductivity' of the solute-carrier gas mixture is measured. FIDs are the type of universal detectors which is capable of detecting various classes of compounds. The major advantage is that its high sensitivity and linearity (Schomburg 1990). The destructive property might be counted as a disadvantage however very small portions of sample are destroyed so that this property is tolerable.

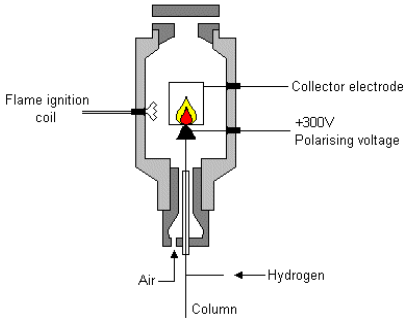

(a)

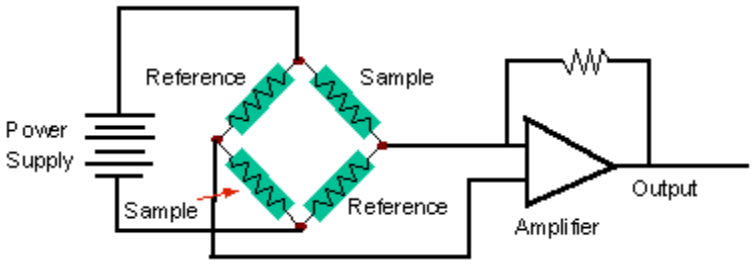

(b)

Figure 2.3. Type of detectors widely used in Gas Chromatography. (a) Flame Ionization Detector (FID), (b) Thermal Conductivity Detector (TCD) (Source:Sheffield Hallam University 2009)

2.2.3. Sample Introduction: Injection Port

During the gas chromatographic analyses, sample introduction is an important step for a successful separation. For packed columns, sample volumes change from tenths of a microliter up to 20 microliters. Capillary columns need much less sample, around 10^{-3} mL. For capillary GC, split/splitless injection is used. Split mode is applied for undiluted samples for preventing the overload of the column, since the sample capacity of this miniaturized column is low (Schomburg 1990).

In split mode the sample is injected through a rubber septum by a microliter syringe, only a small portion of the sample enters the column, and the rest of the sample leaves the column by-passing the column inlet (Schomburg 1990).

Splitless injection mode is used for the dilute samples unlike the split mode. If the dilute samples are split, one observes small peaks with corresponding small signals.

For this reason splitless mode is applied and the sample is directly injected. The splitless mode is advantageous especially during the analysis of dilute samples is performed with temperature programming (Schomburg 1990). Figure 2.4 shows the diagram of a split/splitless injector.

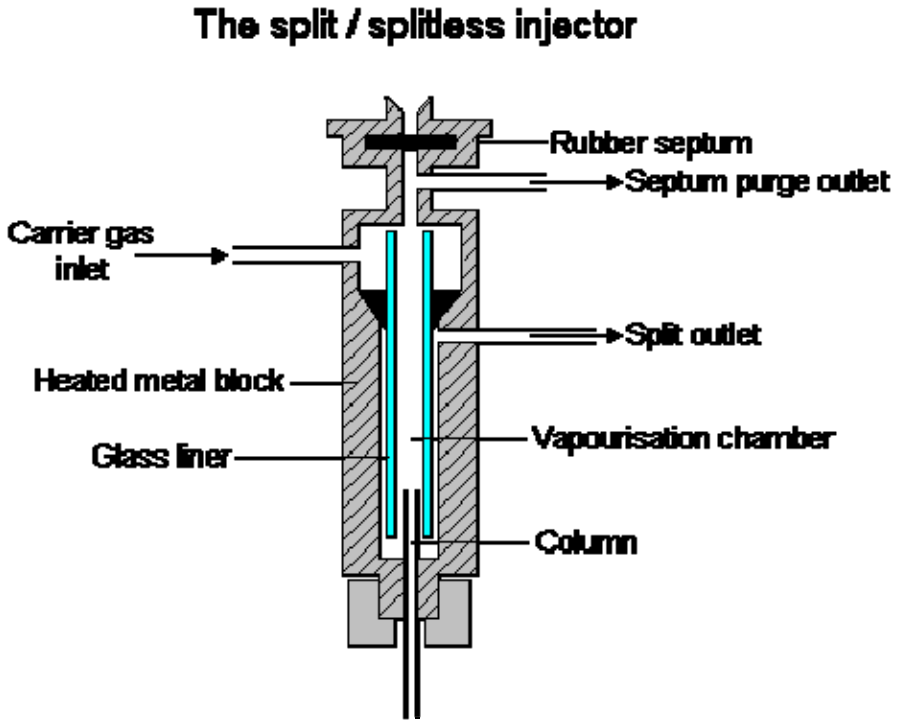

Figure 2.4. The diagram of a split/splitless injector.
(Source:Sheffield Hallam University 2009)

2.3. Temperature Programming

A method in which the column temperature is held constant through the entire analysis is called "isothermal". The total analysis time and the resolution depend on the separation temperature since it is the most important parameter. Therefore the optimization of the temperature should be considered for the reliable separations. The optimal separation temperature adjustment is not possible for the high resolution of samples in different retention sections of the chromatogram. By “temperature programming” this difficulty might be overcome. In this method temperature is usually

increased linearly at different rates following an isothermal condition (Schomburg 1990).

A temperature program allows analytes that elute early in the analysis to separate adequately, while shortening the time it takes for late-eluting analytes to pass through the column. Temperature programming also prevents the peaks of the less volatile sample components becoming too broad.

CHAPTER 3

INFRARED SPECTROSCOPY

3.1. The Principle

Infrared spectroscopy is the study of interaction of infrared light with matter. Infrared spectrum is divided into three different regions which are near infrared (12800-4000 cm^{-1}), mid infrared (4000-200 cm^{-1}), and far infrared (200-10 cm^{-1}). Infrared absorption, emission and reflection spectra are all based upon the assumption that all arise from the changes in energies due to the transitions of molecules from one vibrational or rotational energy state to another. In other words, for a molecule to absorb infrared radiation, there should exist a net dipole moment change in the molecule as a result of vibrational or rotational motions.(Skoog 1998)

Infrared measurements provide both qualitative and quantitative information about an analyte. The correlation between the wavenumbers at which a molecule absorbs IR radiation and its structure allows the identification of the structure of the unknown molecules by investigating the IR spectra. This is why IR spectroscopy is an advantageous and useful tool for chemical analysis.

3.2. Instrumentation

An IR instrument is consisted of an IR radiation source, a sample holder, a wavelength selection device, a detector and a signal processor, basically. All IR instruments require a continuous infrared radiation source and a sensitive IR detector. The types of the sources, sample holders, wavelength selectors, and detectors are selected due to the objectives of a study. The most widely used sources are the Nernst glower (ZrO_2+Y_2O_3), and Globar (SiC). When compared Globar sources provide greater output than that of Nernst glower sources. Quartz cells are the most popular sample holders used in the NIR region. Potassium bromide (KBr) cells are used in the mid-IR and far-IR regions. Dispersive IR instruments use prism or a grating as a

wavelength selector. IR instruments of type nondispersive usually use filters. The most widely used detectors in the IR region are the type of thermal detectors such as thermocouples and bolometers and photoconducting transducers especially the mercury/cadmium telluride transducers which finds widespread use in Fourier Transform instruments. The detailed information of the instrumentation and elements of an IR instrument is given in a number of text books (Skoog 1998).

3.2.1. Dispersive Instruments

The original infrared spectrometers are the dispersive type instruments. These instruments separate the individual frequencies of energy emitted from the infrared source by the use of a prism or grating. An infrared prism works exactly the same as a visible prism and separates visible light into its frequencies. A grating is a more modern dispersive element which separates the frequencies of infrared energy better. The detector measures the amount of energy at each frequency which has passed through the sample (Figure 3.1) (Skoog 1998).

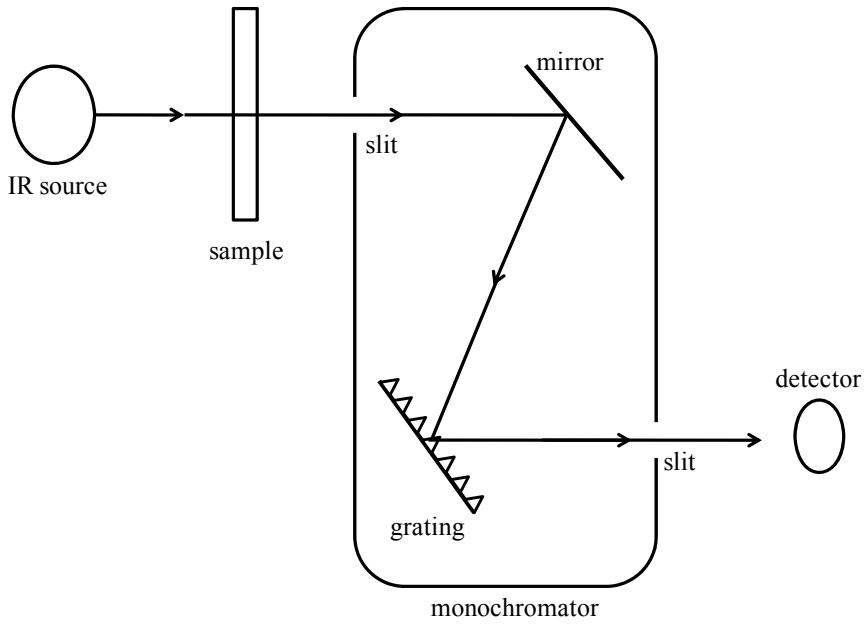

Figure 3.1. A schematic representation of the dispersive instrument.

3.2.2. Nondispersive Instruments

Nondispersive instrument are of type filter or nondispersive photometers which are mostly used for quantitative purposes. The common detector for this type of instrument is a nondispersive IR analyzer (Figure 3.2). These instruments are inexpensive and easy to use (Skoog 1998).

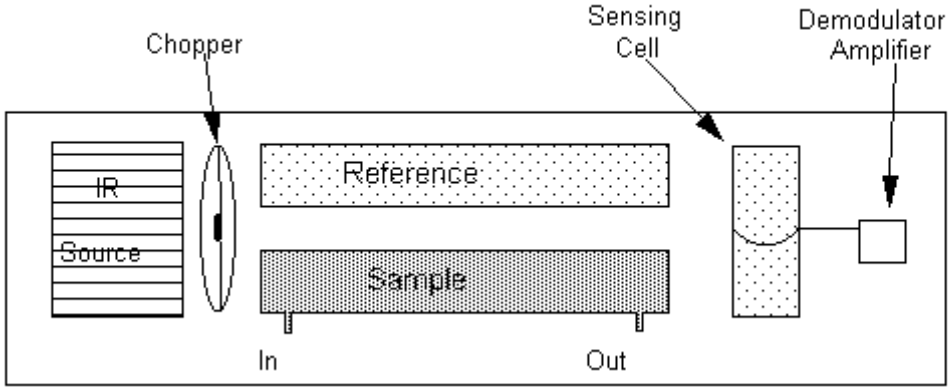

Figure 3.2. A simple nondispersive IR analyzer.
(Source:University of Massachusetts Amherst 2009)

3.2.3. Multiplex Instruments: 'Fourier Transform Instrument'

The most common type of multiplex instrument is of type Fourier Transform. The main difficulty of older technologies is that the slow scanning process. For measuring all the frequencies simultaneously, a device called 'interferometer' is developed. Therefore, the majority of FT instruments are based upon the interferometers.

3.2.3.1. Instrumentation

The purpose of an interferometer is to take the beam, split into two beams, and make one of the beams travel a different distance than the other. The basic

interferometer is a Michelson interferometer which consists of a beamsplitter, moving and fixed mirrors (Figure 3.3).

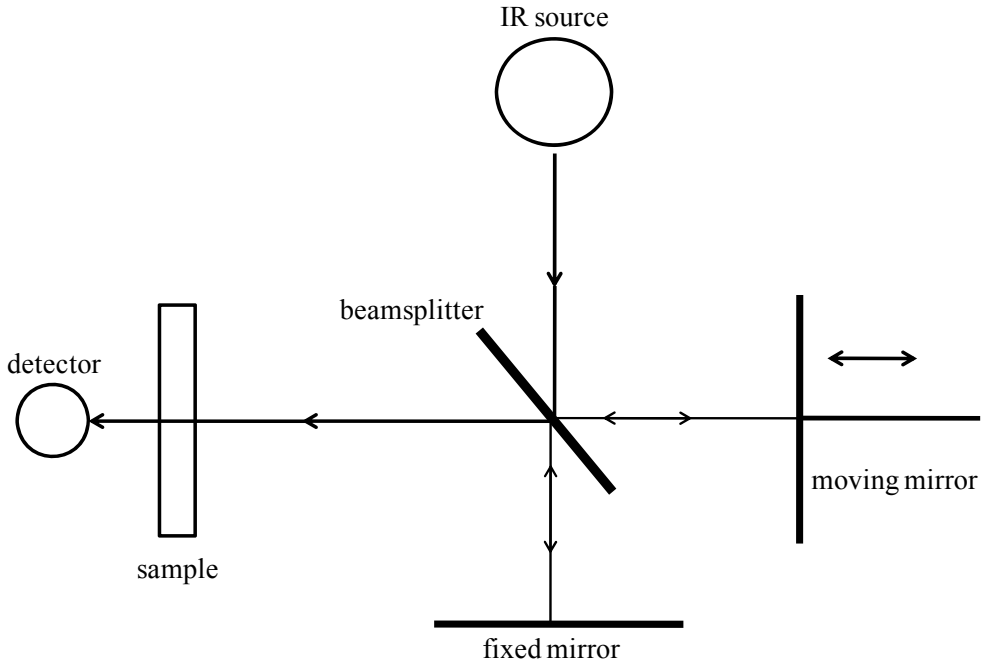

Figure 3.3. An optical diagram for a Michelson interferometer.
(Source: Smith 1996)

The major component of a Michelson interferometer is a beamsplitter. It transmits half of the radiation and reflects half of it. As a consequence the light which is transmitted by the beamsplitter strikes the fixed mirror and the reflected one strikes the moving mirror. Those two beams are recombined after reflecting off the respective mirrors, and leave the interferometer to interact with the sample and reach the detector (Smith 1996).

The resulting signal obtained from the detector is an 'interferogram'. In order to identify the compound in interest, the interferogram should be treated with some mathematical calculations which are called 'Fourier Transformation' (FT). Figure 3.4shows a representation of an interferogram and the spectra obtained after 'decoding' the frequencies by the FT calculations.

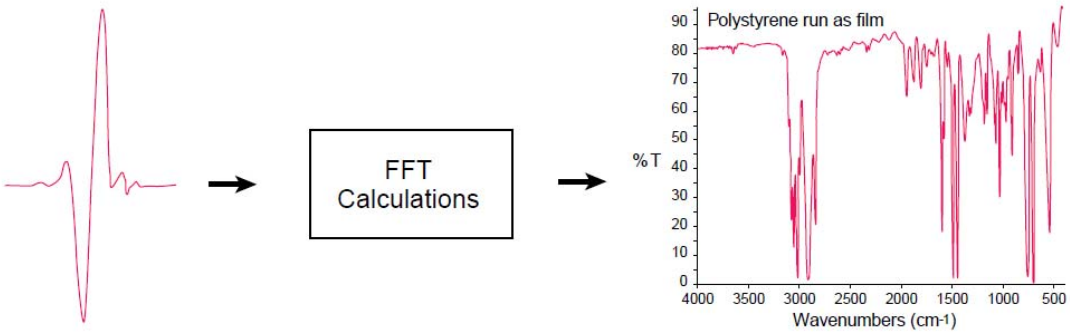

Interferogram Spectrum

Figure 3.4. Schematic representation of an interferogram and a spectrum. (Source:ThermoNicolet 2009)

While working with FTIR instruments, background spectrum should always be collected before measuring the sample since the instrumental and atmospheric contributions that arise from the sample peaks are eliminated by subtracting the background spectrum from the sample spectrum (Smith 1996).

An FTIR instrument is basically a spectrometer which consists of a source, an interferometer (including beamsplitter), and a detector. The figure below represents a schematic diagram for an FTIR instrument (Figure 3.5).

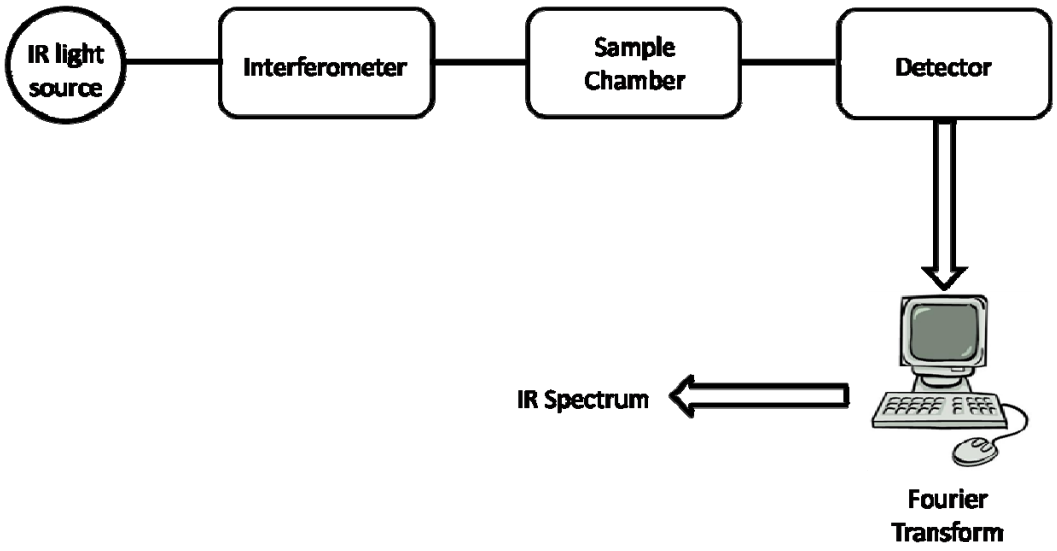

Figure 3.5. Schematic diagram for an FTIR instrument

3.2.3.2. Sampling Techniques

Since every technique has its own specific uses, choosing the right sampling technique is very important. Each technique also has its own advantages and disadvantages. The most common sampling techniques are the transmission and reflectance techniques.

The *transmission technique* is a simple way of obtaining IR spectra in which the light is passed directly through the sample. It is a universal technique since it works for solids, liquids, gases and polymers. However, the major disadvantage is that the thickness of the sample is very important. For instance, samples thicker than 20 microns absorb too much IR radiation so that it becomes impossible to obtain a spectrum (Smith 1996).

KBr pelleting technique finds widespread use while the transmission spectra of solids are collected. The sample/KBr mixture pellets should be prepared carefully since the mixture should be grounded very well and an opaque pellet must be obtained. Otherwise, the light will scatter and cause baseline shifts.

Sealed liquid cells are commonly used during the collection of transmission spectra of liquids. Here, the liquid sample is placed (usually injected with a syringe) between two KBr windows. Those sealed liquid cells are excellent devices for quantitative work since the pathlength is known. They also prevent the evaporation of the sample, so volatile or toxic liquid samples can be analyzed. The only disadvantage is that it is difficult to clean and fill the cell.

Another technique for sampling is the *reflectance techniques*. These techniques differ from transmission techniques in a way that the IR beam interact the sample only on the surface instead of passing through the sample. The major advantage of these techniques is that it shortens the analysis times. However the disadvantage is that these techniques require special accessories which costs expensive. Another disadvantage is the depth of penetration of the IR beam is not known accurately. As a consequence the quantitation might be difficult since it is difficult to determine the pathlength exactly (Smith 1996).

In *specular reflectance*, the angle of incident light is the same with the angle of the reflected light. This type of reflectance occurs on smooth surfaces.

In *Diffuse Reflectance Infrared Fourier Transform Spectroscopy (DRIFTS)*, the angle of the incident light is fixed where the angles of reflections vary from 0 to 360 degrees. This type of reflectance occurs on rough surfaces. This method is used especially for powder and solid samples. The sample preparation is very similar to that for KBr pelleting. The sample is put in the sample cup and IR radiation is focused onto the sample mixture and is scattered, absorbed, transmitted and reflected by the sample, which is named as "diffusely reflected radiation" in short. The diffusely reflected radiation is then collected by another mirror. At last the light reflects off and reaches to the detector. The applications of this technique are widely used in pharmaceutical and chemical industries (Smith 1996).

Another technique is the *Attenuated Total Reflectance (ATR)* which is used to collect the spectra of solids, liquids, semisolids and thin films. The accessory contains a crystal which is IR transparent with high refractive index. The crystal materials are usually zinc selenide (Zn/Se), thallium iodide/thalium bromide (KRS-5). Here the principle is that once the radiation is inside the crystal, an evanescent wave is set up. The sample may interact with this wave and absorb the IR radiation so that its IR spectrum is detected. This evanescent wave is attenuated by the sample's absorbance. This is why the technique is named as 'attenuated total reflectance' (Smith 1996).

CHAPTER 4

MULTIVARIATE DATA ANALYSIS

Modern spectroscopic techniques, offering fast analysis, can generate hundreds of spectra in small time periods for multicomponent samples. However univariate calibration techniques fail to give the efficient results for those types of data. Multivariate calibration techniques are promising for the complex data. These techniques make it possible to relate the instrument responses measured on multiple wavelengths to a chemical or physical property of a sample even though it contains multiple components.

4.1. Calibration Techniques

Calibration which involves the connection of one or more sets of variables together provides the answer for the prediction of a concentration of a constituent in a mixture spectrum or the form of a material by the structural parameters. Applications of calibration techniques find widespread use in many areas of quantitative chemistry. The calibration techniques are divided into two classes basically; *univariate calibration* and *multivariate calibration*. In univariate calibration, there is only one instrumental response which is related to the concentration, whereas multiple responses are related to the concentration in multivariate calibration.

4.1.1. Univariate Calibration

In univariate calibration, two single variables are related to each other which is also called linear regression. The determination of the concentration for a single compound using the response data (such as spectroscopic absorbance at a given wavelength, chromatographic peak area) is the simplest problem that can be solved by applying *'classical calibration'*. Another way of determining the concentration is

applicable when classical calibration is not the appropriate approach, namely *'inverse calibration'*. These methods will be explained in details below.

4.1.1.1. Classical Calibration

In classical calibration, the concentration is related to response (for example spectroscopic measurements) mathematically as shwon in Equation (4.1);

$$\mathbf{a} \approx \mathbf{c} \cdot s \tag{4.1}$$

in which *a* represents the vector of absorbance at one wavelength, *c* is the corresponding concentrations and *s* is a scalar coefficient which is determined by (Equation (4.2));

$$s \approx \left(\mathbf{c}' \cdot \mathbf{c}\right)^{-1} \cdot \mathbf{c}' \cdot \mathbf{a} \tag{4.2}$$

Here *s* relates those parameters mentioned above, where $\mathbf{c}'$ is the transpose of concentration vector. Following the determination of this coefficient the prediction model is built;

$$\hat{a} \approx \hat{c} \cdot s \tag{4.3}$$

where $\hat{a}$ is the scalar of a and $\hat{c}$ is the scalar of c. The model can be tested by calculating the difference between the observed and predicted values which is so-called the *residuals* or *errors*. The smaller the values of the residuals are the better the quality of prediction (Brereton 2000).

4.1.1.2. Inverse Calibration

The classical calibration is not always the most proper method, since it fits model so that all errors arise from the instrumental responses. However, modern instruments are much more reproducible and presents nearly perfect performances so that the errors might only arise from the measurement of concentration during the

sample preparation periods. Eventually, in inverse calibration, the assumption is that the sources of errors are not the instrumental responses but the concentrations. Therefore, the model is built based on the Equation (4.4) and Equation (4.5) are shwon in below;

$$\mathbf{c} \approx \mathbf{a} \cdot b \tag{4.4}$$

$$b = \left(\mathbf{a}' \cdot \mathbf{a}\right)^{-1} \cdot \mathbf{a}' \cdot \mathbf{c} \tag{4.5}$$

Here, b is scalar and the inverse of s which is used in classical calibration. The reason is that the error distributions are different for each of the models (Figure 4.1).

The concentration of an unknown is then predicted by;

$$\hat{c} = \hat{a} \cdot b \tag{4.6}$$

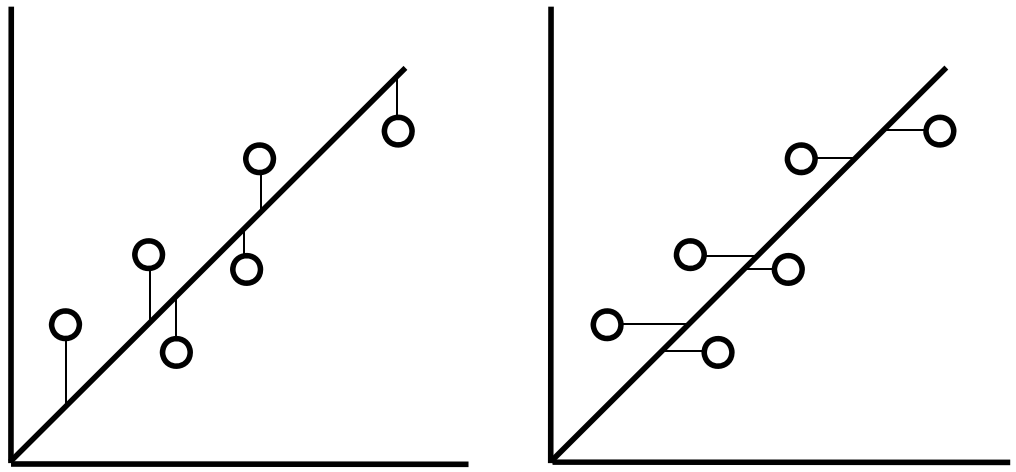

(a) **(b)**

Figure 4.1. The difference between the error distributions in (a) classical and (b) inverse calibration models.

Both of the models should provide very similar predictions unless there are some other factors influencing the data, such as intercept, unexpected noise distributions or outliers. In both of these calibration methods, the intercept is assumed to be zero this is not the case all the time. Since other absorbing species exist in spectrum, this assumption reduces the quality of regression. Therefore, the model should be improved.

More detailed information for improving the model is given in textbooks (Brereton 2000).

4.1.2. Multivariate Calibration Techniques

Multivariate calibration techniques are promising techniques when the univariate calibration techniques are not effectual. These techniques are superior to univariate techniques especially when complex mixtures are in interest. Several multivariate calibration techniques which are widely used are those Classical Least Squares (CLS), Partial Least Squares (PLS) and Inverse Least Squares (ILS) will be described briefly. The newly developed technique, Genetic Inverse Least Squares method will be defined in details.

4.1.2.1. Classical Least Squares (CLS)

Classical least squares (CLS) technique is based on the Beer's Law which states that the absorbance depends on the concentration;

$$A = C \times K \tag{4.7}$$

Since the multi-component samples are in interest, matrix notations are used instead of vector notations. The only difference from classical calibration is that the *A*, *K* and *C* are the matrices of absorbance, absorptivity coefficients multiplied by path length and concentrations, respectively. *K* matrix is estimated as shown in Equation (4.8);

$$K = \left(C' \cdot C\right)^{-1} \cdot C' \cdot A \tag{4.8}$$

where C' refers to the transpose of concentration matrix. Then the predicted concentration of an unknown sample by using its spectral data can be calculated by using the Equation (4.9);

$$\hat{c} = \hat{a} \cdot K' \cdot \left(K \cdot K'\right)^{-1} \tag{4.9}$$

Also the residuals can be calculated as the same in univariate calibration which is the difference between the real concentrations and the predicted ones (c-c').

Calibration model is constructed after measuring the instrumental responses of the standards and forming the related matrices. The model is tested by using an independent set and then the unknown sample concentrations can be calculated by using the calculated K values.

CLS method is advantageous since the calibration models can be constructed only by using several samples. Although the CLS method is easy to apply, it has its limitations. For instance, the concentrations of all components in a complex mixture should be known.

4.1.2.2. Inverse Least Squares (ILS)

The Inverse Least Squares (ILS) method is the inverse expression of the Beer's Law. Here the concentrations are modeled as a function of absorbance;

$$C = A \times P \tag{4.10}$$

where A, P and C represents the matrices of absorbance, the calibration coefficients for each component and concentrations, respectively. P matrix can be calculated as the Equation (4.11);

$$P = \left(A' \cdot A\right)^{-1} \cdot A' \cdot C \tag{4.11}$$

Then the predicted concentrations can be calculated as (Equation (4.12));

$$\hat{c} = \hat{a} \cdot P \tag{4.12}$$

Unless CLS, ILS does not require the whole concentration values for all components present. This method allows picking up the necessary portion of the spectral absorbance that correlates well to the concentrations (Kramer 1998). The most important point is that the selection of variables (e.g. wavelength, wavenumber etc.) during the construction of the calibration models. One important limitation of ILS is

that the variable selection is difficult. Another disadvantage is that the number of wavelengths cannot exceed the number of samples.

4.1.2.3. Partial Least Squares (PLS)

A superior method over ILS is the Partial Least Squares (PLS) technique, when the number of independent calibration samples exceed the number of variables (wavelengths). Since the construction of the model based on the inversion of matrices, a square matrix is necessary. Therefore, PLS reduces the number of variables by calculating the linear combinations of the original variables and uses a small number of these variables for allowing the inversion. In short, PLS is used when factors are many and collinearity between those are high.

4.1.2.4. Genetic Inverse Least Squares (GILS)

Genetic Inverse Least Squares (GILS) is a new generated method which combines inverse least squares with a genetic algorithm. The method is based on genetic algorithm in which the variable selection is achieved and the inverse least squares by which the calibration models are built.

Since in some cases ILS may not offer efficient solutions for a given problem due to the complexity of the data. In this situation, it might be necessary to apply variable selection. Among several methods of variable selection, Genetic Algorithms (GAs) are offering fast and efficient solutions for a given problem (Leardi et.al. 1992, Lucasias et. al. 1993). Genetic Inverse Least Squares (GILS) is a modified version of ILS method in which a small set of wavelengths is selected from a full spectral data matrix and evolved to an optimum solution using GA and has been applied to a number of wavelength selection problems (Özdemir et. al. 2004).

4.2. Genetic Algorithms (GAs)

Darwin's theory of evolution states that individuals who fit better to the environment are more likely to survive and breed, thus are able to transfer their genetic

information to their offspring. However, individuals who do not fit and unable to adapt will eventually be eliminated from the population. This process progresses slowly over a long period of time (or may never end) through generations and the species will evolve into better and fit forms. In the last couple of decades, scientists have been trying to take advantages of the natural evolutions as an improvement concept in the process of solving large-scale optimization problems.

In the 1960's biologists have begun to perform the simulation of genetic systems experiments with computer. The initial work in genetic algorithms was done by Holland who developed a GA in his research on adaptive systems in the early 1960's and is considered the father of the field (Gilbert et. al 1997).

Through years, GA has attracted attention and has been applied to various global optimization problems in many areas including chemometrics (Fontain 1992, Cong and Li 1994, Wienke, et al. 1993, Hibbert 1993, Lucasius and Kateman 1991). In terms of calibration, there have been several applications of GA which was used as a wavelength selection method (Lucasius, et al. 1994, Lucasius and Kateman 1992, Özdemir, et al. 1998a, Özdemir, et al. 1998b, Özdemir and Williams 1999).

Computationally the implementation of a typical GA is quite simple and consists of five basic steps including initialization of gene population, evolution of the population, and selection of the parent genes for breeding and mating, crossover and mutation, and replacing the parents with their offspring. These steps have taken their names from the biological foundation of the algorithm. The flowchart of a typical GA is shown in Figure 4.2.

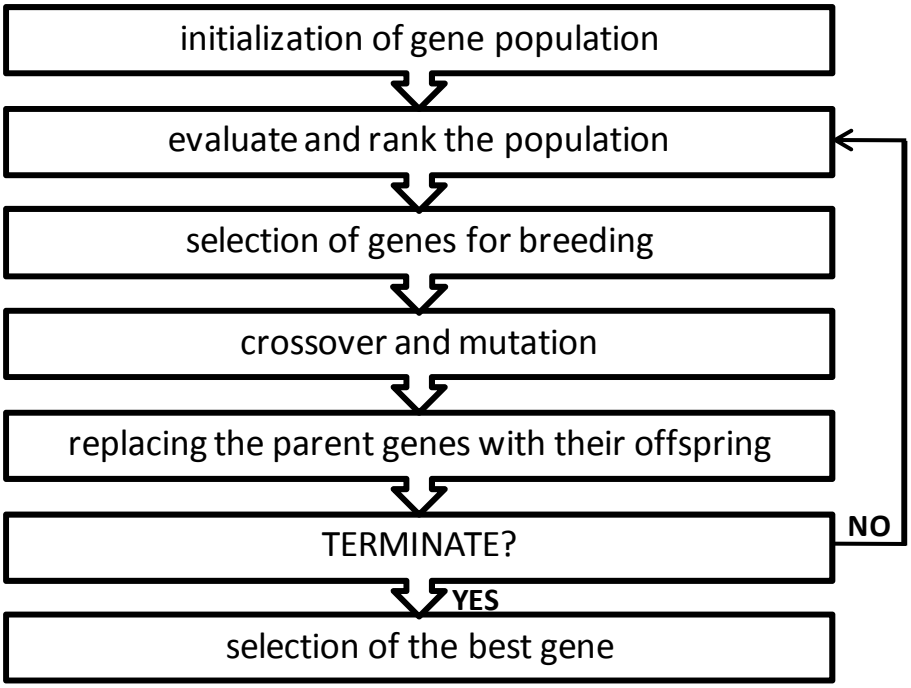

Figure 4.2. Flow chart of general genetic algorithm used in GILS.

4.2.1. Initialization

In the initialization step, the first generation of genes is created randomly with a fixed population size. This random initialization minimizes bias and maximizes the number of recombinations. The algorithm is designed to select initial genes in somewhat biased a random manner, so that it is started with the genes which are better suited to the problem.

The size of the gene pool depends on the nature of the problem, and pre-defined by the user. Note that the larger the population size, the longer the computation time.

A minimum of base pairs is a must in order to allow mating where a gene consists of base pairs between a number of 2 to 50. A base pair which contains two randomly selected wavelengths is then combined with a mathematical operator. Each base pair is then added to give a score which is so-called a gene;

$$S = A_{3879} A_{3643} A_{3539}$$

where A refers to the absorbance value of the selected wavelength. A gene in the genetic algorithm used in GILS is a collection of randolmly selected wavelengths or wavenumbers as shown above. A minimum of two variables must be contained in a gene in order to allow mating where maximum number of variables is limited with number of calibration sample. Each gene is then used to generated ILS calibration models. Figure 4.3is the schematic illustration of the gene for a real process sample.

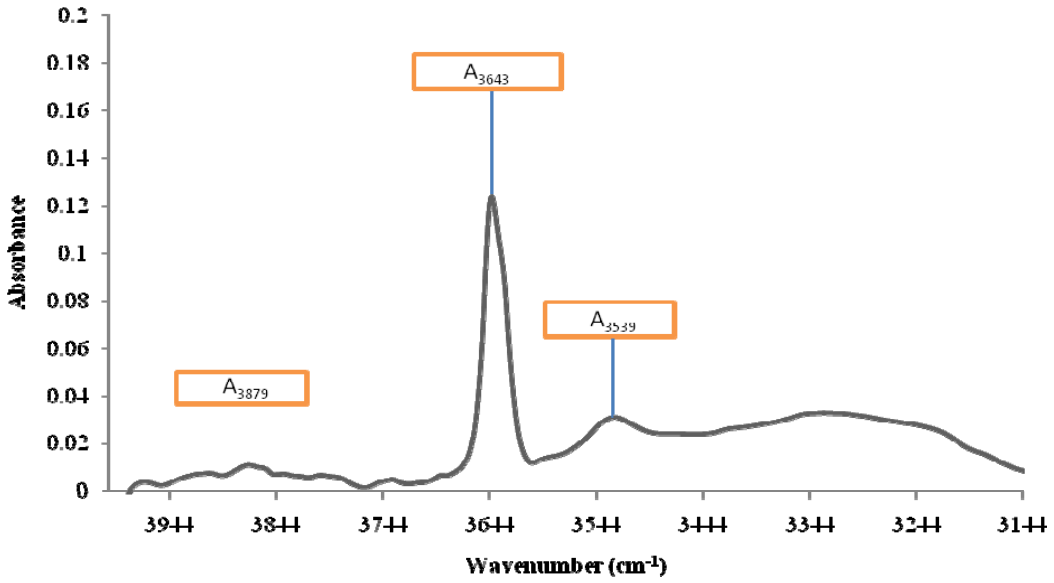

Figure 4.3. The schematic illustration of the gene for a real process sample.

4.2.2. Evaluate and rank the population

In this step, the genes are evaluated using a fitness function which is the recipocal of the standard error of calibration (SEC). Equation (4.13) shows the mathematical formula of SEC.

$$SEC = \sqrt{\frac{\sum_{i=1}^{m}(c_i - \hat{c}_i)^2}{m-2}} \tag{4.13}$$

where c_i is the reference and $\hat{c}_i$ is the predicted values of concentration of i^{th} sample and m is the number of samples. Since if the model is assumed to be linear, the

degrees of freedom is $m - 2$. The slope of the actual vs. reference concentration plot and the intercept are the only two parameters to be extracted. In each step, an increase in the fitness value is intended.

4.2.3. Selection of genes for breeding

This step involves the selection of the parent genes from the current population for breeding according to their fitness value. The main idea is that the genes which have a greater fitness value have a greater chance to survive and a greater probability of contribution to the next generation. The genes which are better suited for the problem will generate a better offspring. Thus, the genes with smaller fitness values will have a less chance to survive.

There are a number of selection methods such as top-down selection, roulette wheel selection. Top down selection is a simple method in which the genes are allowed to mate sequentially (i.e. the first gene mates with the second, and the third with the forth.) after they are ranked in the gene pool. All the members of the current gene are given a chance to breed.

Roulette wheel selection is another selection method in which the chance of selecting the gene is directly proportional with its fitness. Here, each slot represents a gene. Therefore, the largest slot refers to the gene which has the greatest fitness and so the greatest chance to be selected. However, some of the genes might be selected more than once and some might never be selected and thrown out of the pool. Subsequent to the selection of parent genes, they are allowed to mate top down, whereby the first gene is mated with the second, and the third with the fourth. The difference from the top down selection method is that no ranking is done. Therefore, the genes with low fitness might mate with better performing genes resulting in an increased possibility of recombination.

4.2.4. Crossover and mutation

In this step, the genes are broken at random points and then cross-coupled to generate a new offspring. The following example represents how the cross-coupling takes place (Figure 4.4),

$$S_1 = A_{4255}A_{5732} \oplus A_{9237}A_{4890}$$

$$S_2 = A_{5123}A_{8457}A_{9743}A_{7832} \oplus A_{8922}$$

$$S_3 = A_{4255}A_{5732}A_{8922}$$

$$S_4 = A_{5123}A_{8457}A_{9743}A_{7832}A_{9237}A_{4890}$$

Figure 4.4. Mathematical illustration of cross–coupling

where S_1 and S_2 are the parents and S_3 and S_4 are the offspring. "$\oplus$" refers to the point where the crossover takes place. First part of S_1 is cross-coupled with the second part of S_2 to form the offspring S_4. This operation is called *single point crossover* which is the one used in GILS. There are also other types of crossover methods such as two point crossover and uniform crossover, each having their advantages and disadvantages. In the uniform case, each gene is broken at every possible point and many possible combinations are possible in the mating step, thus resulting in more exploitation. However, it is more likely to destroy good genes. Single point crossover will not provide different offspring if both parent genes are identical, which may happen in the roulette wheel selection, and broken at the same point. To avoid this problem, two points crossover, where each gene is broken in two points and recombined, can be used. Single point crossover generally does not disturb a good gene but it provides as many recombination as other types of crossover schemes. Also mating can increase or decrease the number of base pairs in the offspring.

Mutation, which introduces random deviations into the population, can be also introduced into the algorithm during the mating step at a rate of 1% as is typical in GA's, preferably. Replacing one of the wavelengths in an existing gene with a randomly generated new wavelength usually does this. However, it is not used in GILS in this study.

4.2.5. Replacement of the parent genes with their offspring

After crossover, the parent genes are replaced by their off-springs. The ranking process based on their fitness values follows the evolution step. Then the selection for breeding/mating starts again. This is repeated until a predefined number of iterations are reached.

At the end, the gene with the lowest SEC (highest fitness) is selected for model building. This model is used to predict the concentrations of component being analyzed in the validation set. The success of the model in the prediction of the validation set is evaluated using standard error of prediction (SEP) which is calculated as:

$$SEP = \sqrt{\frac{\sum_{i=1}^{m}(c_i - \hat{c}_i)^2}{m}} \qquad (4.14)$$

where m is now, in this case, the number of validation samples.

4.2.6. Termination

The termination of the algorithm is done by setting predefined iteration number for the number of breeding/mating cycles. However no extensive statistical test has been done to optimize it, though it can also be optimized. Since the random processes are heavily involved in the GILS, the program has been set to run predefined number of times for each component in a given multi-component mixture. The best run, i.e. the one generating the lowest SEC for the calibration set and at the same time obtained SEP for the validation set that is in the same range with SEC was subsequently selected for evaluation and further analysis.

GILS has some major advantages over the classical univariate and multivariate calibration methods. GILS is not only quite simple in terms of the mathematics involved in the model building and prediction steps, but also has the advantages of the multivariate calibration methods, since it uses the whole spectra to extract the relevant information. By selecting a subset of instrument responses, it is able to eliminate nonlinearities that might be present in the full spectral region.

CHAPTER 5

EXPERIMENTATION

This project covers the determination of additives and contaminants in aluminum rolling base oil used in ASSAN Aluminum Corp.(ASSAN Alüminyum San. ve Tic. A.Ş., Tuzla, İstanbul, TURKEY) which is one of the leading aluminum producers in Turkey. The lubricants which are used as additives to reduce the constructive effects of friction and the mechanical cooling lubricants which may often cause contamination were determined by means of Gas Chromatography (GC) and Fourier Transform Infrared (FTIR) Spectroscopy. Gas chromatography is the reference technique which was then compared with the results of FTIR spectroscopy by using the multivariate calibration techniques, Genetic Algorithm based Inverse Least Squares (GILS).

The rolling base oil named as Linpar 13-14 which is linear paraffinic oil with 13-14 carbon chain length was obtained from Sasol (Sasol Italy S.p.A. Milano, ITALY). The additive Nafol 1214S is a blend of linear alcohols with 10-16 carbon chain length and used as antioxidant and wetting agent. It is also supplied by Sasol, Italy. Another additive that was used in this study is Cindolube SR 99 AP which is purchased from Houghton (Houghton Italia S.p.A, Genova, ITALY). Cindolube SR is a performance additive lubricant used as antioxidant and wetting agent. Hydrotex Alu 16 and 46 (Belgin Madeni Yağlar Ticaret ve Sanayi A.Ş., Kocaeli, TURKEY) were used in the aluminum rolling mills as the hydraulic oils. A number of gear oils were also investigated in this study as the possible source of contaminations in aluminum rolling lubricating oils. Among them, Recompound Alu 100, 220, 320 and 460 that are also purchased from Belgin, were used in this study. Since they are commercial products, the original names are not mentioned by the producer company so that their commercial names will be used to describe each. Table 5.1 shows the commercial names for the cooling lubricants and additives.

Table 5.1. The commercial names for the cooling lubricants and additives.

Base oil	Additives	Cooling Lubricants
Linpar	Nafol	Hydrotex Alu 16
	Cindolube	Hydrotex Alu 46
		Recompound Alu 100
		Recompound Alu 220
		Recompound Alu 320
		Recompound Alu 460

Aluminum sheet and foil production is accomplished by using ten different systems due to their purposes. The system names will also be coded shortly. Table 5.2 represents the names of the systems, the purposes which are used during the production process and the additives used in those systems.

Table 5.2. Names of the aluminum foil and sheet production lines and the additives used in those systems.

Cold Mill Systems	Additive Used	Foil Mill Systems	Additive Used	Sheet Mill Systems	Additive Used
SH1	Cindolube	FH1	Nafol	C1	Nafol
SH2	Cindolube	FH2	Nafol	C2	Cindolube
		FH3	Nafol	C3	Nafol
		FH4	Nafol	C4	Cindolube

As indicated before, the refence method was chosen to be GC. The GC (GC–2010, Shimadzu, Kyoto, Japan) is equipped with a fused silica capillary column (OPTIMA 5, 5% phenyl – 95% dimethylpolysiloxane (30.0 m/0.25 mm/0.25 μm). A flame ionization detector is used.

For the GC analyses, both additive and contaminant standards were prepared. All standards were prepared in the base oil Linpar. Since the real process samples contain fixed amounts of additives (Nafol and Cindolube), concentration range (by weight percent concentration; w/w %) is held at those ranges. In real samples, the tolarable amount of Cindolube additive is around 5.0 - 7.0% (w/w %) in base oil Linpar, where the Nafol is around 0.7 - 1.0% (w/w %). The concentration ranges for both the additive and contaminant standards are given in Table 5.3. The reason of which the

'total Alu' standards were used will be mentioned in Chapter 6. But briefly, since the most of the contamination is caused by Alu 46, Alu 100, Alu 220, Alu 320 and Alu 460 and the GC profiles are very similar, these contamination can only be detected as total amount. The real process samples were also analyzed by GC for assigning the reference values which are then be compared with the FTIR-GILS results.

Table 5.3. Concentrations of the GC standards of the additives and contaminants.

Sample	Nafol concentration (w/w %)	Cindolube concentration (w/w %)	Total Alu concentration (w/w %)
1	0.2125	2.0141	0.3382
2	0.5065	4.9415	0.7166
3	0.7026	6.0050	1.3680
4	1.0036	8.0000	2.4199
5	1.2635	10.0170	3.7702
6	1.5105		5.0105
7	2.0022		7.5441
8			10.0143

During GC analyses, a temperature programme was used for better separation. The temperature programme parameters are given in Table 5.4 which lasts 23 minutes. Since the boiling points of those components are around 200°C, the temperature of the column was raised upto 250°C. The initial column temperature is 100°C and the injector temperature is 250°C. The detector temperature is adjusted to 320°C. The split injection mode is used with a ratio of 10 and the injection volume is adjusted as 1 μL.

Table 5.4. The GC temperature programme parameters.

Rate	Temperature(°C)	Hold time(min)
-	100	2
10	150	2
10	200	2
10	250	2

Spectrum 100 FTIR spectrometer (Perkin Elmer, Waltham, MA, USA) equipped with an Deuterated Triglycine Sulfate (DTGS) detector, Michelson interferometer, KBr beamsplitter and a quartz/halogen source. For FTIR spectroscopic analyses, the standards which were prepared for GC analyses were used again. During spectroscopic analyses, a teflon liquid cell with a window material KBr is used. The pathlength is maintained by using spacers of 0.5 mm. The measurements are done in the range between 450–4000 cm^{-1}. The scan number is adjusted as 8, while the resolution is set to 4 cm^{-1}. The same standards were measured which were used in GC analyses. The real process samples were also measured.

CHAPTER 6

RESULTS AND DISCUSSION

The mechanical cooling lubricants causing contamination and the additives which are necessary for permanent lubrication, are analyzed using both the chromatographic and spectroscopic techniques. In this chapter, the results of gas chromatographic and FTIR spectroscopic analyses was examined. The contaminants and additives in a series of real process samples are described quantitatively, using GILS and the results was investigated. This chapter includes two sections, and those two sections are also subdivided into two parts; the contaminant analysis and the additive analysis. The first section covers the gas chromatographic analysis while the second is covering the FTIR spectroscopic results.

6.1. Gas Chromatographic Analysis

As mentioned before GC is assigned as the reference method for the comparison of the GILS results which is acquired by using FTIR spectroscopic data. The Recompound Alu series (Alu 100, Alu 220, Alu 320, and Alu 460) and Hydrotex Alu series (Alu 16 and Alu 46) which are used for mechanical cooling objectives and causing contamination in production, and Nafol and Cindolube which are used as the additives for maintaining the permanent lubrication were analyzed in GC. The chromatograms are investigated and the most intense and specific peaks for each component was chosen to build calibration models using classical calibration. For this reason calibration standards were prepared for each component. Since Linpar is used as base oil for lubrication objectives in all process systems, the standards were prepared in Linpar. Figure 6.1 shows the chromatogram of pure Linpar.

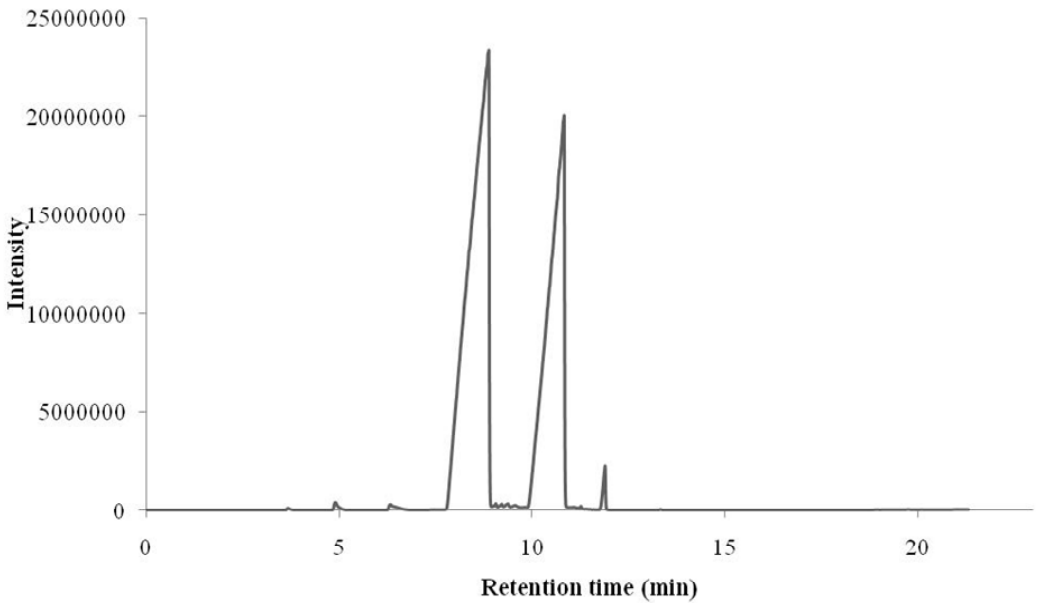

Figure 6.1. GC chromatogram of pure Linpar.

As can be seen from the chromatogram given in Figure 6.1, there are two main peaks around 8.0 and 11.0 minutes and an additional small peak around 11.5 minute. Due to the intense peaks on the chromatogram which suppresses the chromatogram, it is not clear from the above chromatogram that the chromatographic profile after 12.0 minutes contains no detectable peak, it was apparent from a close examination of the whole chromatogram that pure Linpar showed no peaks after 12.0 minutes.

6.1.1. Contaminant Analysis

The leaks from the mechanical cooling lubricants cause contamination resulting in serious staining problems on products. Recompound Alu series oils (Alu 100, Alu 220, Alu 320, Alu 460 and Hydrotex Alu series oils (Alu 16, Alu 46) which are used for the gear and hydraulic systems are the contaminants.

Figure 6.2, Figure 6.3, Figure 6.4 and Figure 6.5 represents the chromatograms of Recompound Alu series and Hydrotex Alu series respectively (1.0% (w/w %) solution of these compoents in base oil Linpar). As can be seen from these chromatograms, among the all Recompound and Hydrotex Alu series, only Alu 16 gave a distinctively different chromatographic profile from all the other components. In

addition, all the peaks are observed after 12 minutes which provided a chance to analyze these components apart from base oil Linpar.

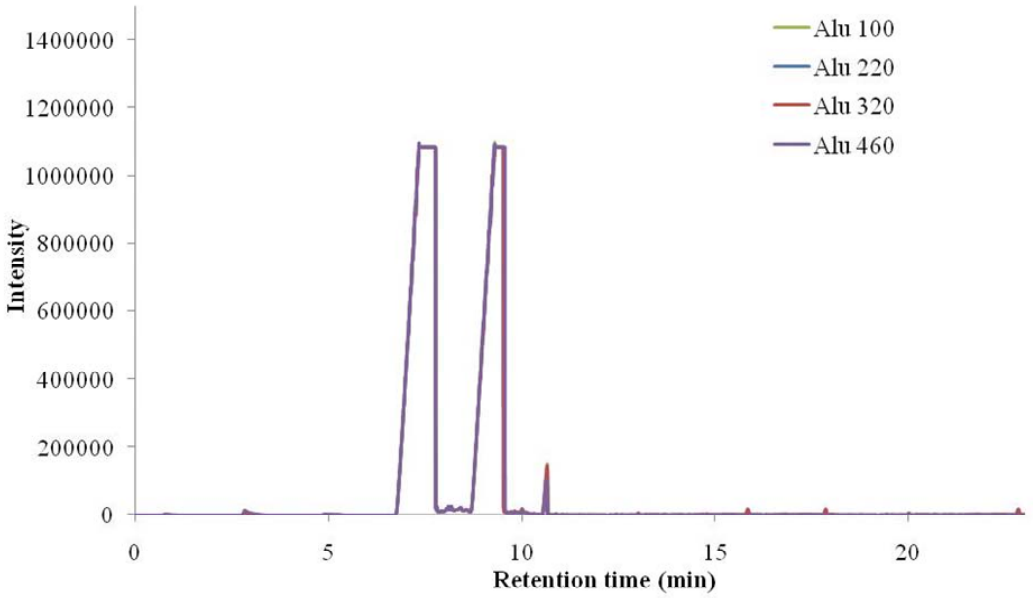

Figure 6.2. GC chromatograms for Recompound Alu 100, Alu 220, Alu 320, and Alu 460 components (between 0.0–23.0 minutes).

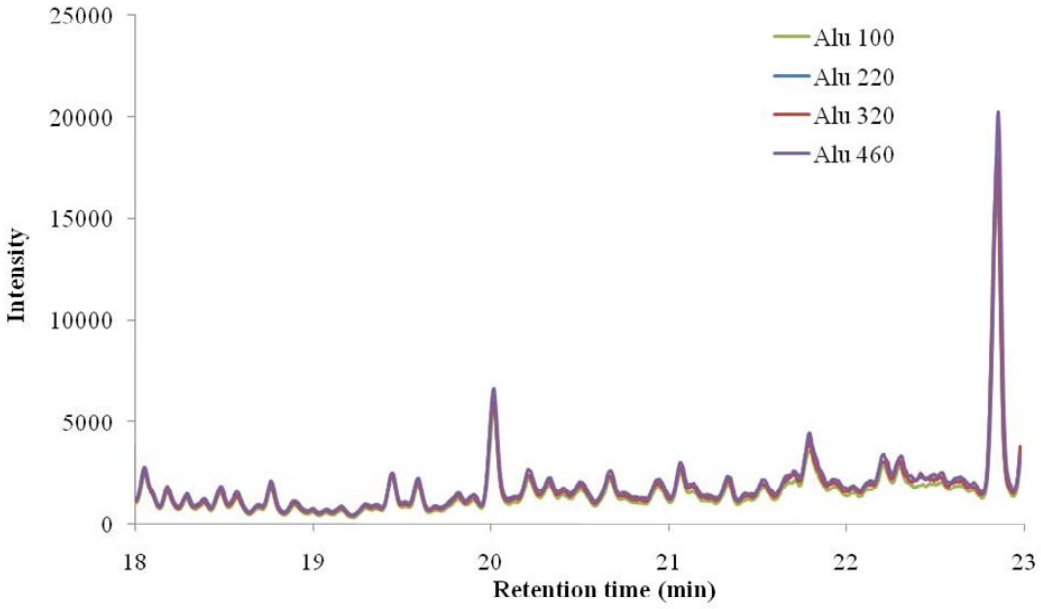

Figure 6.3. GC chromatograms for Recompound Alu 100, Alu 220, Alu 320, and Alu 460 components (between 18.0-23.0 minutes).

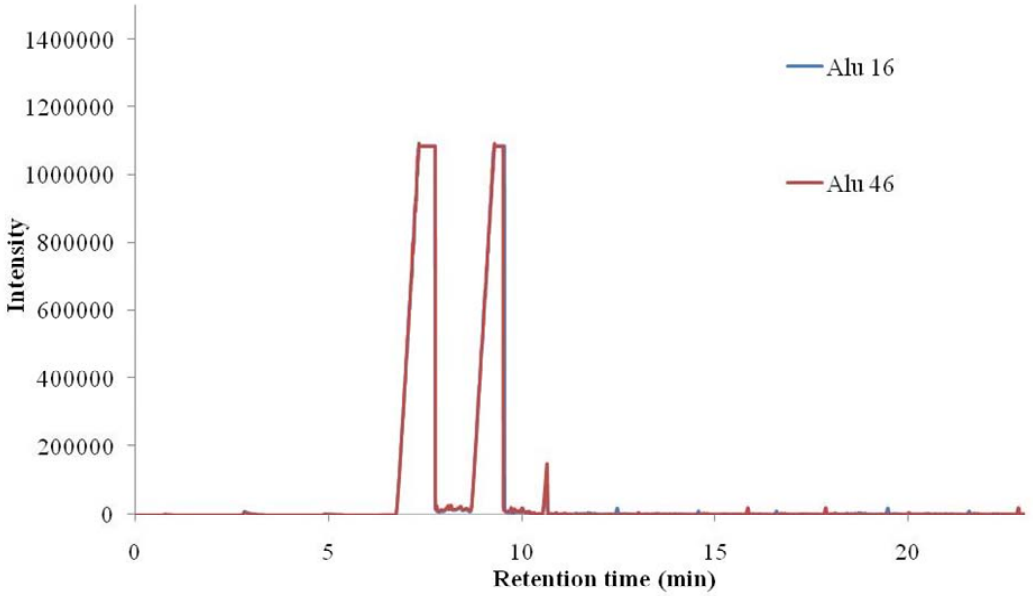

Figure 6.4. GC chromatograms for Recompound Alu 16 and Alu 46 components (between 0.0-23.0 minutes)

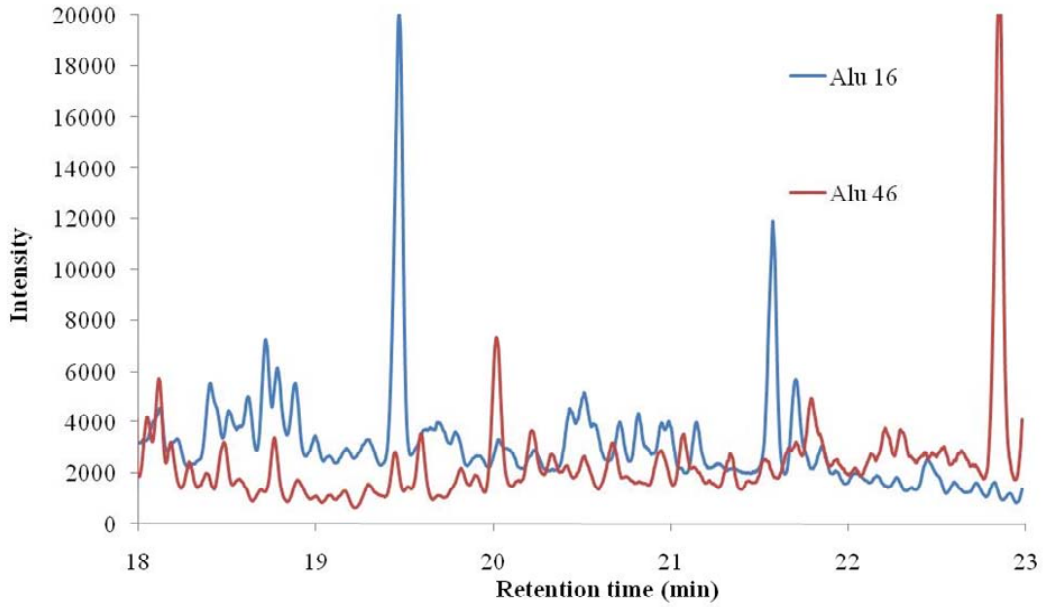

Figure 6.5. GC chromatograms for Hydrotex Alu 16 and Alu 46 components (between 18.0-23.0 minutes).

As can be seen from the Alu 16 chromatogram, there are two distinct peaks around 19.5 minutes and 21.5 minutes which are not seen in other Alu components. Because it was not possible to separate Alu components, chromatographic analysis of these components were performed as total Alu (Alu 46, Alu 100, 220, 320, and 460) and as Hydrotex Alu 16.

Figure 6.6 shows chromatograms of real process samples taken from C1, C2, C3, FH1, and SH1 production lines.

When the whole chromatogram is examined it is not possible to visually observe the peaks for Alu components since the main Linpar peaks dominating the chromatogram. However, when the intensity scale for those components were adjusted, it is clear that the real process samples do contain the possible contaminant peaks. As a result, this profile illustrates that the determination of contaminants in real samples could be possible by using GC technique.

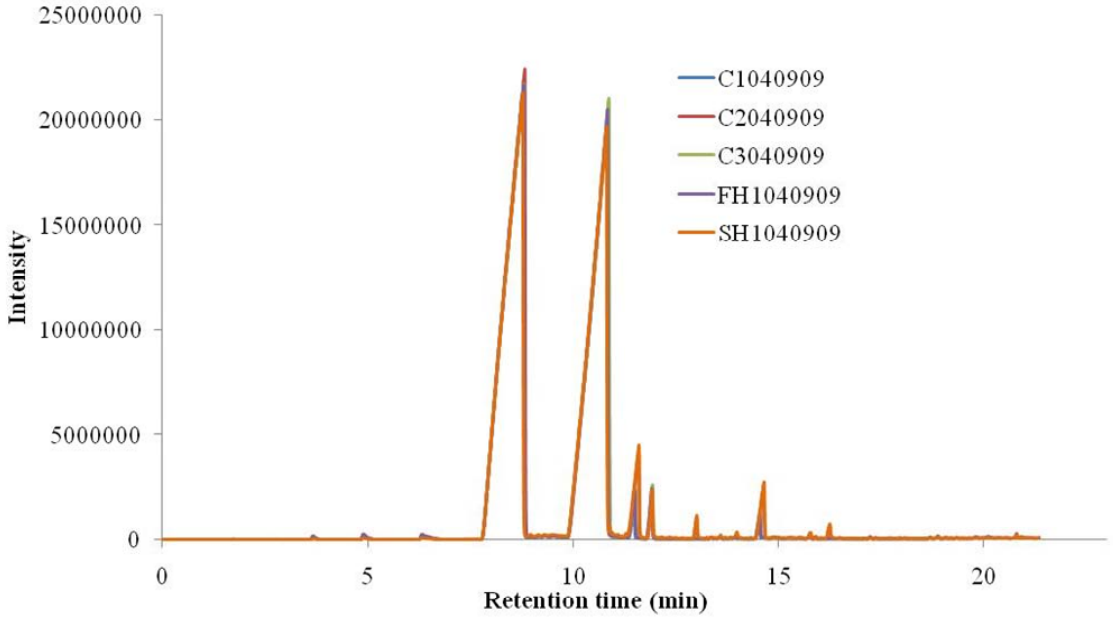

(a)

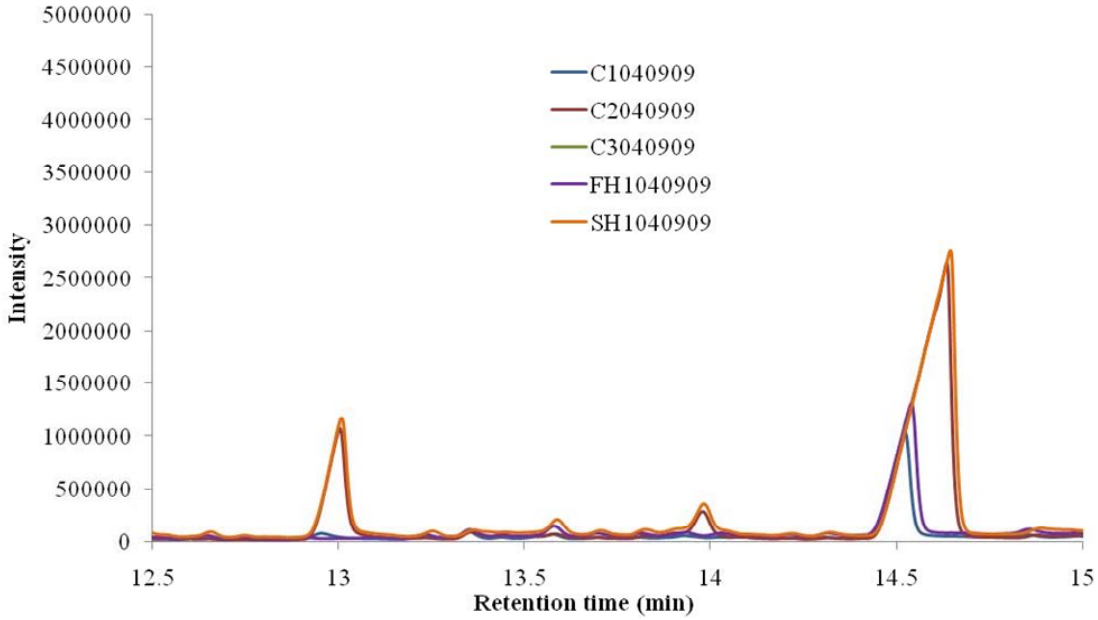

(b)

Figure 6.6. GC chromatogram of real samples within the retention times (a) 0.0–23.0 minutes, (b) 12.5–15.0 minutes.

The chromatographic profiles illustrate that Recompound Alu series oils (Alu 100, 220, 320 and 460) have very identical chemical composition giving very similar chromatograms, with an intense peak at around 17.63 minute. This makes it impossible to identify the Recompound Alu series (Figure 6.7).

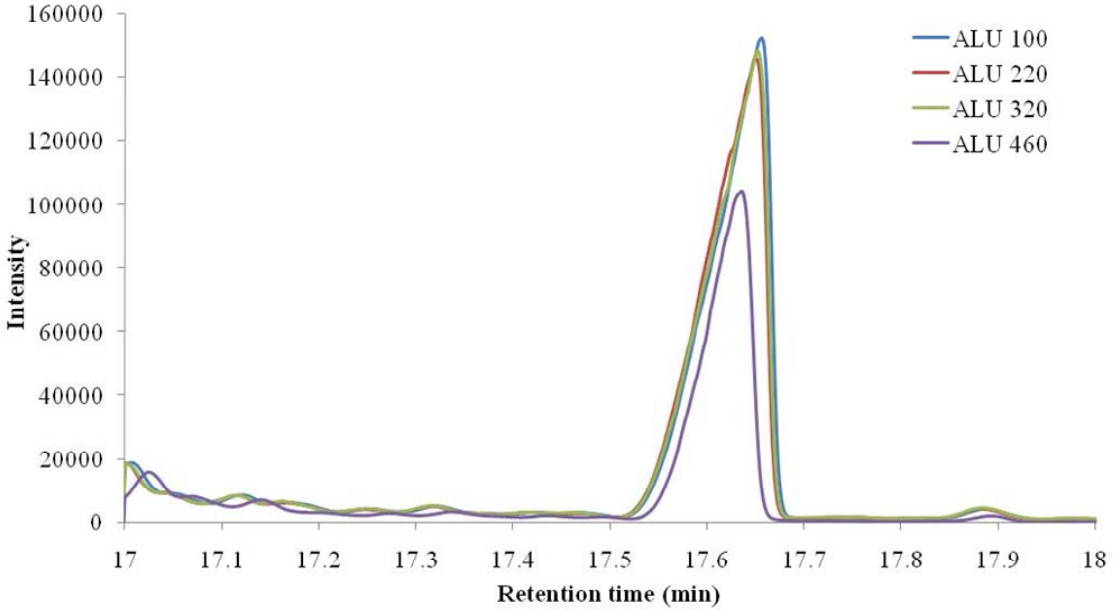

Figure 6.7. GC chromatograms for Alu 100, Alu 220, Alu 320, and Alu 460 components between 17.0 and 18.0 minutes retention times.

When the contaminant chromatograms are investigated, it is obvious that good separation cannot be established for all of the components.

On the other hand, only one of the Hydrotex Alu series compounds (Alu 16, and Alu 46), Alu 16 can be distinguished. There is an intense peak for Alu 16 component at a retention time of 21.5 minutes (Figure 6.8). This peak does not overlap any other component peaks so that making it possible to use for quantification.

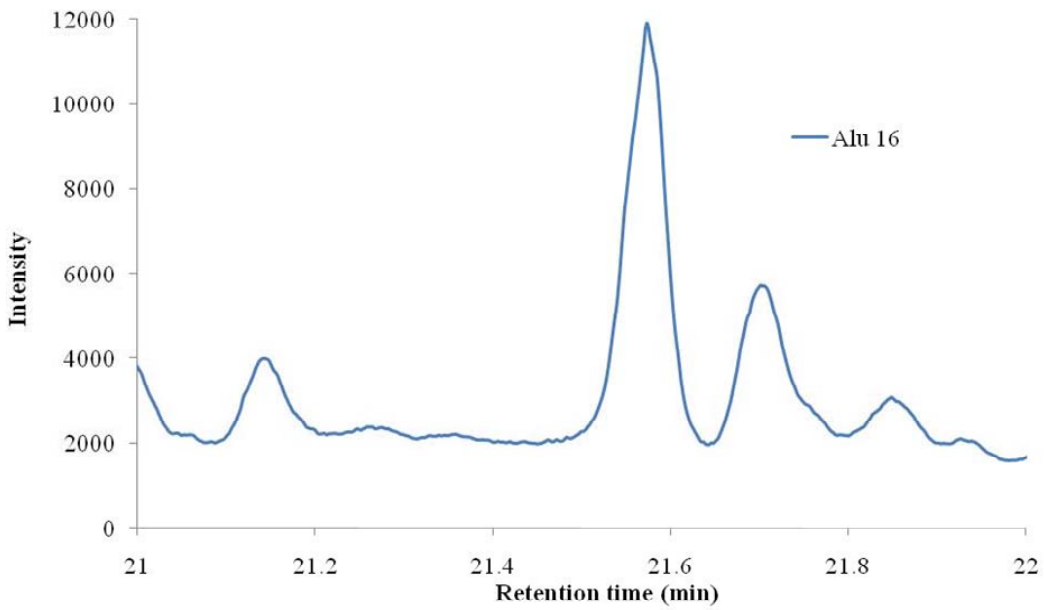

Figure 6.8. GC chromatogram for Alu 16 component between 21.0 and 22.0 minutes retention times.

For this reason, Alu 16 standards were prepared between a concentration range of 0.1% (w/w %) and 5.0% (w/w %) (Table 6.1).

Table 6.1. Concentrations of Hydrotex Alu 16 standards (w/w %).

Sample	Hydrotex Alu 16 Concentrations (w/w %)
1	0.1553
2	0.5258
3	1.0099
4	2.0118
5	2.9959
6	4.0087
7	4.9697

Although the peaks at 19.5 minute are much more intense than that of 21.5 minute peaks, it is not appropriate to use 19.5 minute peak, because it overlaps with another components (Alu 46, Figure 6.8) peak. Therefore calibration model for Alu 16

component is built due to 21.5 minute peak, using the peak areas. The calibration model is constructed for Hydrotex Alu 16 standards (Figure 6.9). As can be seen from the figure, the model seems to be quite successful with an R^2 value of 0.9988.

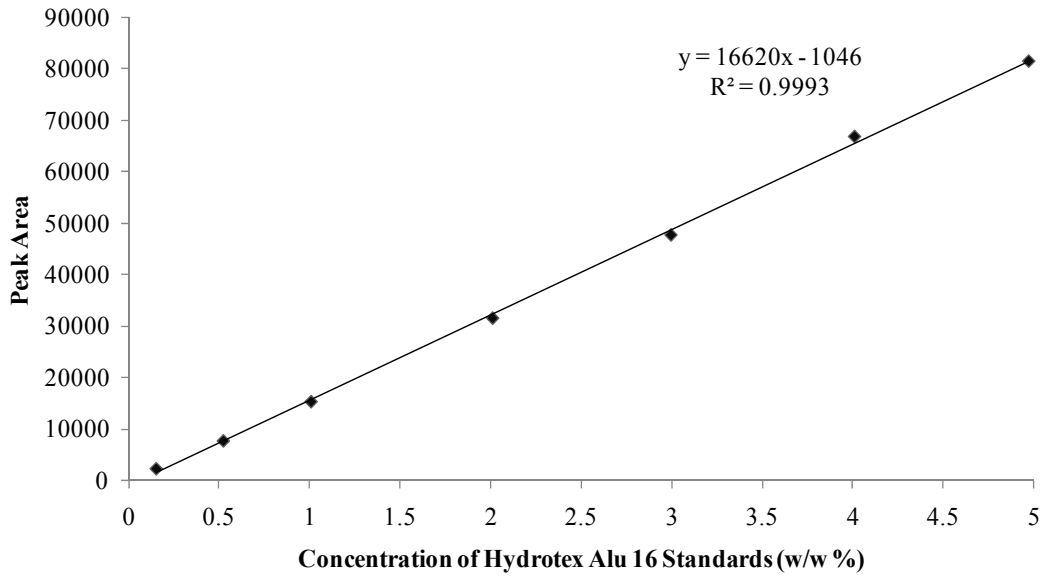

Figure 6.9. Calibration curve for Hydrotex Alu 16 component.

The real samples collected from 10 different process systems were analyzed. The calibration model was used to calculate the Alu 16 amount in the real samples. Figures below show the graphical distribution of predicted concentrations for the 10 different type of process samples which are C1, C3 (Figure 6.10), FH1, FH2, FH3, and FH4 (Figure 6.11), and C2, C4 (Figure 6.12), SH1 and SH2 (Figure 6.13), respectively. The predicted concentrations vary between 0.16% and 0.42% (w/w %) for C1, C3 samples, and between 0.09 and 0.49% (w/w %) for FH1 and FH2, FH3 and FH4 and between 0.07 and 0.77% (w/w %) for C2, C4, SH1 and SH2 samples.

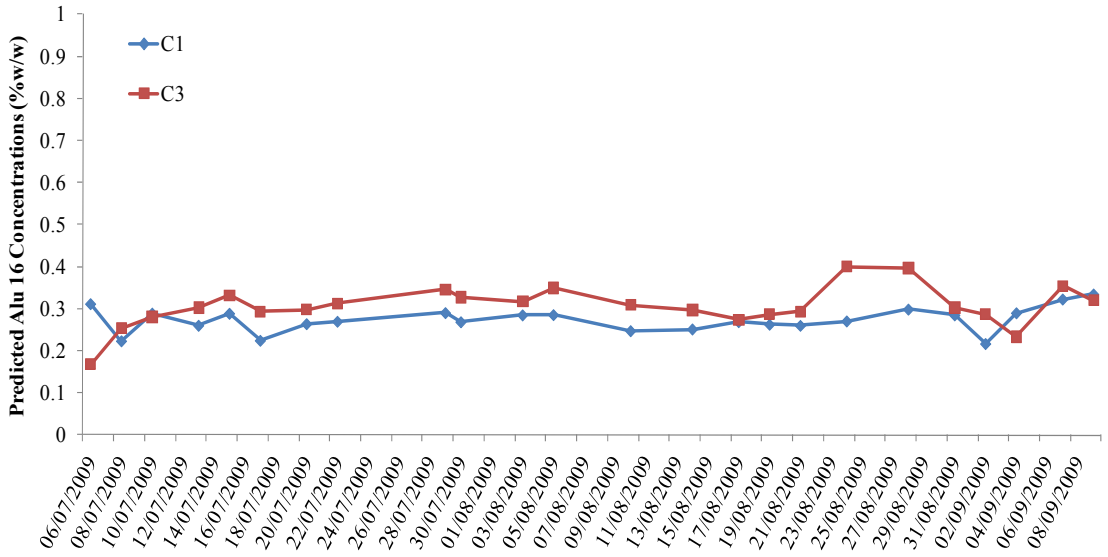

Figure 6.10. The predicted Hydrotex Alu 16 concentrations for the C1, C3 real process samples collected and analyzed in July, August, and September 2009.

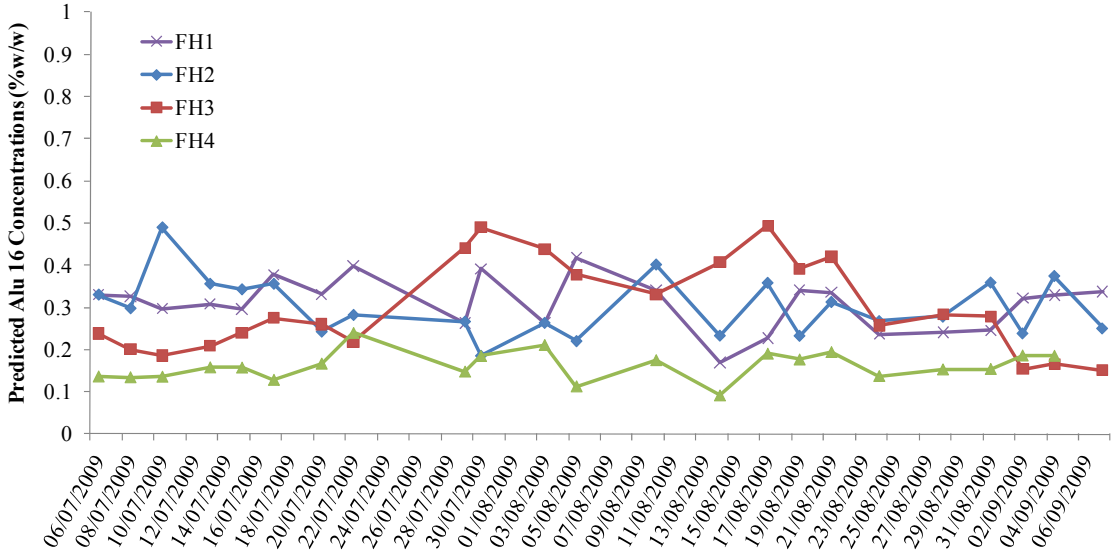

Figure 6.11. The predicted Hydrotex Alu 16 concentrations for the FH1, FH2, FH3, and FH4 real process samples collected and analyzed in July, August, and September 2009.

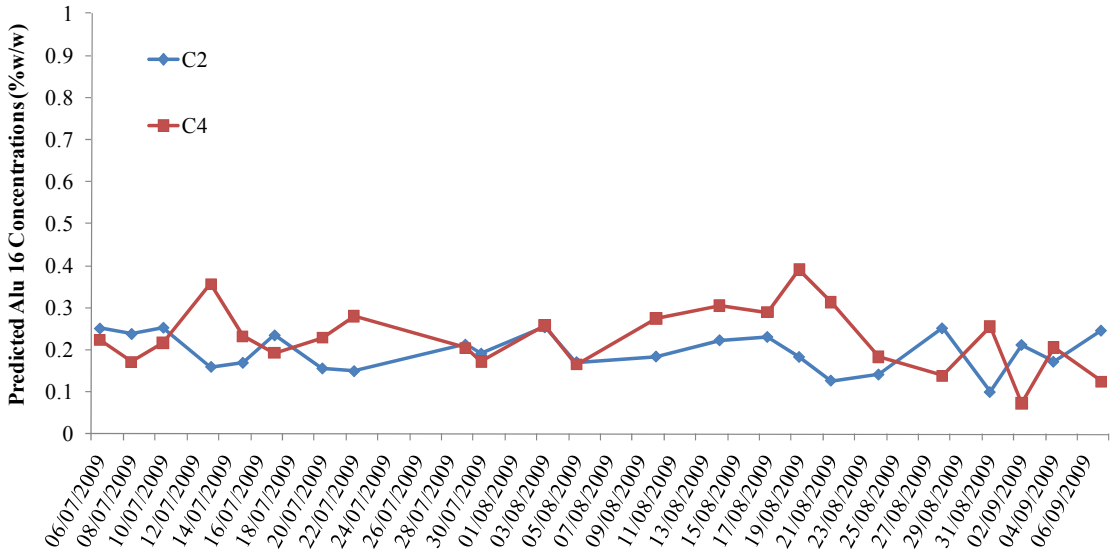

Figure 6.12. The predicted Hydrotex Alu 16 concentrations for the C2, C4, real process samples collected and analyzed in July, August, and September 2009.

,

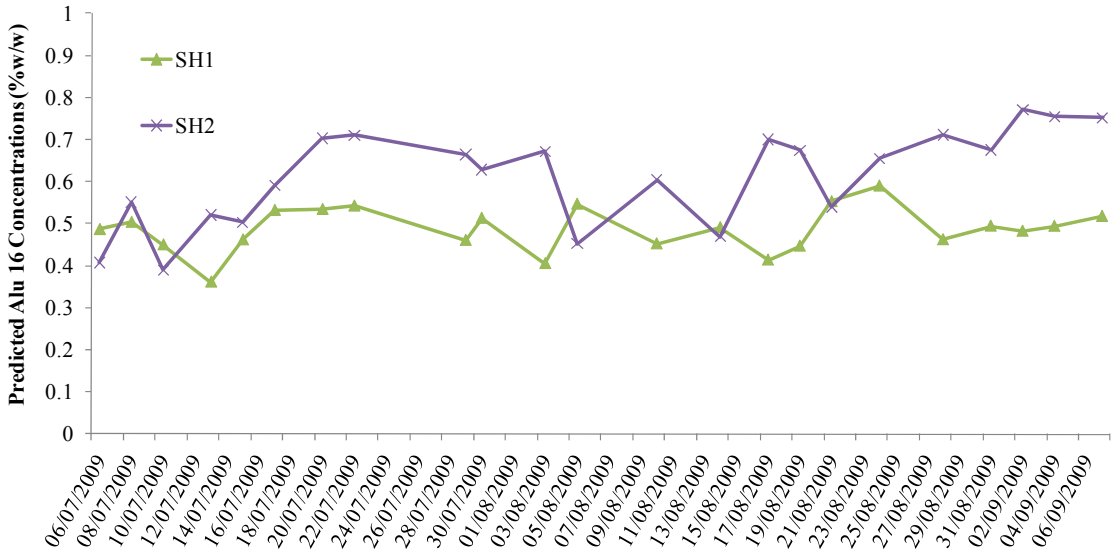

Figure 6.13. The predicted Hydrotex Alu 16 concentrations for the SH1 and SH2 real process samples collected and analyzed in July, August, and September 2009.

Another Hydrotex component is Alu 46. However, as mentioned before, all the components, especially the Alu series follow very similar trends so that it could not be possible to distinguish Alu 46 chromatographically.

Alu 46 has no specific and intense peak to be identified in the real process samples. For this reason, Alu 46 was analyzed with Recompound Alu series in total Alu amount in the samples.

Since Recompound Alu series and Hydrotex Alu 46 component shows the similar chromatographic profiles, Alu impurities in the lubrication systems can be detected totally. Due to this reason, a five-component stock solution including Recompound Alu 100, 220, 320 and 460 and Hydrotex Alu 46, is prepared.

Eight calibration standard solutions from this stock are also prepared between a concentration range of 0.33% and 10.01% (w/w %) (Table 6.2).

Table 6.2. Concentrations of total Alu standards (w/w %).

Sample	Total Alu Concentrations (w/w %)
1	0.3382
2	0.7166
3	1.3680
4	2.4199
5	3.7702
6	5.0105
7	7.5441
8	10.0143

Total Alu standards having identifiable peaks between 15.00 and 21.00 minutes are linearly related with concentrations (Figure 6.14). Especially 15.73 minute peaks are chosen for the construction of the calibration models. Figure 6.15 illustrates the calibration curves constructed by using the peak areas at the related retention times.

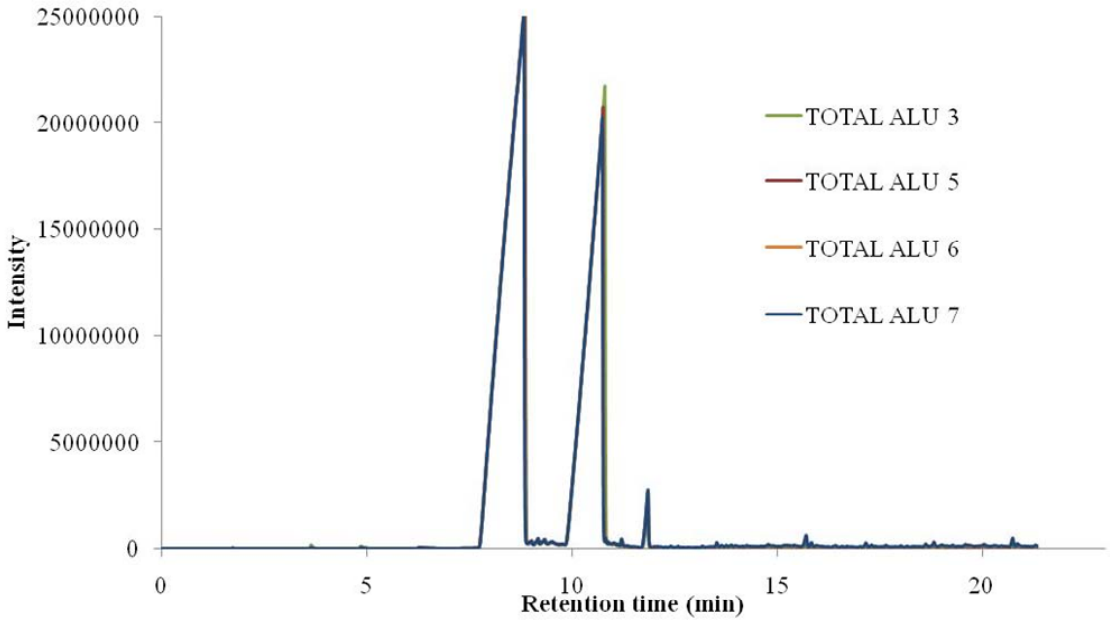

(a)

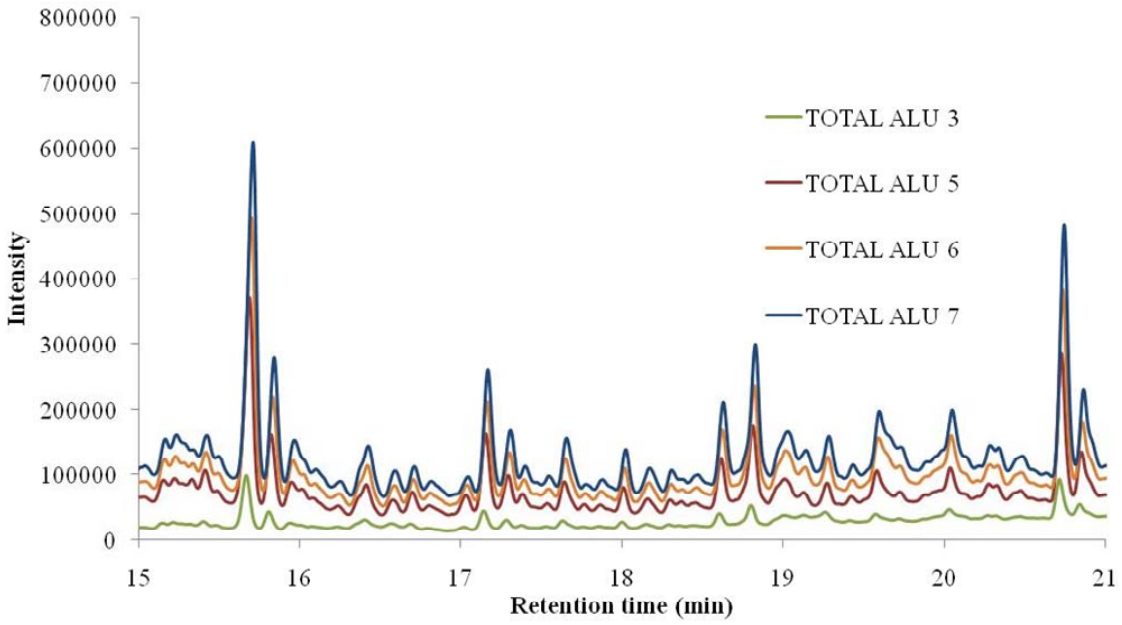

(b)

Figure 6.14. GC Chromatograms of Total Alu standards, (a) between the retention times 0.0–23.0 minutes, and (b) between the retention times 15.0–21.0 minutes.

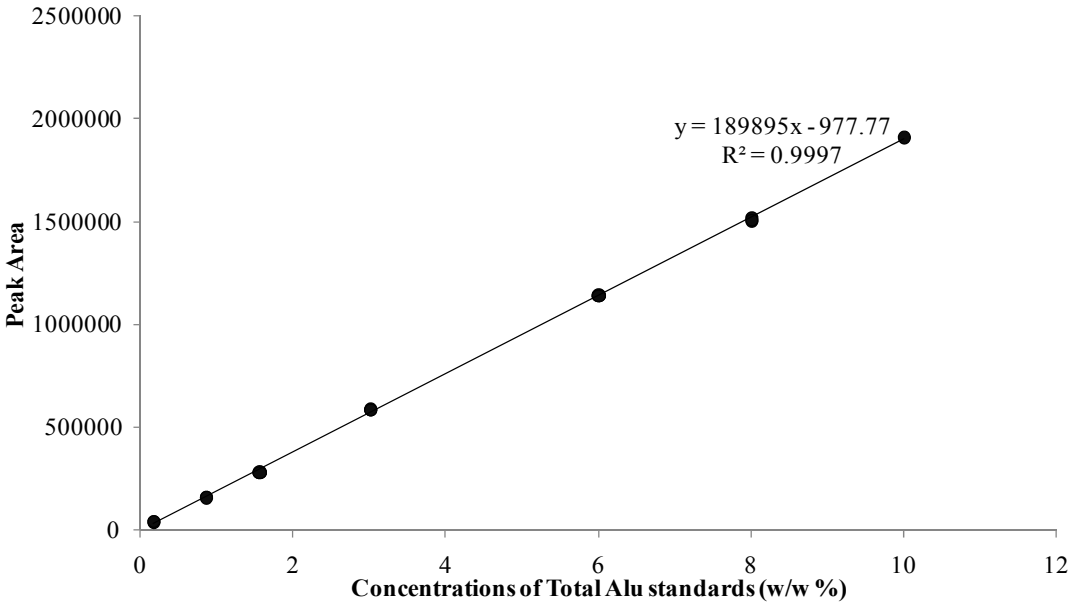

Figure 6.15. Calibration curve for Total Alu standards at 15.73 minute peak.

The R^2 values for those calibration curves which are constructed by using the 15.73 and 20.77 minute peaks are satisfactory. Since 15.73 minute peak give a better calibration plot, the total Alu amount in the real process samples are predicted using the 15.73 minute peaks.

Figures below illustrate the line graphs of predicted concentrations of the real process samples collected and analyzed in July, August and September 2009.

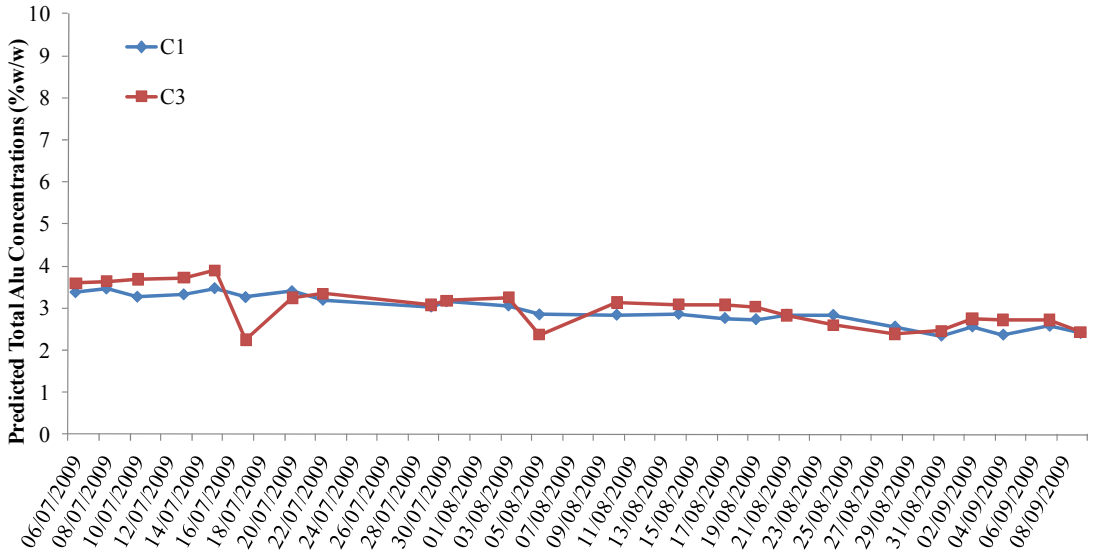

Figure 6.16. The predicted total Alu concentrations for the C1, C3 real process samples in July, August and September 2009.

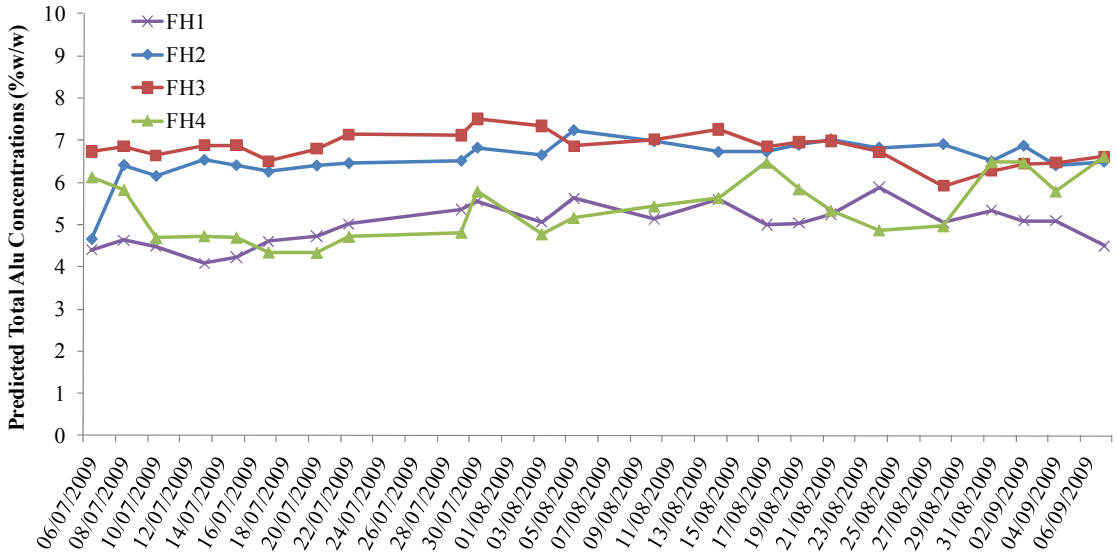

Figure 6.17. The predicted total Alu concentrations for the FH1, FH2, FH3, and FH4 real process samples in July, August and September 2009.

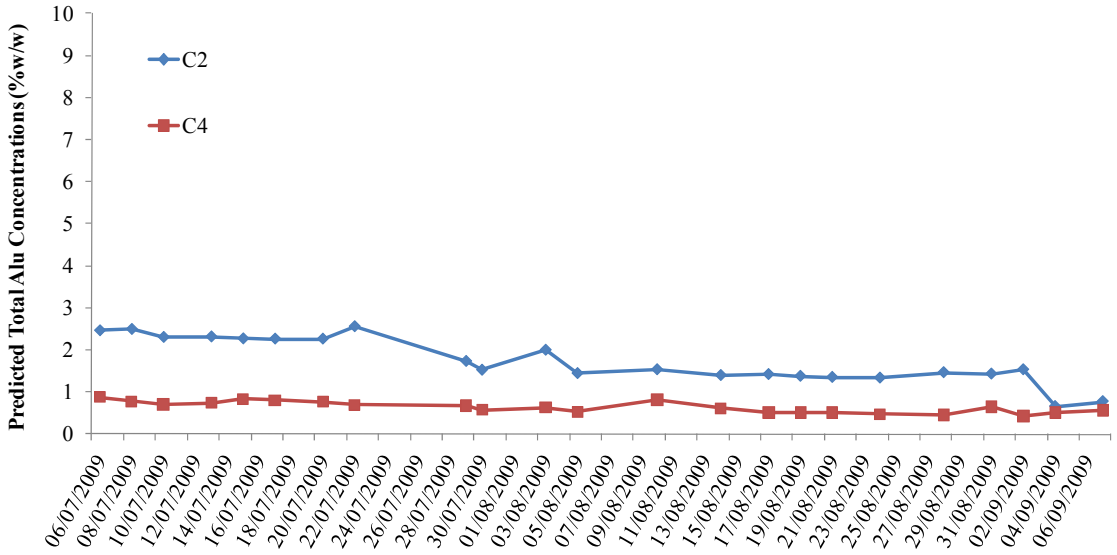

Figure 6.18. The predicted total Alu concentrations for the C2, C4 real process samples in July, August and September 2009.

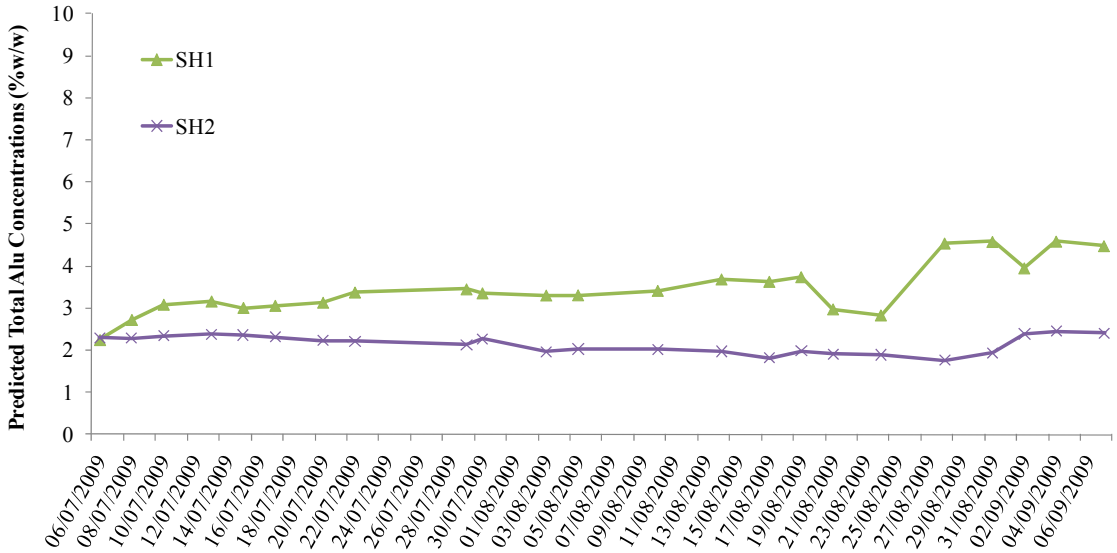

Figure 6.19. The predicted total Alu concentrations for the SH1 and SH2 real process samples in July, August and September 2009.

The results show that the total Alu amount for C1, C3, (Figure 6.16) varies between 2.25%–5.88% (w/w %), for FH1, FH2, FH3 and FH4 (Figure 6.17) system samples is around 4.33% to 7.50% (w/w %). In C2, C4, (Figure 6.18) and SH1 and

SH2 (Figure 6.19) system samples this amount is predicted between a range from 0.42% and 4.59% (w/w %). Those amounts are acceptable for the production.

FH2, FH3, FH4, system samples have the highest amount of total Alu which varies between 4.33% and 7.50% (w/w %) from time to time. This means that an intervention is necessary on the spraying amount of mechanical cooling lubricants On the other hand; the total Alu amounts in C2, C4, SH1 and SH2 system samples are 0.42% and 4.59% (w/w %), respectively.

Through the contaminant analysis, it is clearly seen that the mechanical cooling lubricants which cause the contamination should be controlled. The reason of the fluctuation in those line plots can be described as the effect of change in the oils. In other words fresh mechanical cooling lubricants are added in those huge tanks in the plant. Those fluctuations prove this statement.

6.1.2. Additive Analysis

The additives are used for maintaining the permanent lubrication. Nafol and Cindolube are used for this purpose in aluminum production systems. For good quality products the amounts of these additives should be controlled. The tolerable limits for those additives are 0.7-1.0% (w/w %) for foil production systems and 4.0-6.0% (w/w %) for sheet production systems, which are accepted and used in ASSAN Aluminum.

Table 6.3 represents the concentrations of Nafol and Cindolube standards which were used to build the calibration model for each additive component. The gas chromatographic analysis of Nafol and Cindolube additives was done. Initially calibration standards were prepared and analyzed.

Table 6.3. Concentrations of Nafol and Cindolube standards (w/w %) used in GC analysis

Sample	Nafol concentration (w/w %)	Cindolube concentration (w/w %)
1	0.2125	2.0141
2	0.5065	4.9415
3	0.7026	6.0050
4	1.0036	8.0000
5	1.2635	10.0170
6	1.5105	
7	2.0022	

The figures below represent the gas chromatographic profile for Nafol and Cindolube standards (Figure 6.20 and Figure 6.21).

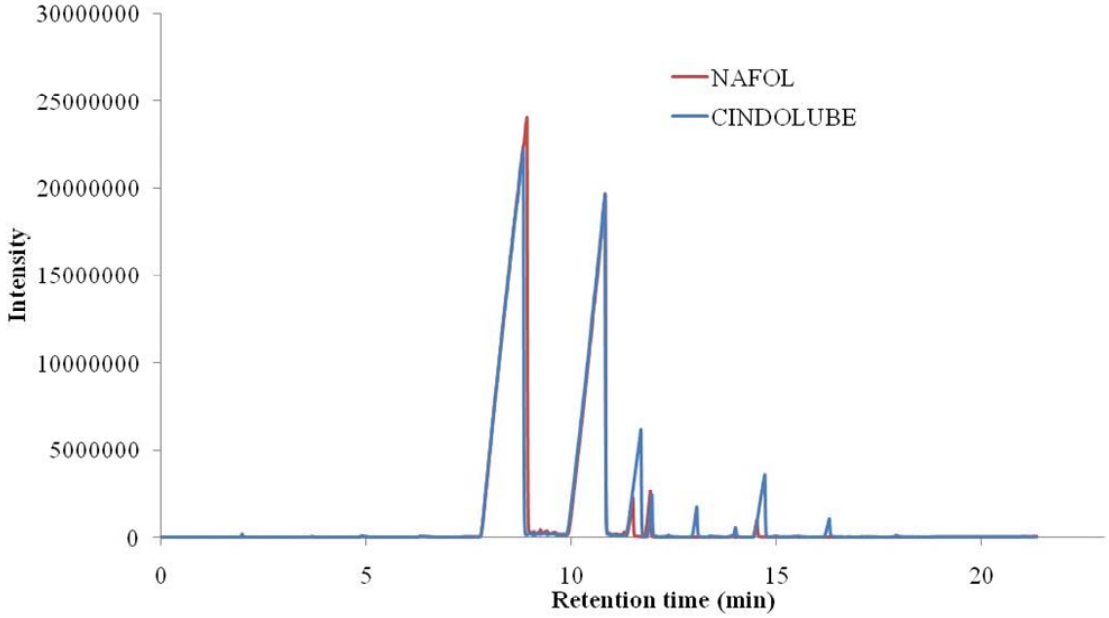

Figure 6.20. GC chromatograms of Nafol and Cindolube standards between retention times of 0.0-23.0 minutes.

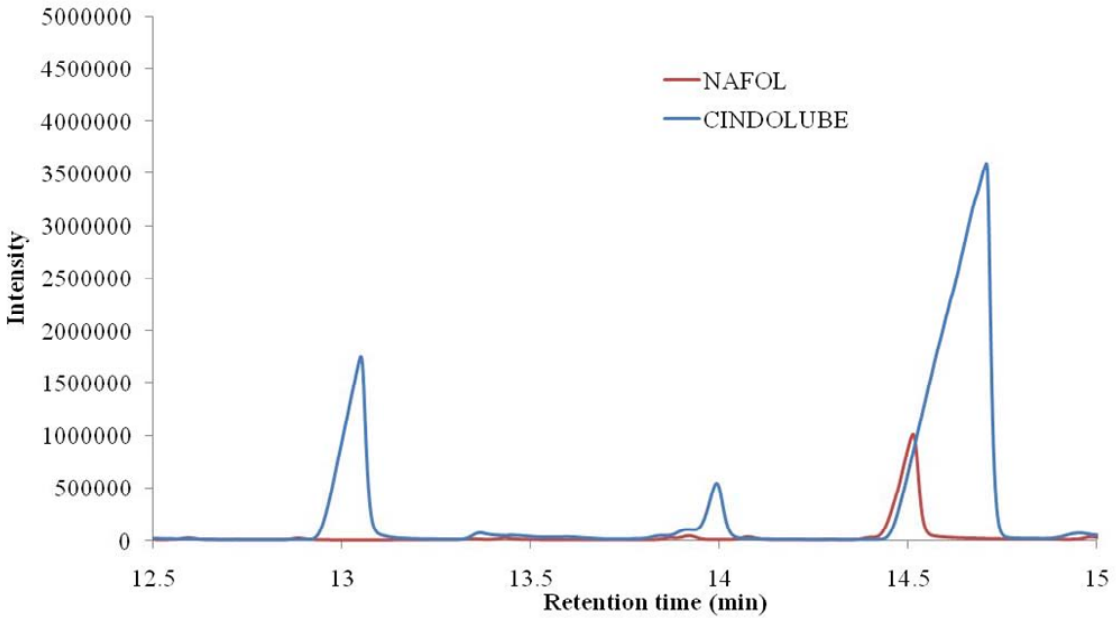

Figure 6.21. GC chromatograms of Nafol and Cindolube standards between retention times of 12.5- 15.0 minutes.

Cindolube additive gives a characteristic peak not only at around 12.99 minute, but also at around 13.80 and 14.50 minutes. On the other hand Nafol additive also give a characteristic peak at around 14.50 minute. Apparently, both of these additives represent similar chromatographic profiles, because they have very similar compositions except Cindolube contains some different material which is not clarified by the producer company. However in real process samples, these additives are not used at the same time, meaning that the samples which include Nafol additive, does not include Cindolube. Thus, for the construction of the calibration models, 14.5 minute peaks, and 12.99 minute peaks are used for Nafol and Cindolube, respectively.

Figure 6.22 and Figure 6.23 represents the chromatographic profiles for the samples containing Nafol additive which are collected from C1 and FH1 production lines. Since those samples have intense peaks at 14.5 minute, it supports the claims that these peak areas are possible to use for the construction of the calibration models.

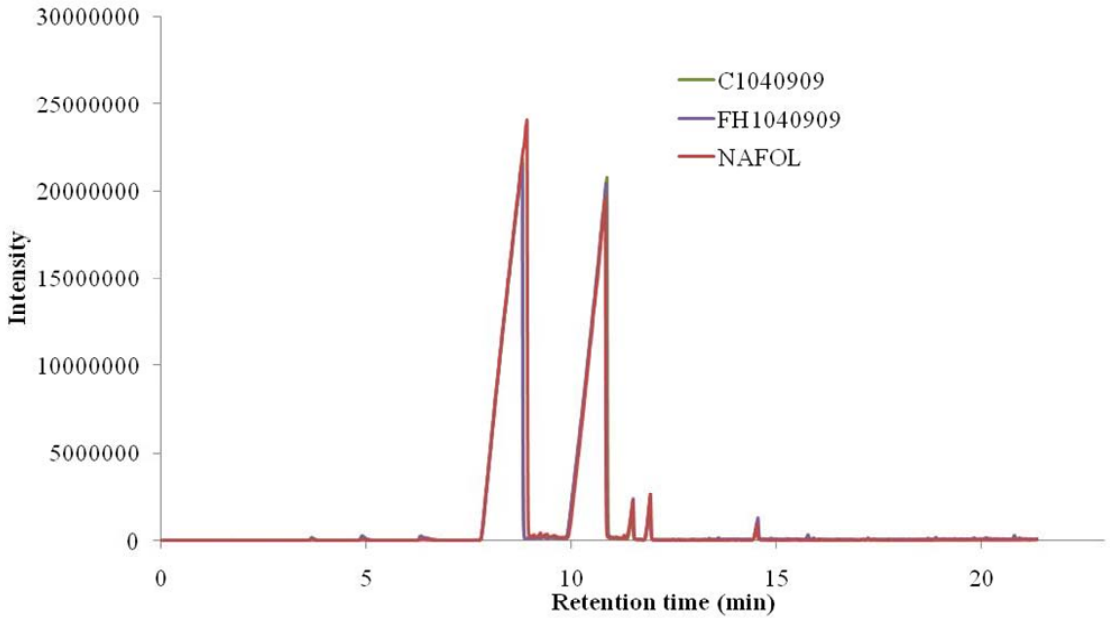

Figure 6.22. GC chromatograms of Nafol standard with real samples between retention times 0.00-23.00 minutes.

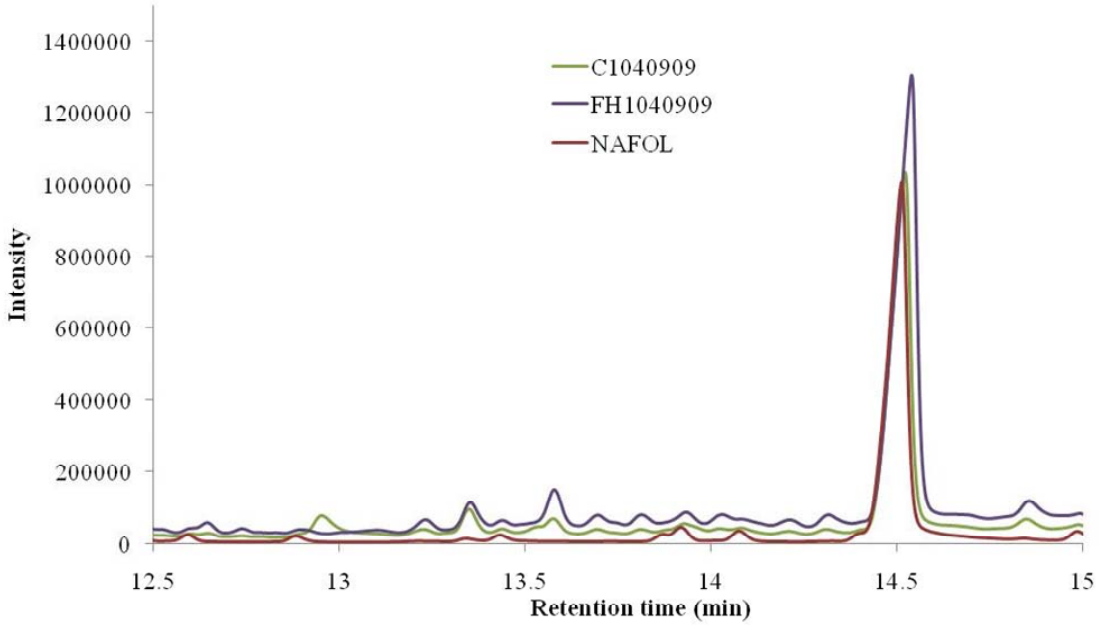

Figure 6.23. GC chromatograms of Nafol standard with real samples between retention times 12.5 and 15.0 minutes.

Figure 6.24 and Figure 6.25 represents the chromatographic profiles for the samples containing Cindolube additive which are collected from C2 and SH1 production lines. Since those samples have intense peaks at 12.99 minute, it supports the claims that these peak areas are possible to use for the construction of the calibration models.

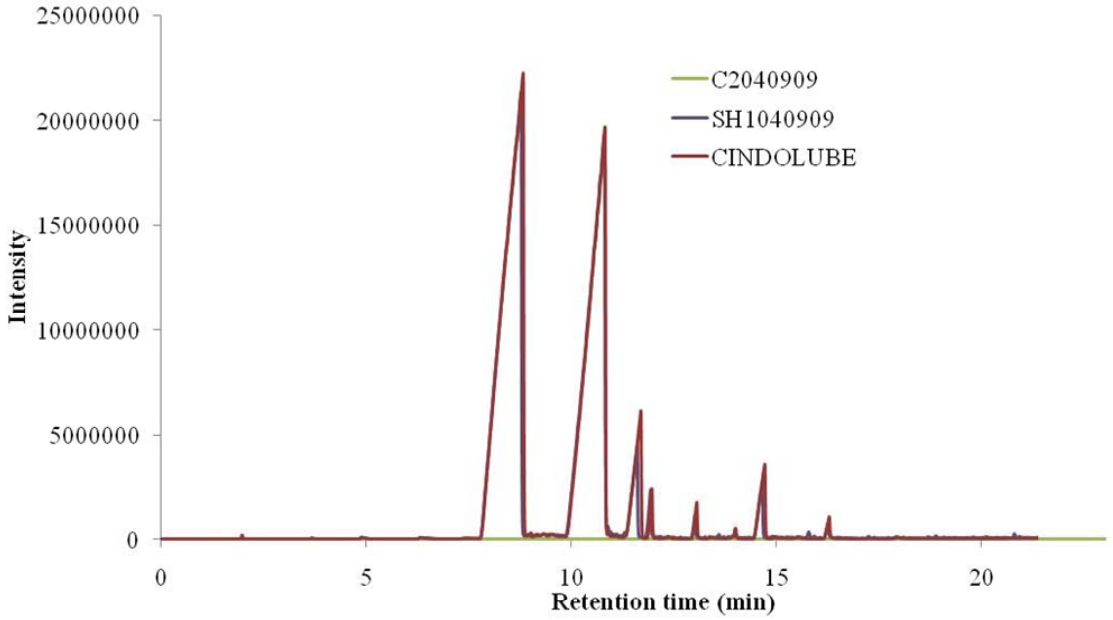

Figure 6.24. GC chromatograms of Cindolube standard with real samples between retention times 0.0 and 22 minutes.

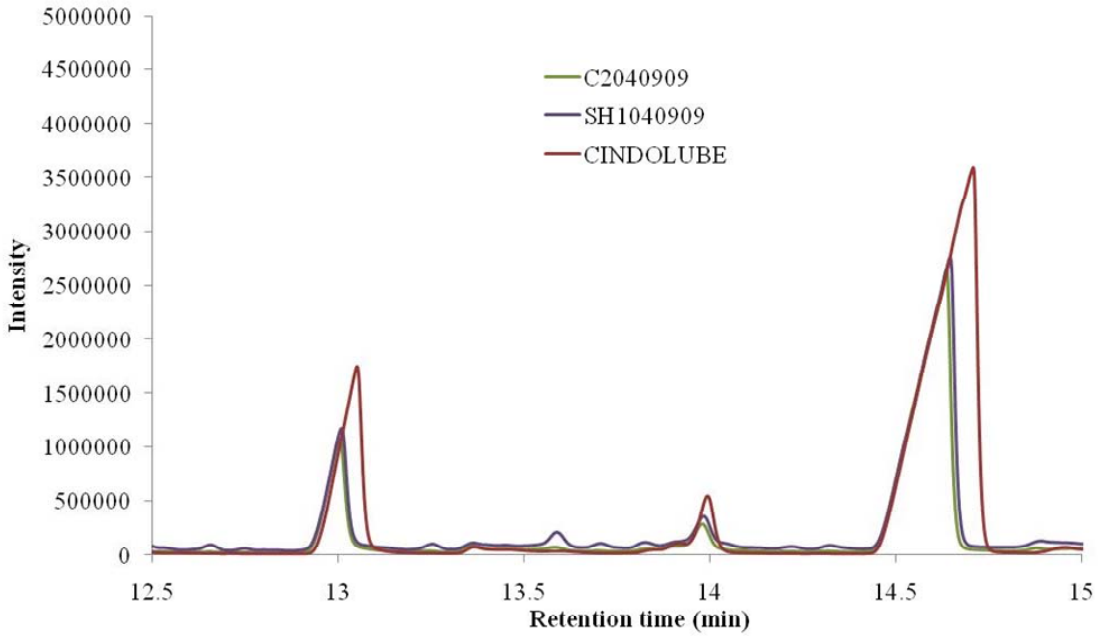

Figure 6.25. GC chromatograms of Cindolube standard with real samples between retention times 12.5 and 15.0 minutes.

After deciding which peak to use, the calibration models were built for each component. As indicated before, 12.99 and 14.50 minute peaks are used for Nafol and Cindolube, respectively. R^2 values illustrate that successful calibration model for Nafol can be constructed (Figure 6.26).

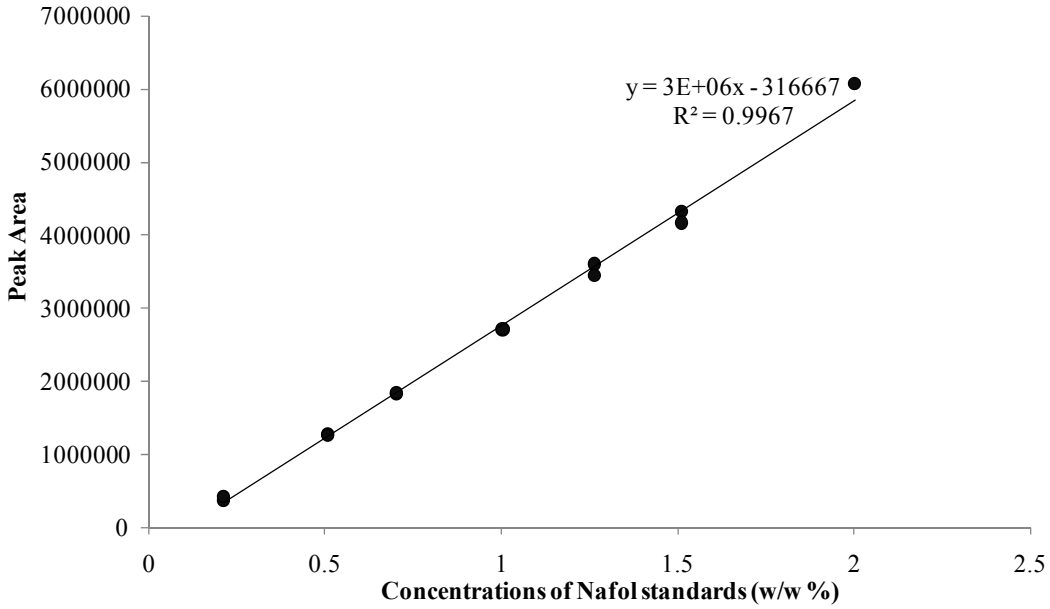

Figure 6.26. Calibration curve for Nafol standards.

Using the above calibration models, real process samples which were collected in July, August and September 2009 were also analyzed. C1, C3, and FH1, FH2, FH3, and FH4 system samples which contain Nafol additive are illustrated in Figure 6.27 and Figure 6.28, respectively.

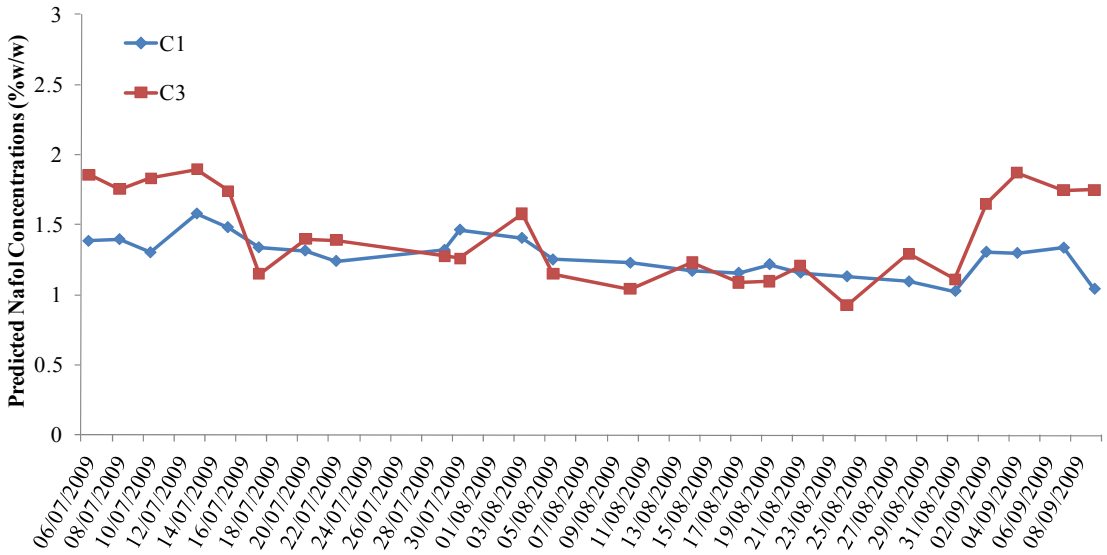

Figure 6.27. The predicted Nafol concentrations for the C1, C3 real process samples in July, August, and September 2009.

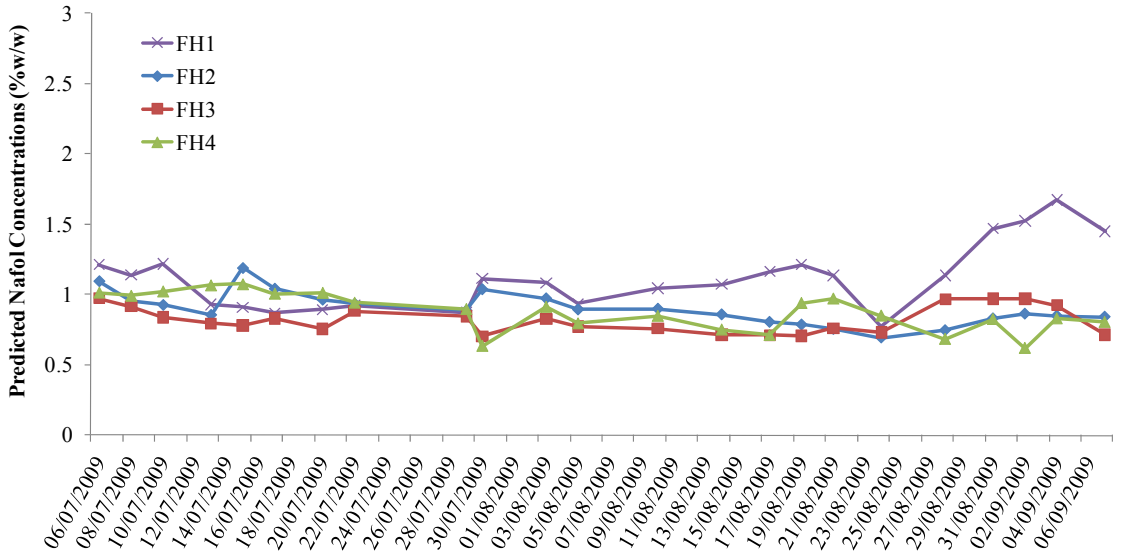

Figure 6.28. The predicted Nafol concentrations for the FH1, FH2, FH3, and FH4 real process samples in July, August, and September 2009.

The calibration curve for Cindolube additive is given in Figure 6.29. Using this curve equation, real process sample concentrations were also calculated. Figure 6.30 and Figure 6.31 is the graphical illustration of the predicted concentrations of the real samples in Cindolube containing systems which are C2, C4, and SH1, SH2, respectively.

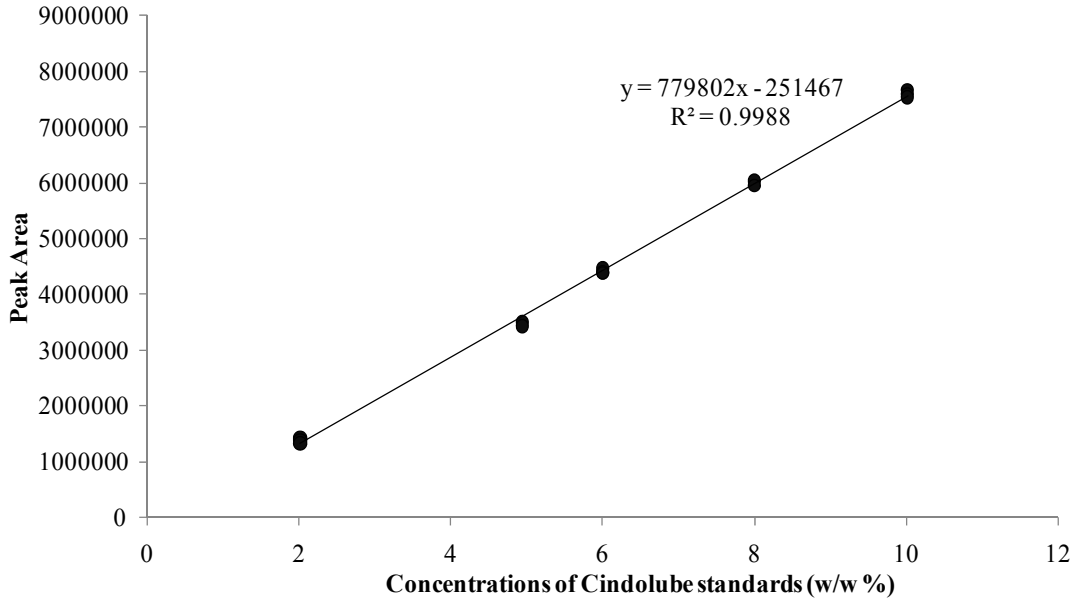

Figure 6.29. Calibration curve for Cindolube standards.

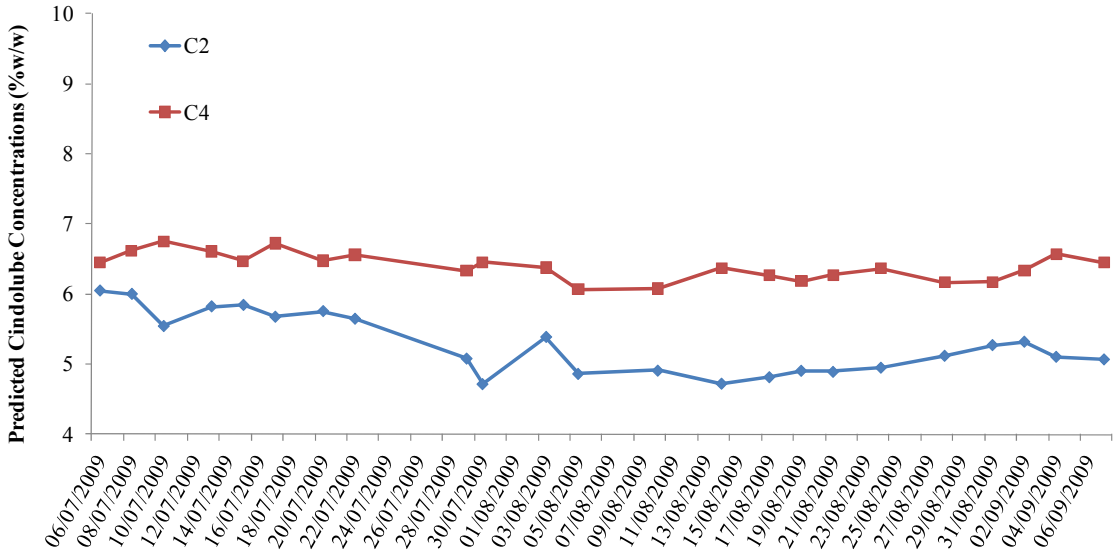

Figure 6.30. The predicted Cindolube concentrations for the C2, and C4 real process samples in July, August, and September 2009.

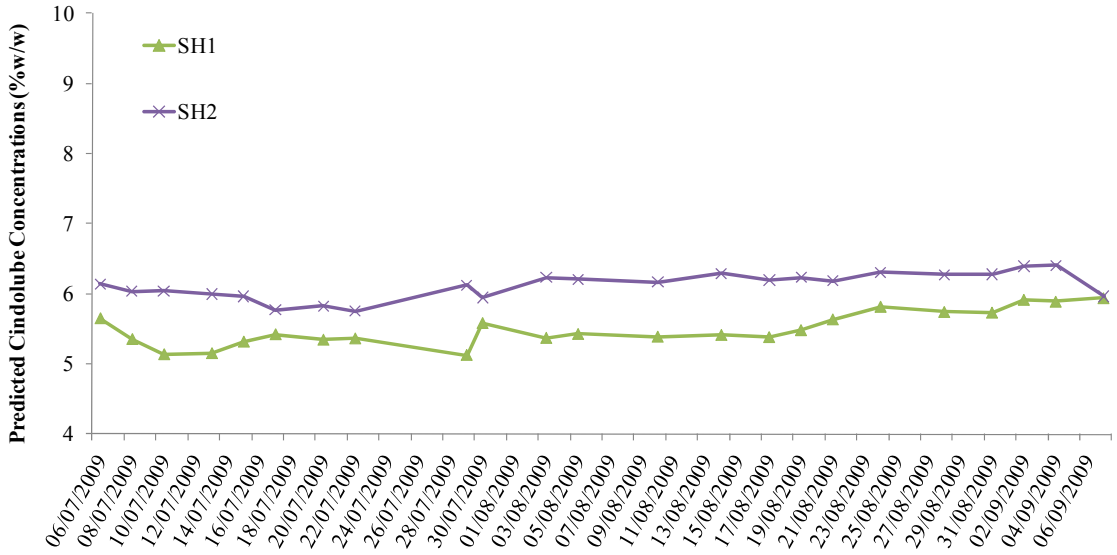

Figure 6.31. The predicted Cindolube concentrations for the SH1, and SH2 real process samples in July, August, and September 2009.

6.2. Fourier Transform Infrared (FTIR) Spectroscopic Analysis

The complex mixtures of the lubricating oils were analyzed by using FTIR. By using the spectra obtained from the spectroscopic analysis, calibration models were constructed for every component. Reference values are needed for the construction of the models using the multivariate calibration techniques. The reason is that the necessity of the knowledge about the composition and concentration informations. Those necessary reference values could be obtained by using two different ways. One is to prepare synthetic samples in laboratory conditions which mimics the real system and then those complex mixtures were subjected to the spectroscopic analysis, and the spectral data is then used for construction of the calibration models. However, there is a better way in which a reference analysis is used if there exists. In other words, the real samples are analyzed by the reference method, and regarding to the obtained results, the spectroscopic results, which were used for the construction of the calibration models, are then compared.

As indicated at the beginning of this chapter, GC is assigned as the reference method for the comparison of the GILS results which are acquired by using FTIR spectroscopic data. This section covers the investigation of the FTIR results combined

with GILS and also comparison with the reference technique: GC. The real process samples were all analyzed with FTIR and the spectral data matrices were used in GILS to predict both the contaminant concentration and the additive concentration. Those results obtained by using FTIR-GILS were compared with the reference method, GC. However, some of the contamination source components, such as Alu 46, Alu 320, and Alu 460, were analyzed only by FTIR spectroscopy, and the calibration models were built using the synthetic mixtures by GILS. Then the contamination in real samples was predicted.

Figures below show the spectra of the additive and contaminants in Linpar. Figure 6.32 illustrates the FTIR-ATR spectra of the additives and contaminants, whereas Figure 6.33 shows the real samples' spectra before eliminating the noisy regions. Finally, Figure 6.34 shows the real samples' spectra after eliminating the noisy regions. The FTIR-ATR technique was used at first, in order to observe the spectroscopic profiles of the additives, contaminants and the real process samples. However the spectra did not provide efficient information especially for the real samples. Thus the FTIR measurements were carried out by using a teflon liquid cell, with a window material KBr. The pathlength is maintained by using spacers of 0.5 mm.

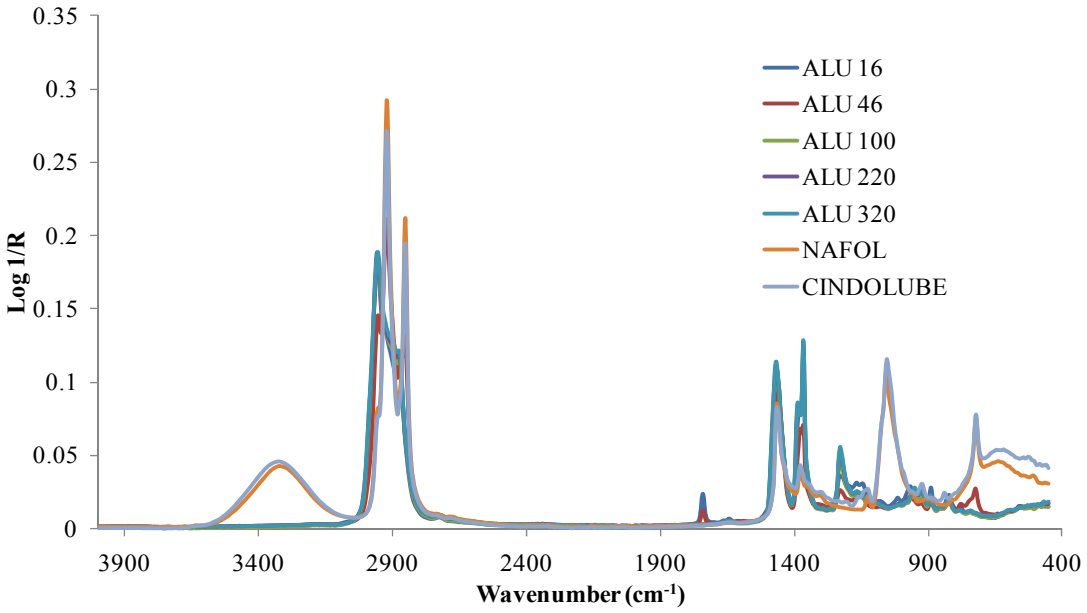

Figure 6.32. ATR-FTIR spectra of the contaminants and additives.

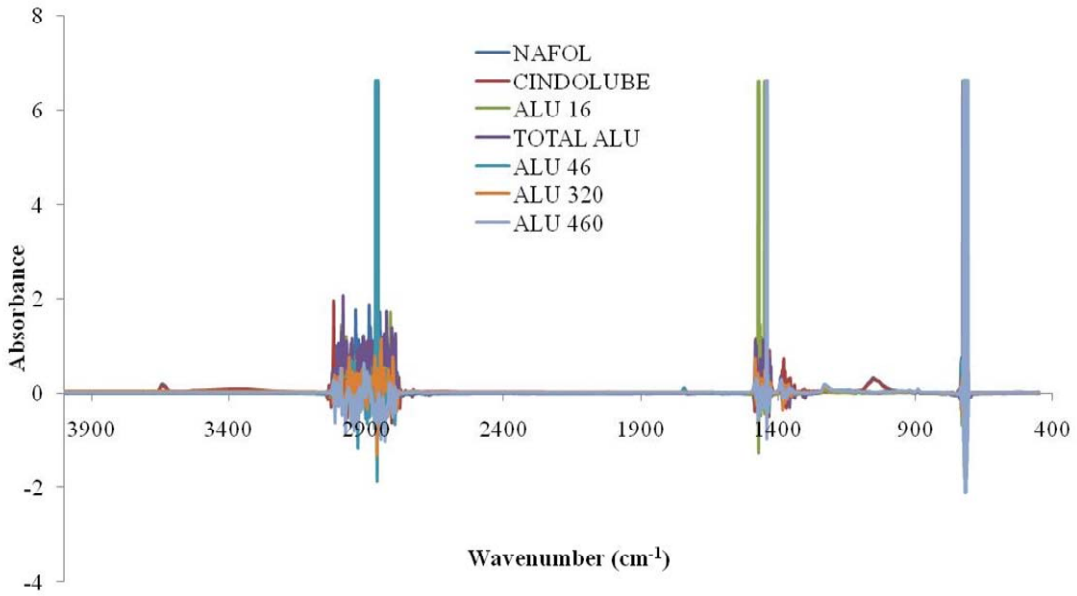

Figure 6.33. The original FTIR spectra of the contaminants and additives taken with liquid cell.

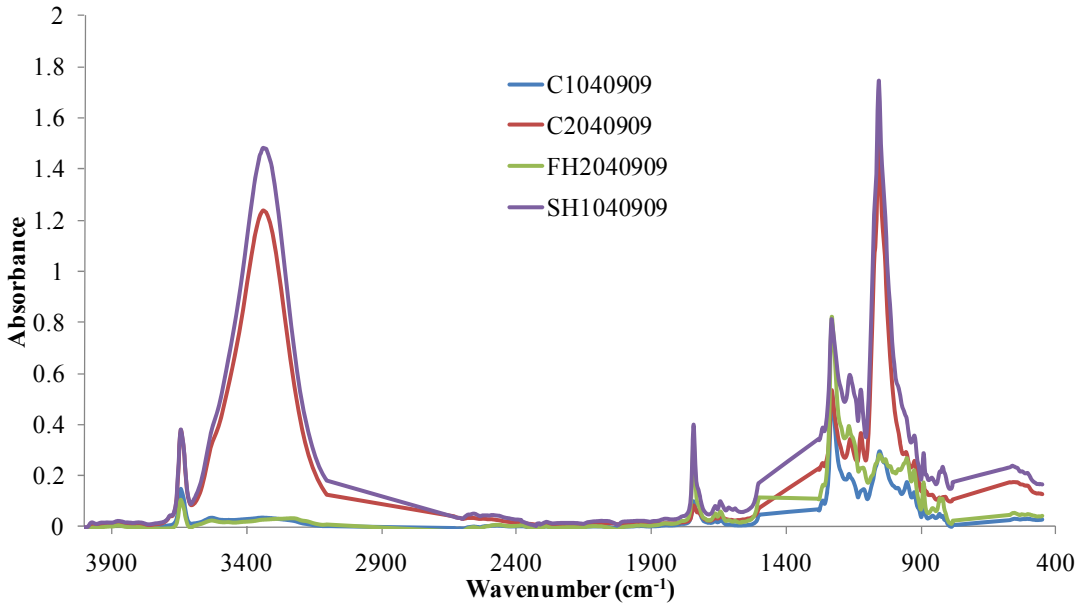

Figure 6.34. The FTIR spectra (with liquid cell) of the real process samples after eliminating the noisy regions.

During the spectroscopic analyses, since Linpar is used as base oil for lubrication objectives in all process systems, all spectra should be recorded after Linpar is measured as a blank. As a result of using Linpar as background, all the other impurities in real process samples might be eliminated and clear illustration of the pure component peaks is tried to be provided (Figure 6.35). Although the blank solution is Linpar, another point that should still be taken into consideration is that the percent weight of Linpar in both synthetic standards and process samples is around 90% (w/w %). Hereby, when the blank spectra are subtracted from the real sample spectra, some negative intensities and noisy regions are observed. Thus, these regions are eliminated and then GILS is applied for the construction of calibration models.

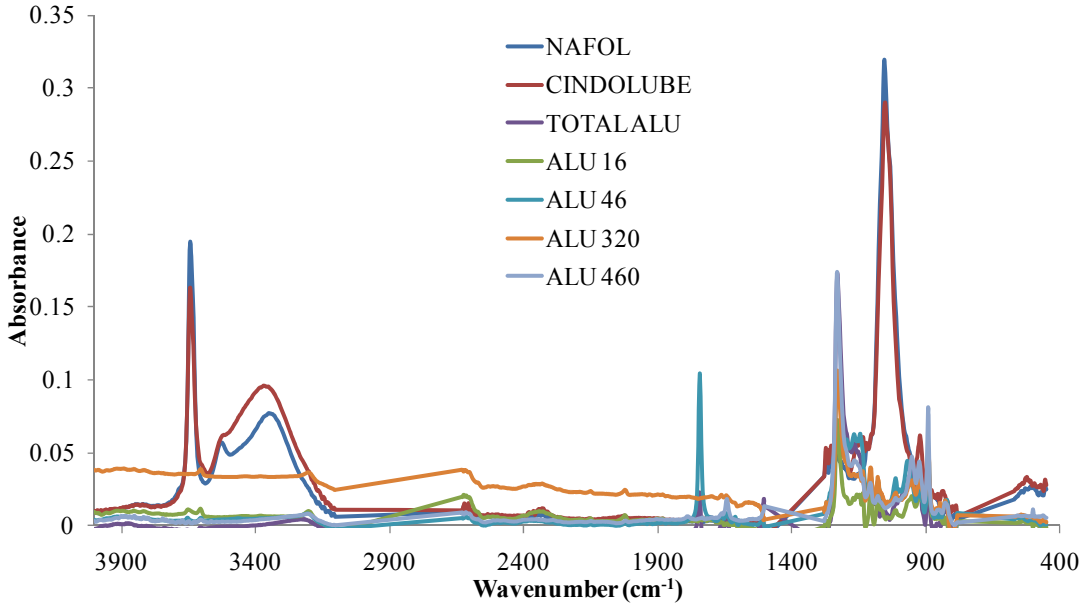

Figure 6.35. The FTIR spectra of the contaminants and additives after eliminating the noisy regions.

The reason of those noisy regions appears is that the Linpar is used as background. However, as mentioned before, the samples contain a large amount of Linpar (around 90.00% (w/w %)), but still not the same as pure Linpar which is used as background. Therefore, the noisy regions are eliminated in real samples, also. The regions which were eliminated are listed in Table 6.4 It can be seen that the eliminated wavenumber ranges are the ones where Linpar gives intense peaks. Thus when Linpar is

used as background, it means that a Linpar spectrum is subtracted from the other samples' spectra, so that a negative intensity is observed.

Table 6.4. The list of wavenumber regions that were eliminated.

	Wavenumber (cm^{-1})
1	3101-2629
2	1501-1279
3	781-570

After the noisy regions are subtracted, the spectra seem to be clearer (Figure 6.35). The peaks around 900 cm^{-1} wavenumber belongs to the Alu components causing the contamination, and can be assigned as the olefinic C-H bonds. The peak around 1050 cm^{-1} belongs to the Nafol and Cindolube components which are the additives having very identical compositions. The intense peaks belong to the C-O stretching in phenols or alcohols, since those additives contain fatty alcohols. The peak around 1230 cm^{-1} regarding to the Alu components, assigned as the O-H bending in alcohols and phenols. Since the Alu components contain sulfur and nitrogen in their composition, the peak around 1650 cm^{-1} can be defined as the N-H stretching in urethanes (R-O-CO-N). (Williams, Fleming 1995). Another peak regarding to Alu components is at around 1760 cm^{-1} wavenumber, which is possibly the carbonyl absorption. 3218 and 3790 cm^{-1} peaks belonging to Nafol and Cindolube, can be assigned as the N-H stretching in amide group (-CONH-) and O-H stretching, respectively (Vahaoja et. al. 2005).

On the other hand, since the real process samples have identical spectral profiles with very low concentration values, the visual interpretation will not be possible. Thus, the univariate calibration will not be a solution for the prediction of the contaminants and so for the additives. An alternative solution is using the multivariate calibration techniques in which the calibration models are constructed by taking the linear combinations of the information in a spectrum, relating them to the concentrations. However, there may be regions that do not have linear relationship with the concentration, or, there may be some noisy regions which prevent the construction of successful calibration models. In such situations, the spectral region which supplies the best correlation for the concentrations should be selected. Therefore, genetic algorithms

serve as a variable selection method. In this study, a genetic algorithm based inverse least squares method (GILS) which was developed by our research group was used for these purposes.

This section is also divided into sub-sections in which the GC-compared results for contaminants, Alu 16 and Total Alu, and additives, Nafol and Cindolube, where the calibration and prediction were both done with the real samples, and the FTIR-GILS results where the calibration model is constructed by using the synthetic samples of the contaminants Alu 46, Alu 320 and Alu 460, and the model is tested by the real samples.

6.2.1. Contaminant Analysis

Contaminants, Total Alu and Alu 16, were analyzed by using both GC and FTIR. The spectral data were used in GILS for the construction of the calibration model. Through the data analysis, the GILS was set to run 100 times with 50 iterations and 30 genes. Figure 6.36 represents the FTIR spectra of the Total Alu and real samples.

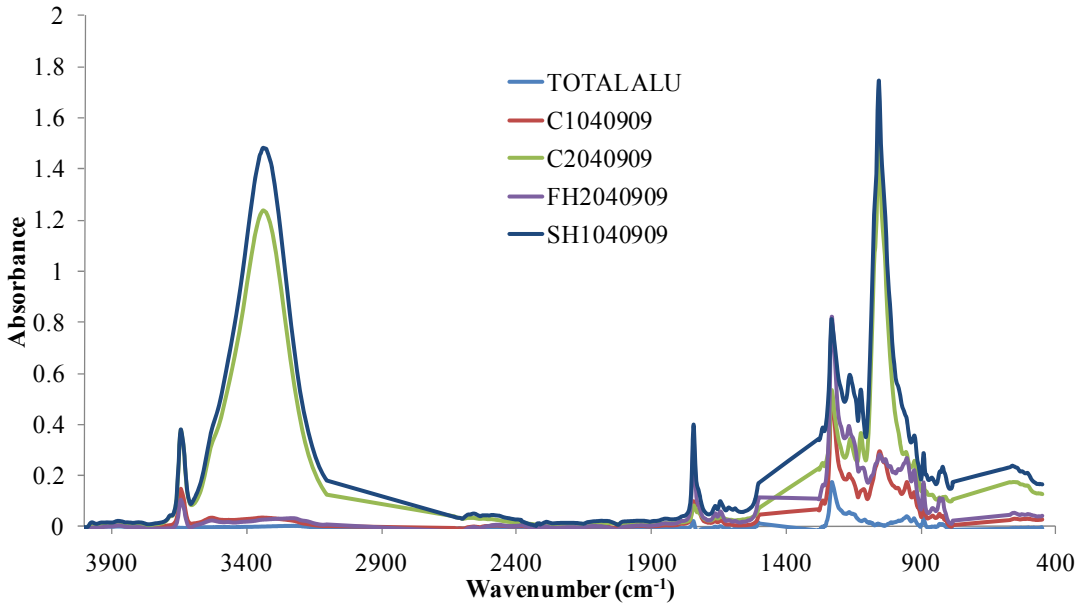

Figure 6.36. FTIR spectra of Total Alu and real samples collected from 4 different production lines.

After the FTIR measurements of the real samples were completed, the data is transferred to another computer for the data analysis and were divided into two sets as the calibration and validation sets. For the Total Alu analysis, 39 of the real process samples which were analyzed by GC were involved in the calibration set and another 38 were assigned as the validation set (Table 6.5).

Table 6.5. The concentrations of the calibration and validation sets for the Total Alu contaminant.

Calibration Set for Total Alu (w/w %)				**Validation Set for Total Alu (w/w %)**			
1	2.76	**21**	3.67	**1**	2.75	**20**	3.56
2	2.67	**22**	3.93	**2**	2.65	**21**	3.80
3	2.78	**23**	3.21	**3**	2.82	**22**	3.36
4	2.55	**24**	5.05	**4**	2.58	**23**	5.49
5	2.58	**25**	5.50	**5**	3.03	**24**	5.17
6	3.04	**26**	5.92	**6**	2.85	**25**	5.84
7	2.91	**27**	6.63	**7**	1.92	**26**	6.39
8	1.76	**28**	7.32	**8**	1.96	**27**	6.08
9	2.08	**29**	7.13	**9**	2.11	**28**	6.98
10	2.72	**30**	7.36	**10**	2.84	**29**	7.00
11	2.96	**31**	7.62	**11**	3.16	**30**	7.45
12	3.09	**32**	6.69	**12**	3.16	**31**	4.48
13	2.81	**33**	3.90	**13**	2.92	**32**	4.31
14	3.00	**34**	4.16	**14**	0.72	**33**	4.05
15	0.69	**35**	4.41	**15**	0.68	**34**	4.18
16	0.69	**36**	4.15	**16**	0.69	**35**	4.32
17	0.66	**37**	2.00	**17**	0.67	**36**	2.02
18	0.65	**38**	2.02	**18**	0.68	**37**	2.04
19	3.31	**39**	2.08	**19**	3.24	**38**	1.95
20	3.43						

After the model is constructed, the total Alu concentrations in the real samples were predicted. The actual versus predicted concentrations are shown on a plot in Figure 6.37. As it can be seen, the correlation coefficient is 0.9993. The standard error of calibration (SEC) and standard error of prediction (SEP) values, which were indicated in the figure, are 0.0510% (w/w %) and 0.0818% (w/w %), respectively. Thus, it can be concluded that the model is quite successful.

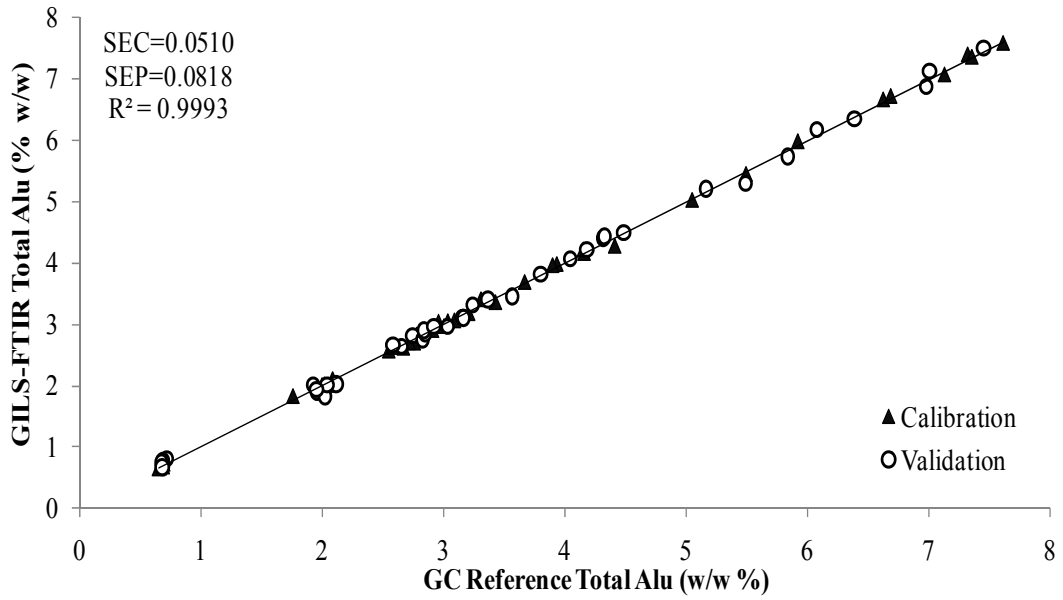

Figure 6.37. The actual versus predicted concentrations for Total Alu in real samples.

The predicted concentrations of Total Alu in real samples which are shown in the line plots in are in between 1.64% and 4.83% (w/w %) for the samples collected from C1, C3 production lines (Figure 6.38), between 3.77 to 6.42% (w/w %) for the samples of FH1, FH2, FH3 and FH4 systems (Figure 6.39) and between 0.87 and 4.34% (w/w %) for C2, and C4, (Figure 6.40) ,SH1 and SH2 system samples (Figure 6.41).

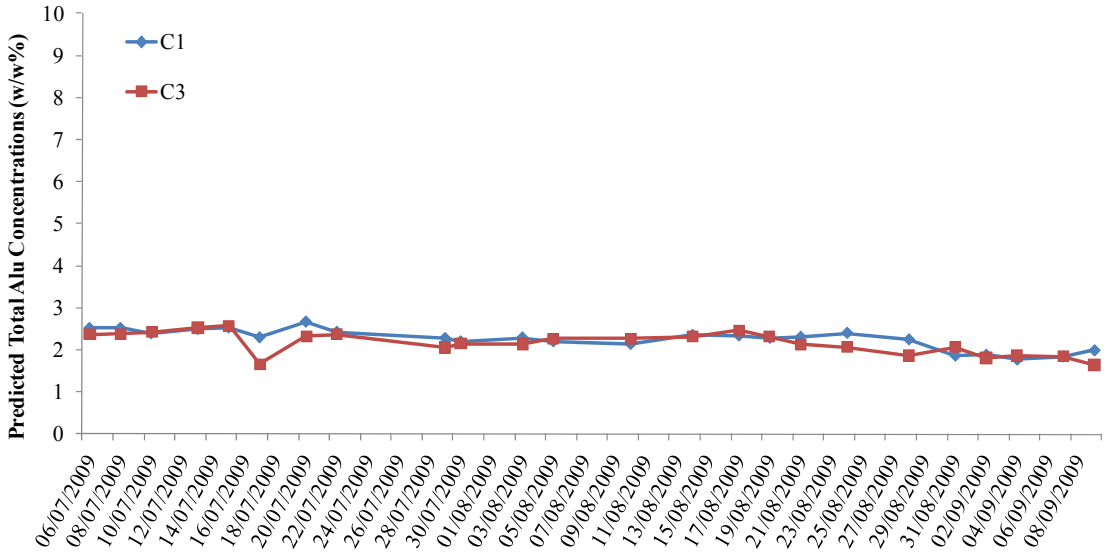

Figure 6.38. The line graphs of the predicted concentrations of Total Alu contaminant in real process samples of C1, C3 systems collected in July, August and September 2009.

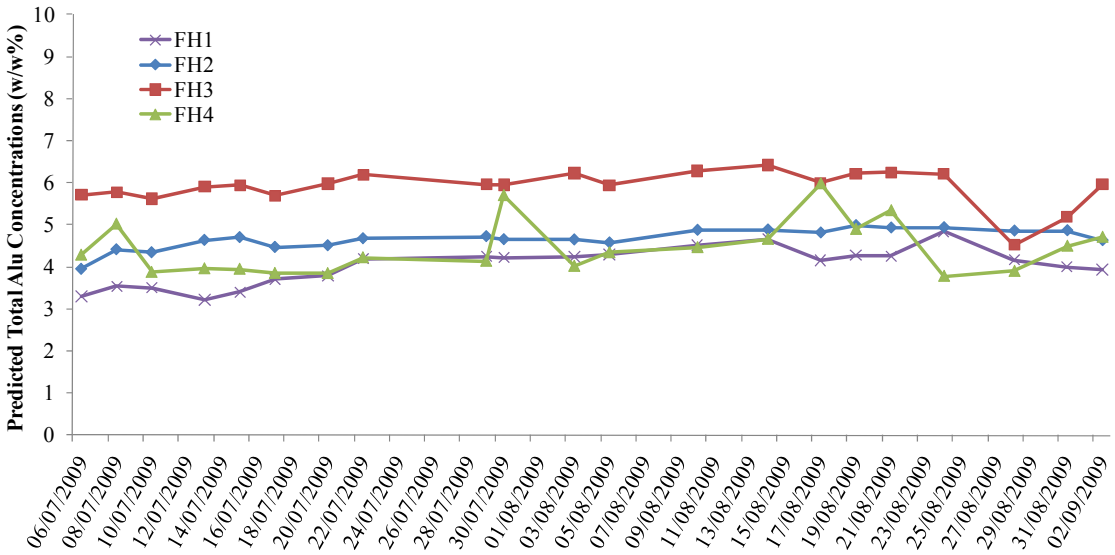

Figure 6.39. The line graphs of the predicted concentrations of Total Alu contaminant in real process samples of FH1, FH2, FH3, and FH4 systems collected in July, August and September 2009.

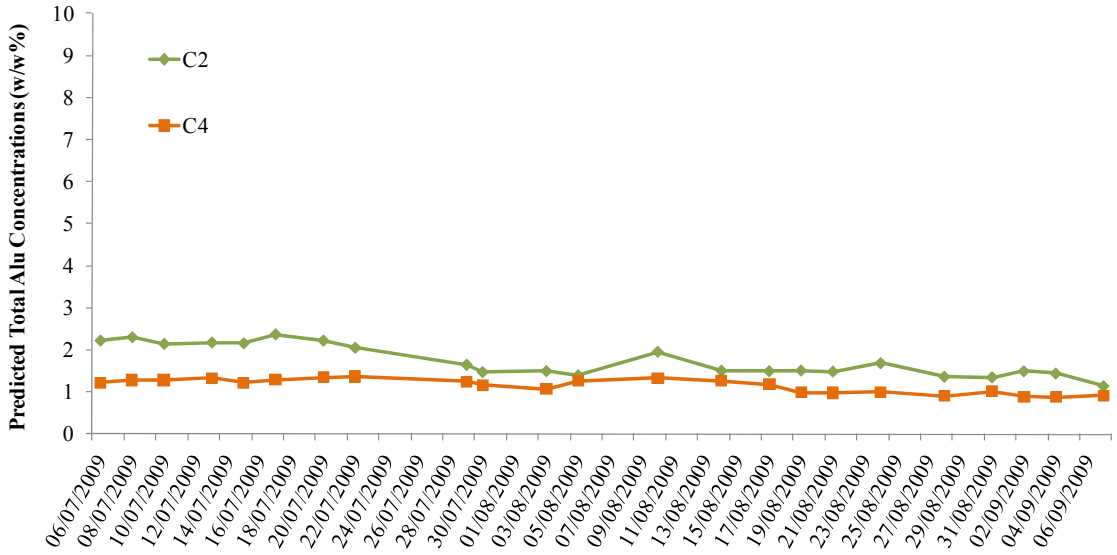

Figure 6.40. The line graphs of the predicted concentrations of Total Alu contaminant in real process samples of C2, and C4, systems collected in July, August and September 2009.

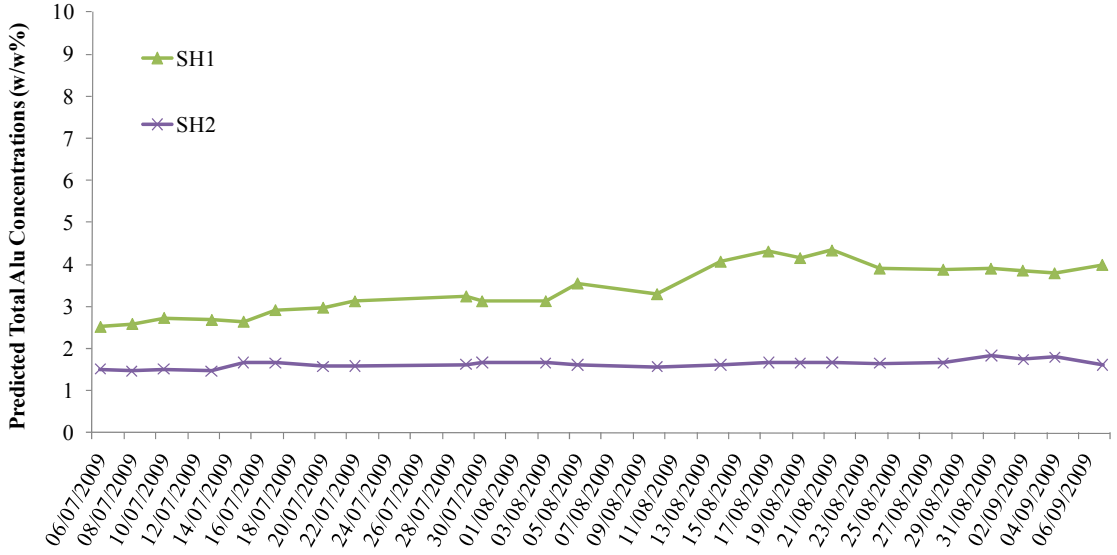

Figure 6.41. The line graphs of the predicted concentrations of Total Alu contaminant in real process samples of SH1 and SH2 systems collected in July, August and September 2009.

The profile is changing from month to month, and sample to sample. The reason is that those mechanical cooling lubricants which cause contaminations are circulating in the huge oil tanks and changed after only specific periods. In other words the mechanical cooling lubricants in those huge tanks in the plant are partially changed with the fresh ones periodically. The oils in those tanks would not be very clean, since only a particular volume can be changed during the process, meaning that there is still old is present in the tank even if the new volume had been added. Those fluctuations prove this statement.

Figures below show the line plots for the comparison of FTIR-GILS results with the reference results obtained from GC. Figure 6.42 is plotted for C1 and C3 samples, Figure 6.43 is for FH1 and FH2 samples, Figure 6.44 is for FH3 and FH4 samples, Figure 6.45 is for C2 and C4 samples and Figure 6.46 is for SH1 and SH2 samples The plots support the claims that the model is quite successful since the predicted results are in good agreement with the ones obtained from GC method.

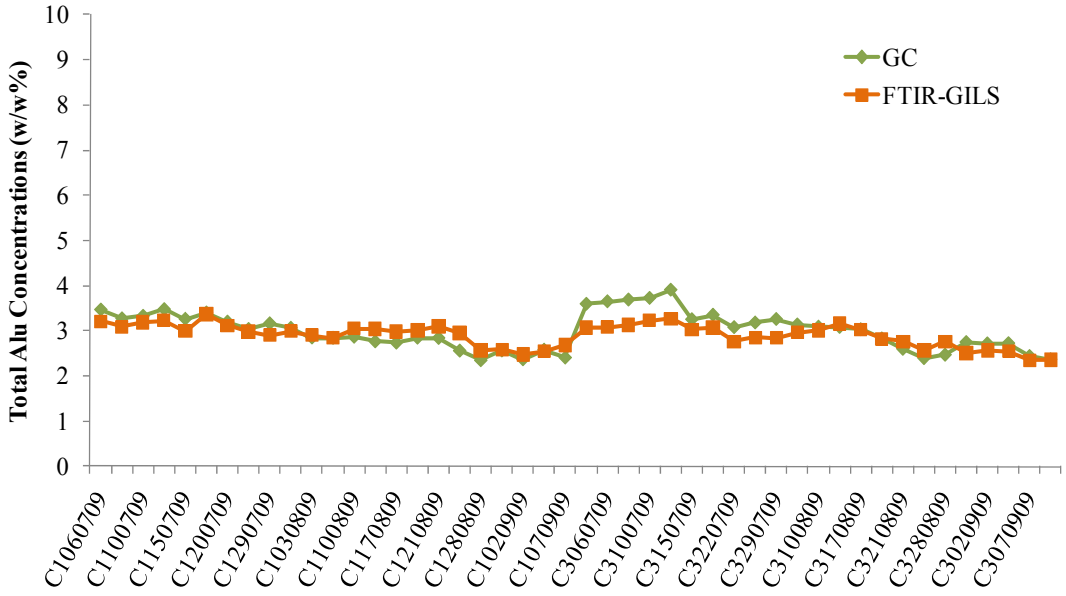

Figure 6.42. The comparison of FTIR-GILS predicted results with the GC-Reference results for the C1 and C3 real process samples collected in July, August, and September 2009.

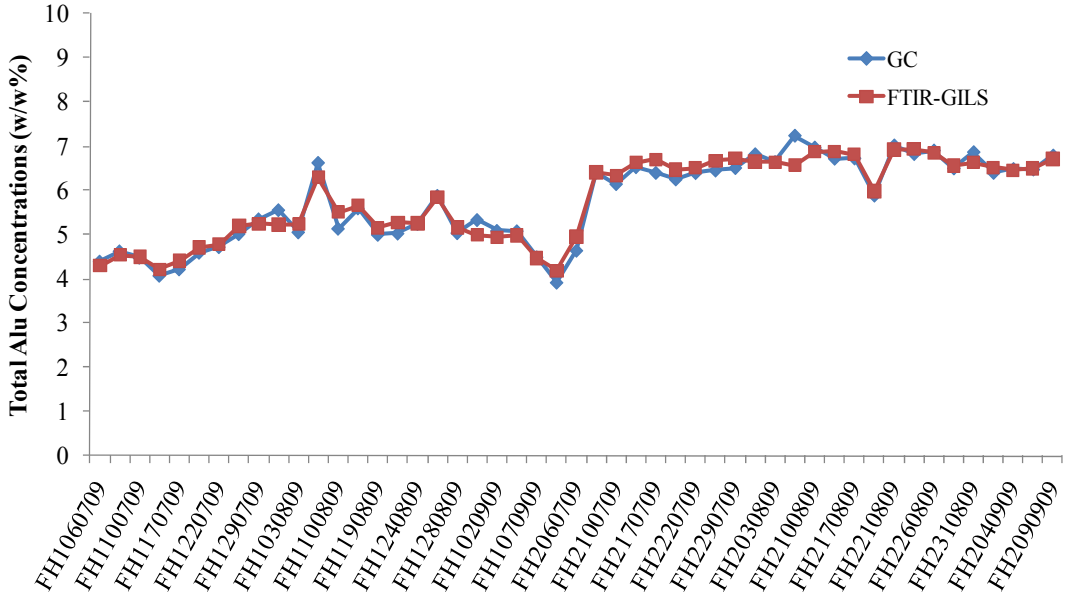

Figure 6.43. The comparison of FTIR-GILS predicted results with the GC-Reference results for the FH1 and FH2 real process samples collected in July, August, and September 2009.

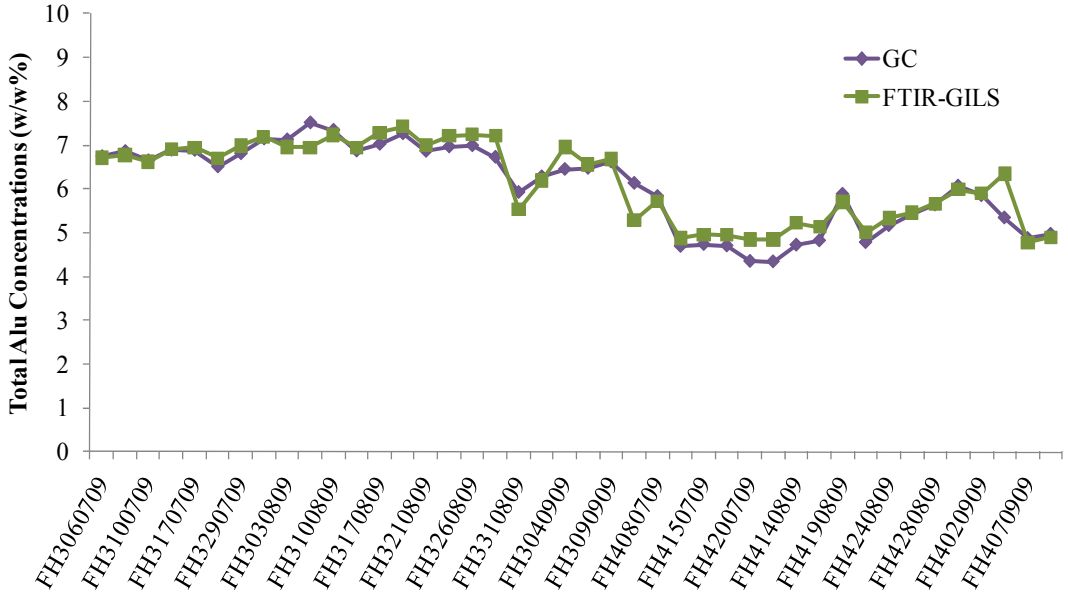

Figure 6.44. The comparison of FTIR-GILS predicted results with the GC-Reference results for the FH3 and FH4 real process samples collected in July, August, and September 2009.

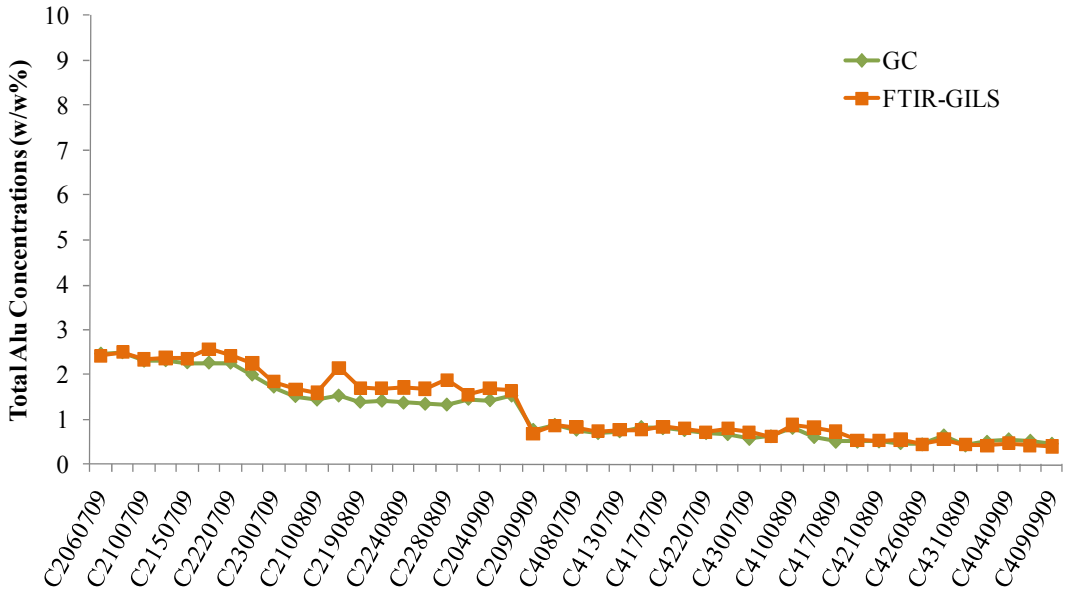

Figure 6.45. The comparison of FTIR-GILS predicted results with the GC-Reference results for the C2 and C4 real process samples collected in July, August, and September 2009.

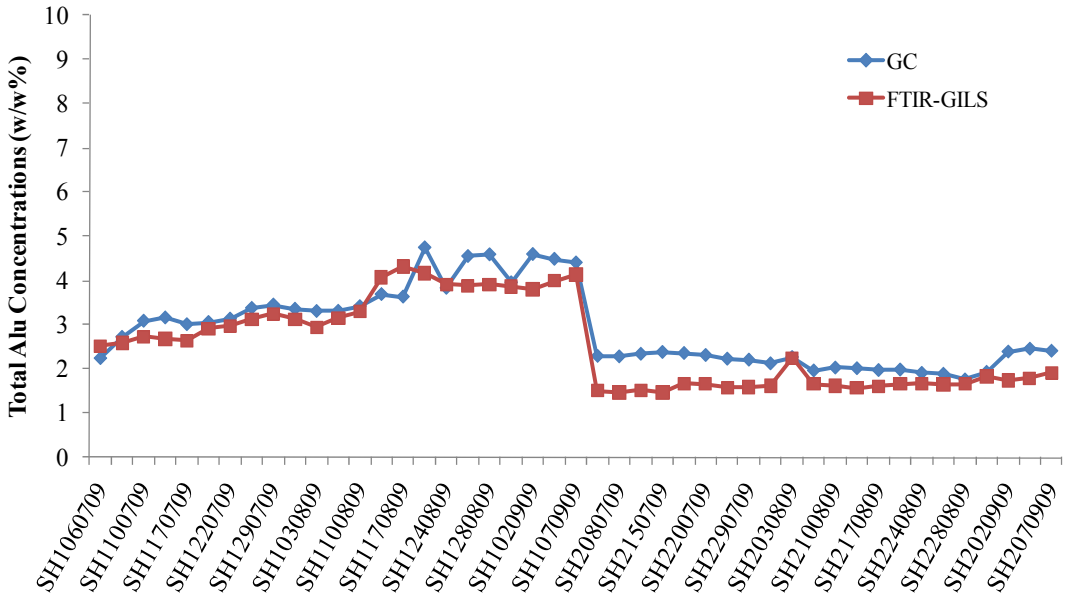

Figure 6.46. The comparison of FTIR-GILS predicted results with the GC-Reference results for the SH1 and SH2 real process samples collected in July, August, and September 2009.

Table 6.6. The concentrations of the calibration and validation sets for the Alu 16 contaminant.

Calibration Set for Alu 16 (w/w %)				Validation Set for Alu 16 (w/w %)			
1	0.34	**39**	0.19	**1**	0.31	**39**	0.18
2	0.33	**40**	0.26	**2**	0.31	**40**	0.20
3	0.32	**41**	0.17	**3**	0.27	**41**	0.18
4	0.30	**42**	0.15	**4**	0.28	**42**	0.19
5	0.22	**43**	0.19	**5**	0.29	**43**	0.21
6	0.32	**44**	0.20	**6**	0.33	**44**	0.18
7	0.40	**45**	0.18	**7**	0.33	**45**	0.19
8	0.26	**46**	0.19	**8**	0.34	**46**	0.19
9	0.30	**47**	0.17	**9**	0.32	**47**	0.19
10	0.33	**48**	0.20	**10**	0.35	**48**	0.19
11	0.33	**49**	0.21	**11**	0.36	**49**	0.19
12	0.38	**50**	0.34	**12**	0.36	**50**	0.31
13	0.37	**51**	0.29	**13**	0.29	**51**	0.31
14	0.36	**52**	0.29	**14**	0.40	**52**	0.25
15	0.40	**53**	0.28	**15**	0.30	**53**	0.24
16	0.29	**54**	0.23	**16**	0.23	**54**	0.22
17	0.35	**55**	0.24	**17**	0.32	**55**	0.28
18	0.45	**56**	0.27	**18**	0.40	**56**	0.23
19	0.41	**57**	0.25	**19**	0.32	**57**	0.27
20	0.37	**58**	0.25	**20**	0.38	**58**	0.24
21	0.43	**59**	0.25	**21**	0.41	**59**	0.26
22	0.36	**60**	0.24	**22**	0.33	**60**	0.28
23	0.16	**61**	0.13	**23**	0.12	**61**	0.11
24	0.12	**62**	0.09	**24**	0.12	**62**	0.09
25	0.12	**63**	0.08	**25**	0.12	**63**	0.12
26	0.13	**64**	0.11	**26**	0.11	**64**	0.10
27	0.13	**65**	0.11	**27**	0.14	**65**	0.12
28	0.16	**66**	0.08	**28**	0.16	**66**	0.10
29	0.13	**67**	0.11	**29**	0.15	**67**	0.13
30	0.12	**68**	0.11	**30**	0.15	**68**	0.10
31	0.16	**69**	0.78	**31**	0.16	**69**	0.73
32	0.17	**70**	0.71	**32**	0.19	**70**	0.69
33	0.18	**71**	0.85	**33**	0.16	**71**	0.93
34	0.16	**72**	0.94	**34**	0.16	**72**	0.88
35	0.17	**73**	0.89	**35**	0.13	**73**	0.88
36	0.15	**74**	0.89	**36**	0.24	**74**	0.96
37	0.11	**75**	0.93	**37**	0.18	**75**	0.92
38	0.19			**38**	0.18		

Another set of GC compared FTIR-GILS results is the Alu 16 contaminant. The same procedure was applied for this component too. The data obtained was divided into two sets as the calibration and validation sets. 75 of the real process samples which were analyzed by GC were involved in the calibration set and another 75 were assigned as the validation set (Table 6.6). The GILS parameters are again set to 50 runs, with 100 iterations and 30 genes.

After the model is constructed, the Alu 16 concentrations in the real samples were predicted. The actual versus predicted concentrations are shown on a plot in Figure 6.47. As it can be seen, the correlation coefficient is 0.9386 and the SEC and SEP values are 0.0247% (w/w %) and 0.0545% (w/w %), respectively. Thus, it can be concluded that the model is quite successful.

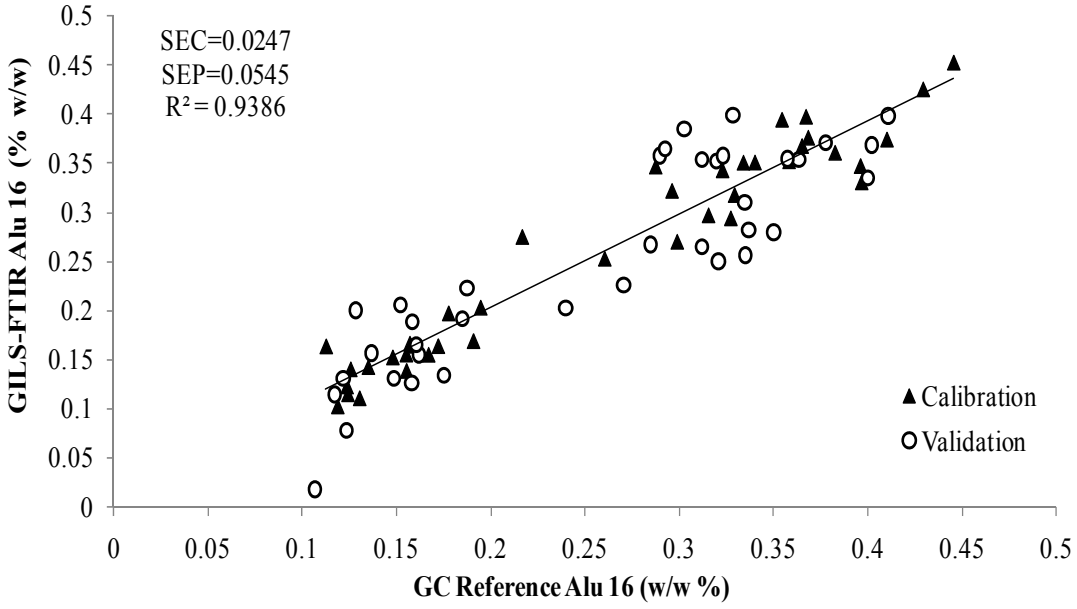

Figure 6.47. The actual versus predicted concentrations for Alu 16 in real samples.

The predicted concentrations of Alu 16 in real samples which are shown in Figure 6.48 are in between 0.02 and 0.38% (w/w %) for the samples collected from C1, and C3, varies from 0.02 to 0.46% (w/w %) for the samples of FH1, FH2, FH4, (Figure 6.49) and 0.10 to 0.81% (w/w %) for the SH1 and SH2 systems (Figure 6.50). Those amounts are very low, and still in the tolerable limits. As mentioned before C2, and C4

process samples contain Cindolube. Those production lines have similar additive and contaminant concentrations. Although C2 and C4 samples were predicted; they were not included in the figures. The C2 and C4 samples might have been predicted however the amounts are very low. The reason could be that the contamination in those system samples is at very low level so that it could not be detected.

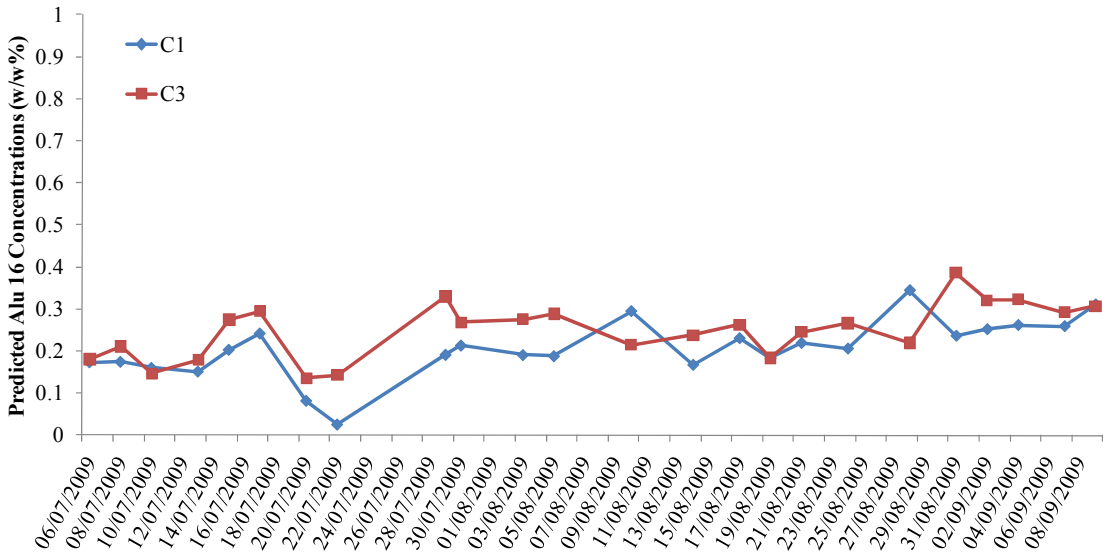

Figure 6.48. The line graphs of the predicted concentrations of Alu 16 contaminant in real process samples of C1, and C3 systems collected in July, August and September 2009.

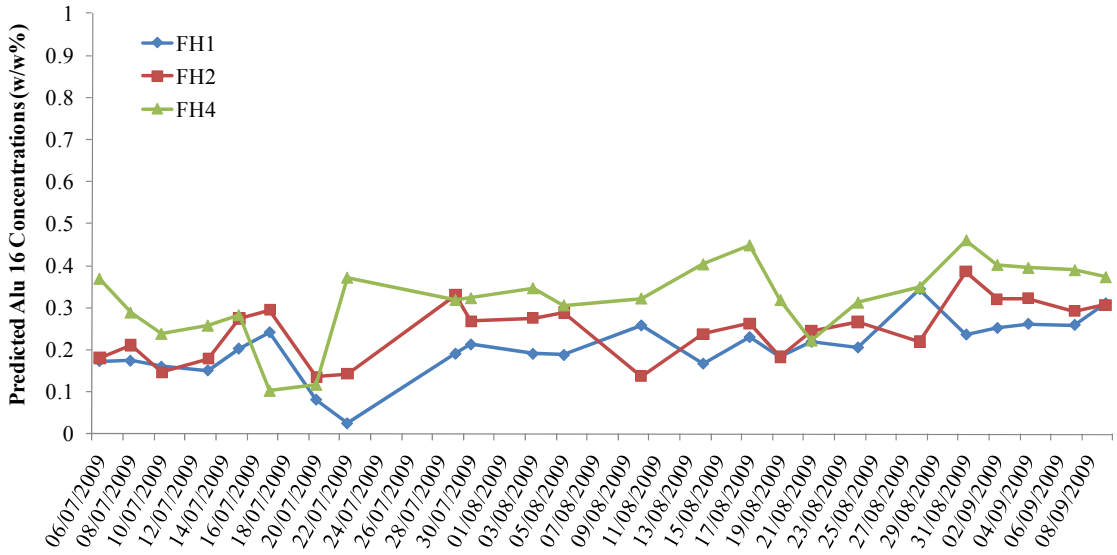

Figure 6.49. The line graphs of the predicted concentrations of Alu 16 contaminant in real process samples FH1, FH2, and FH4 systems collected in July, August and September 2009.

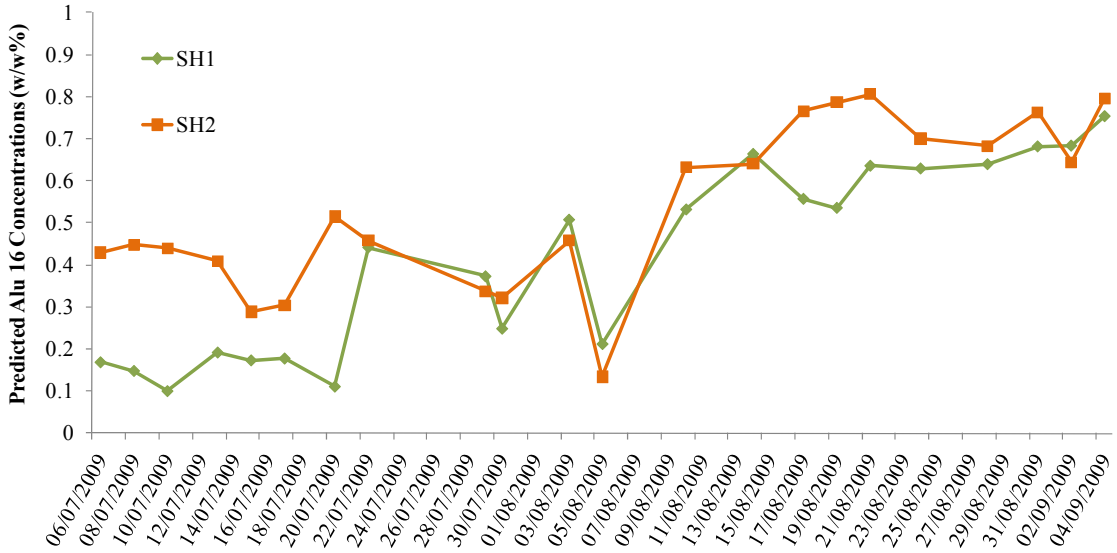

Figure 6.50. The line graphs of the predicted concentrations of Alu 16 contaminant in real process samples SH1 and SH2 systems collected in July, August and September 2009.

Following the prediction of those contaminants, Alu 16 and Total Alu, the results were compared with the predicted results from the reference method, GC. Figure 6.51, Figure 6.52, and Figure 6.53 show the line plots for the comparison of FTIR-GILS results with the reference results obtained from GC. The plots support the claims that the model is quite successful since the predicted results are in good agreement with the ones obtained from GC method.

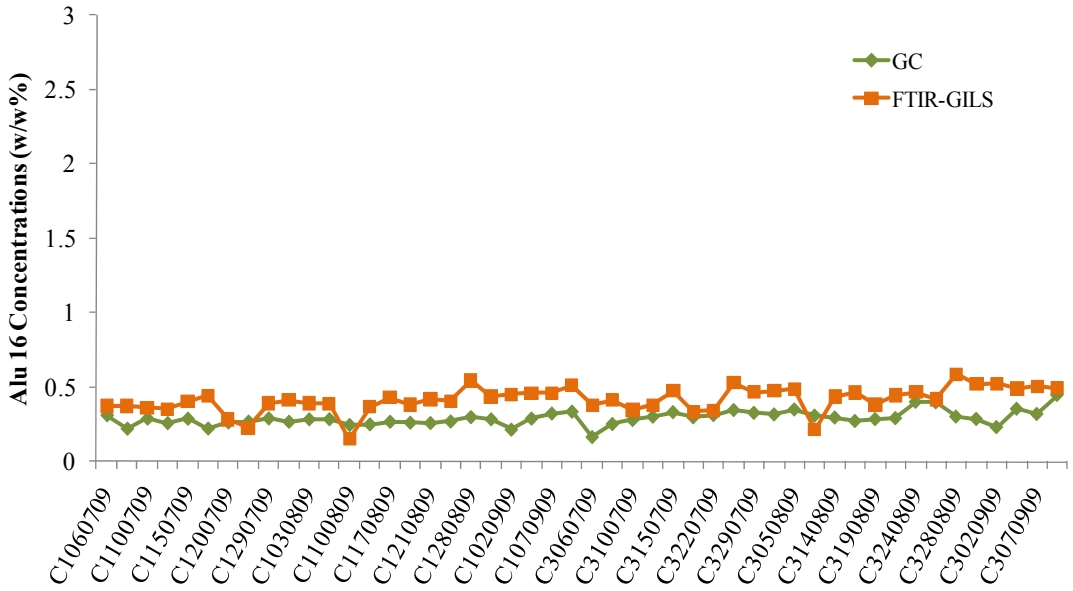

Figure 6.51. The comparison of FTIR-GILS predicted results with the GC-Reference results for the C1 and C3 real process samples collected in July, August, and September 2009.

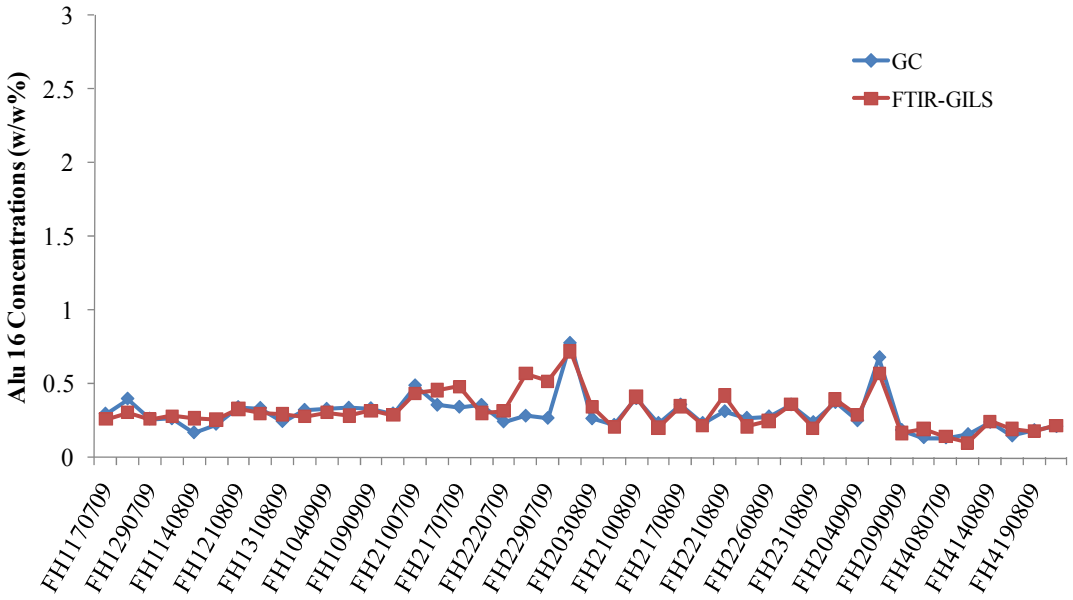

Figure 6.52. The comparison of FTIR-GILS predicted results with the GC-Reference results for the FH1, FH2 and FH4 real process samples collected in July, August, and September 2009.

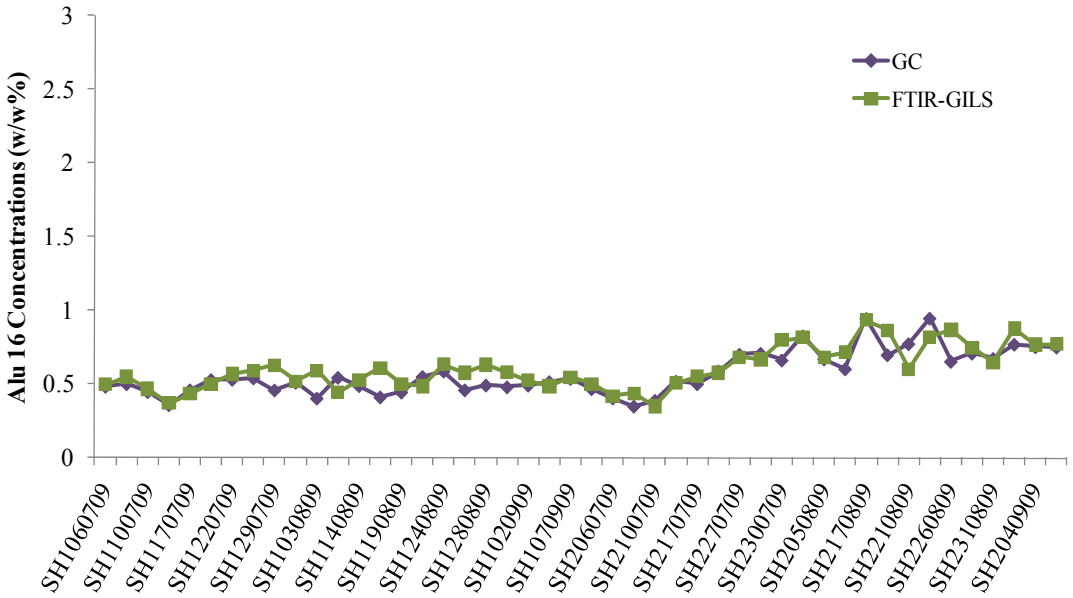

Figure 6.53. The comparison of FTIR-GILS predicted results with the GC-Reference results for the SH1 and SH2 real process samples collected in July, August, and September 2009.

The rest of the contaminants, Alu 46, Alu320 and Alu 460 could not be detected with GC, but still it is possible to predict those contaminant amounts in real samples by using synthetic samples. The samples which were prepared to mimic the system, contain Nafol around 0.80% (w/w %) and also three other components; Alu 46, Alu 320 and Alu 460. Those samples were analyzed with FTIR and the data obtained was used with GILS for the construction of the calibration models, then the concentrations in real samples were predicted.

The table below (Table 6.7) represents the concentrations of the Alu 46, Alu 320 and Alu 460 in the synthetic samples which were used as calibration set and validation set. 31 samples were assigned as the calibration set and 15 samples as the validation set.

Table 6.7. The concentrations of the calibration and validation sets for the Alu 46, Alu 320 and Alu 460 contaminant.

Calibration Set (w/w %)			**Validation Set (w/w %)**		
ALU 46	**ALU 320**	**ALU 460**	**ALU 46**	**ALU 320**	**ALU 460**
1.15	0.97	1.95	1.62	1.67	1.93
1.33	0.92	0.59	1.82	1.81	1.47
0.40	0.66	0.15	0.93	1.69	0.26
0.39	1.41	1.30	1.13	1.90	0.53
0.84	0.42	0.90	0.33	1.81	1.45
0.04	1.02	0.50	0.44	1.22	1.88
0.93	0.34	0.23	1.37	1.50	0.36
0.71	1.27	0.54	1.30	1.33	0.66
1.75	1.26	1.17	1.33	0.22	1.00
1.85	1.97	0.15	0.35	1.19	0.44
1.52	0.03	0.86	1.84	0.83	0.03
0.08	1.01	1.87	0.74	1.13	0.03
0.10	0.38	1.65	1.83	1.67	1.32
1.32	0.57	1.48	1.69	0.57	1.82
1.38	1.99	0.36	0.69	0.81	0.39
1.54	0.25	0.89			
1.34	0.61	0.34			
0.57	0.53	0.94			
1.27	1.96	1.44			
0.38	1.86	0.61			
0.21	0.23	1.08			
0.18	1.88	1.48			
1.26	1.13	0.18			
0.18	1.87	1.34			
1.91	0.45	0.38			
1.63	0.18	1.76			
0.88	1.91	0.03			
0.67	0.96	1.37			
0.97	1.95	1.75			
1.10	0.76	1.78			
0.49	0.59	1.08			

The model is constructed for the Alu 46 and the real versus actual concentration graph is plotted (Figure 6.54). The R^2 value is 0.9999 which represents that the model constructed is successful. The SEC and SEP values are calculated as 0.0064% (w/w %) and 0.0080% (w/w %), respectively.

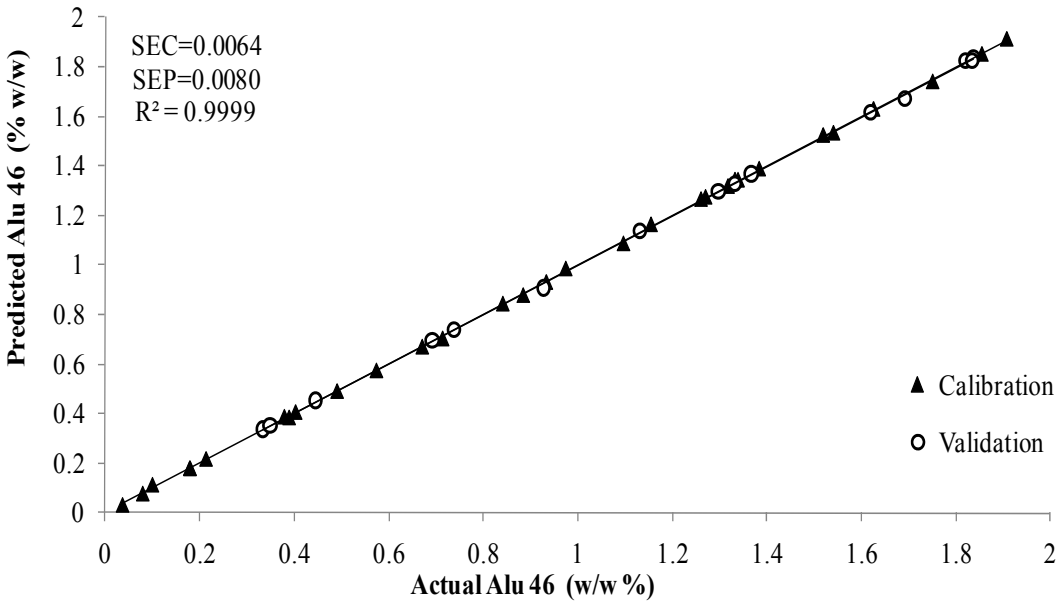

Figure 6.54. The actual versus predicted concentrations for Alu 46.

The predicted concentrations for the real samples are shown in figures below. Figure 6.55 shows the C1, C3 system samples where the concentrations are between 1.33 to 2.88% (w/w %), Figure 6.56 represents the FH1, FH2, FH3, and FH4 samples within a predicted concentration range between 2.02 and 4.14 % (w/w %), and Figure 6.57 illustrating the C2, C4, and Figure 6.58 is for SH1 and SH2 samples' predicted concentrations varying from 0.49 to 1.52% (w/w %). Since the contamination amount is tolerable up to those limits, the results are in good agreement with the intended amounts.

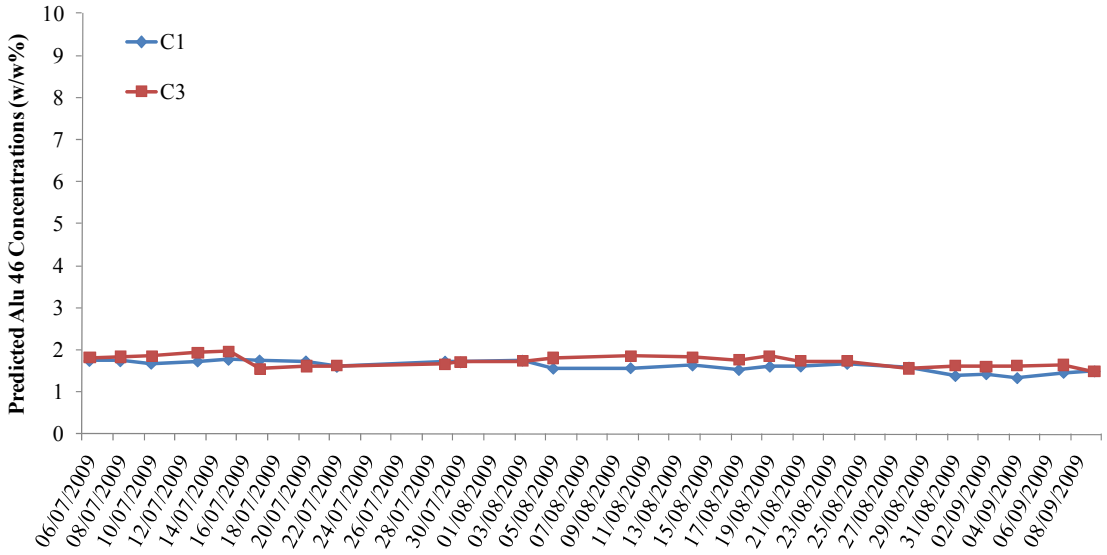

Figure 6.55. The line graphs of the predicted concentrations of Alu 46 contaminant in real process samples of C1, and C3 systems collected in July, August and September 2009.

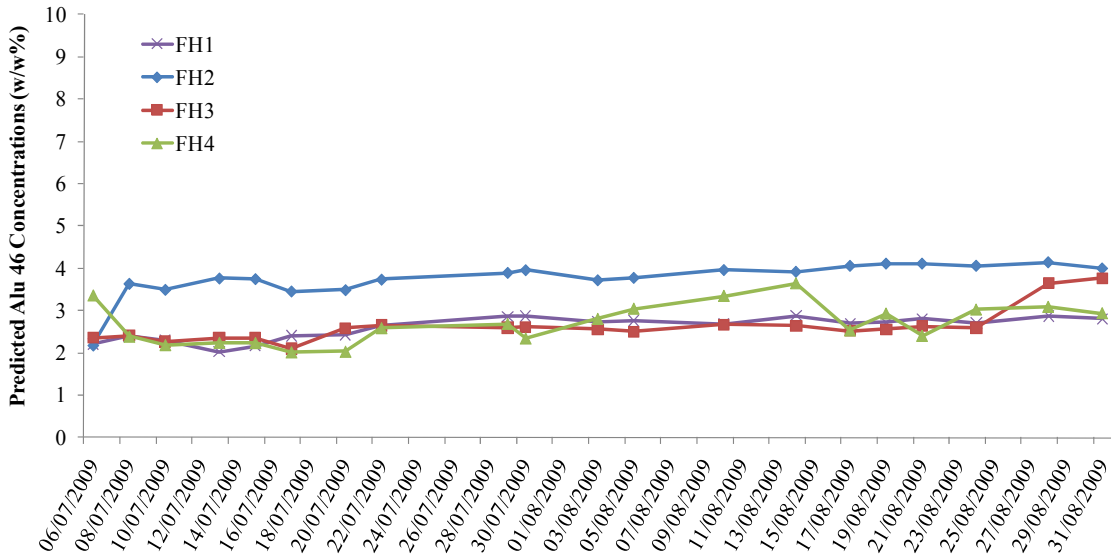

Figure 6.56. The line graphs of the predicted concentrations of Alu 46 contaminant in real process samples of FH1, FH2, FH3 and FH4 systems collected in July, August and September 2009.

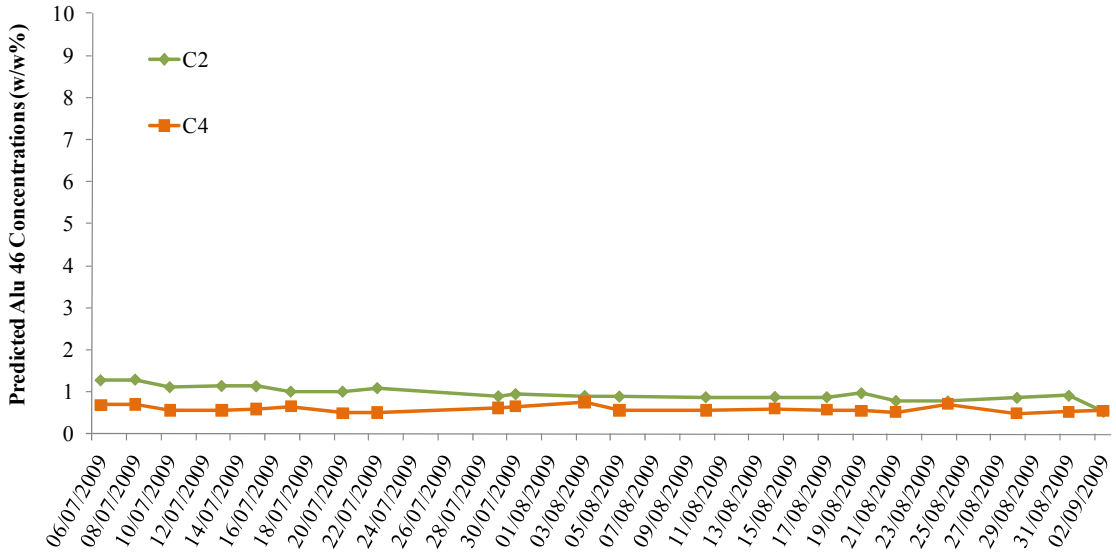

Figure 6.57. The line graphs of the predicted concentrations of Alu 46 contaminant in real process samples of C2 and C4 systems collected in July, August and September 2009.

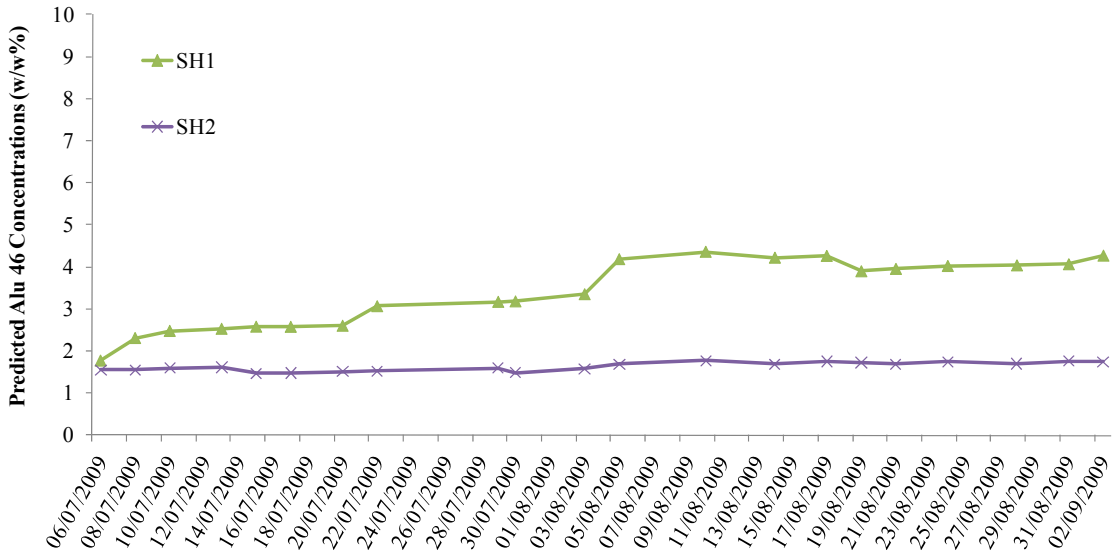

Figure 6.58. The line graphs of the predicted concentrations of Alu 46 contaminant in real process samples of SH1 and SH2 systems collected in July, August and September 2009.

Another component which was investigated is Alu 320. The calibration and validation set concentrations for Alu 320 were given in Table 6.7. 31 out of 46 synthetic samples were assigned as the calibration set and the rest 15 were used in validation set.

The calibration model is built using the calibration set samples and was tested using the validation set. The actual versus predicted results were plotted (Figure 6.59).

It is clear that the model is quite successful with an R^2 value of 0.9996, a SEC value of 0.0290% (w/w %) and SEP value of 0.0315% (w/w %).

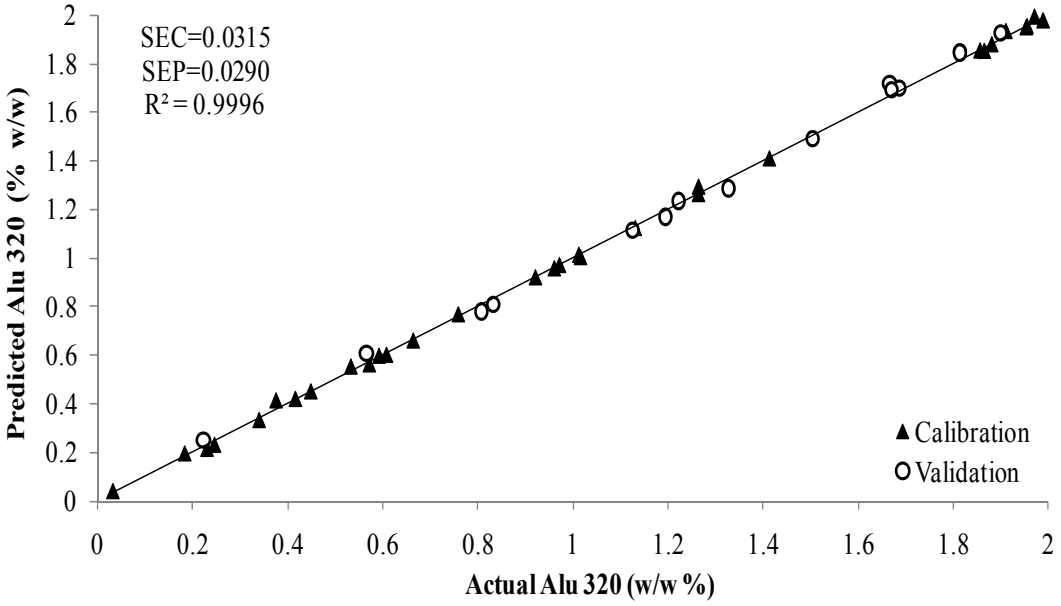

Figure 6.59. The actual versus predicted concentrations for Alu 320.

The predicted Alu 320 concentrations for the real process samples are given in figures below. The predicted concentration ranges vary between 2.41 and 4.21% (w/w %) for C1, C3, system samples (Figure 6.60), 2.27 and 5.90% (w/w %) for FH1, FH2, FH3, and FH4 systems (Figure 6.61), and 0.66 and 3.01% (w/w %) for the C2, C4 (Figure 6.62), and SH1 and SH2 system samples (Figure 6.63). The line plots show the distribution of those concentrations through the 3-month period.

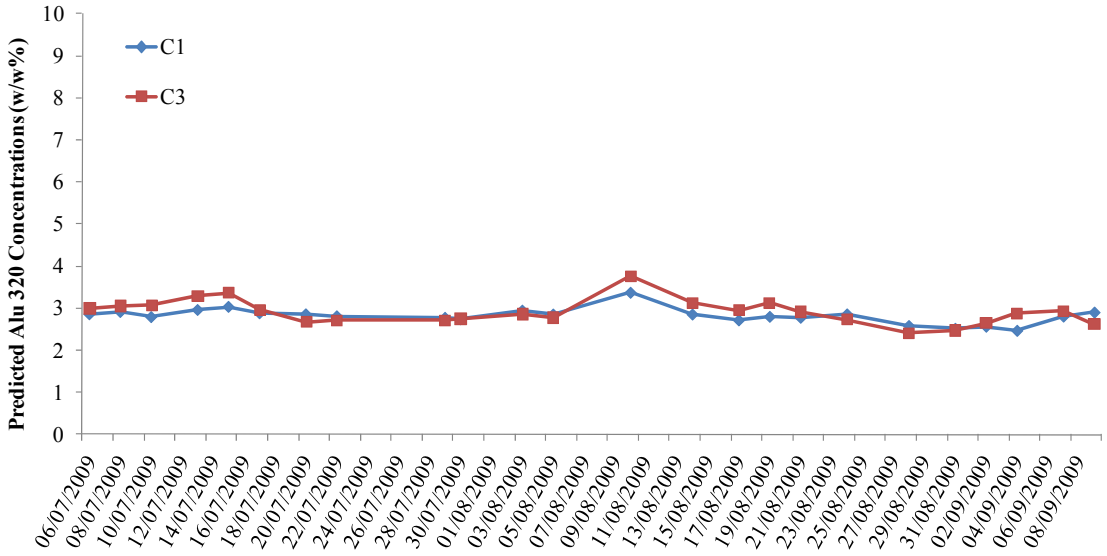

Figure 6.60. The line graphs of the predicted concentrations of Alu 320 contaminant in real process samples of C1, C3 systems collected in July, August and September 2009.

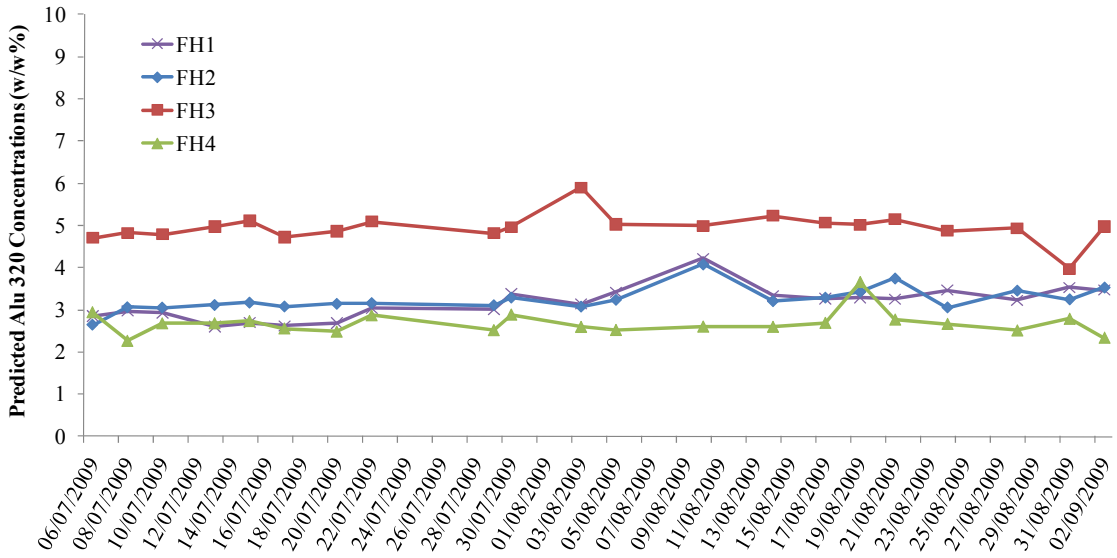

Figure 6.61. The line graphs of the predicted concentrations of Alu 320 contaminant in real process samples of FH1, FH2, FH3 and FH4 systems collected in July, August and September 2009.

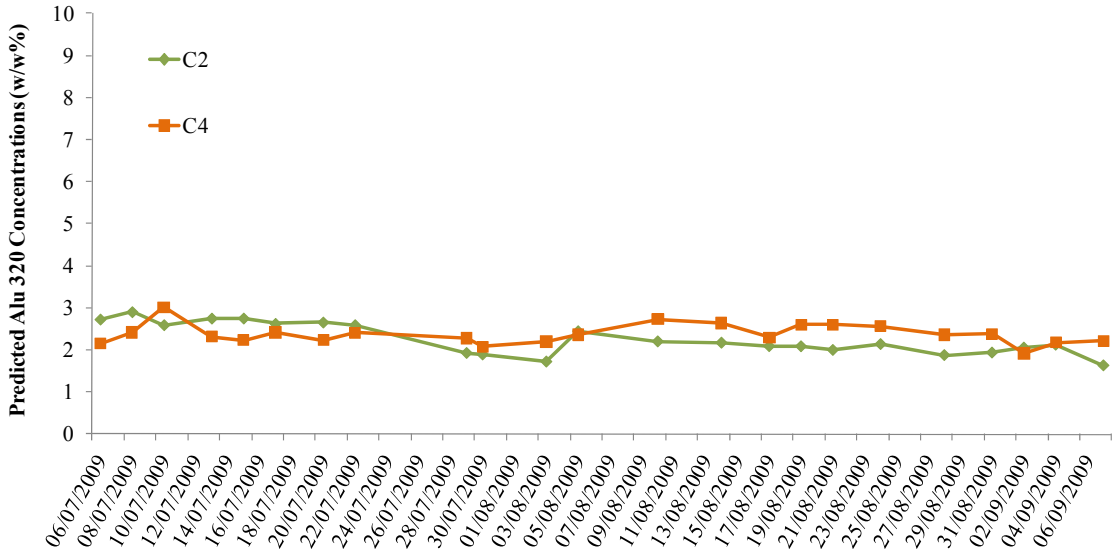

Figure 6.62. The line graphs of the predicted concentrations of Alu 320 contaminant in real process samples of C2 and C4 systems collected in July, August and September 2009.

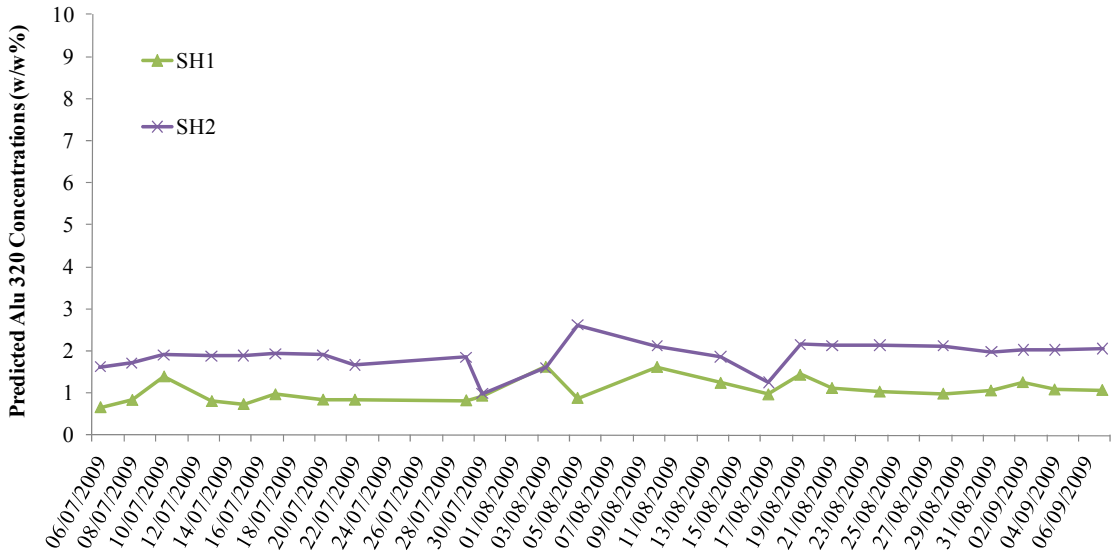

Figure 6.63. The line graphs of the predicted concentrations of Alu 320 contaminant in real process samples of SH1, and SH2 systems collected in July, August and September 2009.

The last contaminant which was investigated is Alu 460. The calibration and validation sets which were used through the construction and testing of the model is given in Table 6.7.

The calibration model is built using the calibration set samples and was tested using the validation set. The actual versus predicted results were plotted (Figure 6.64).

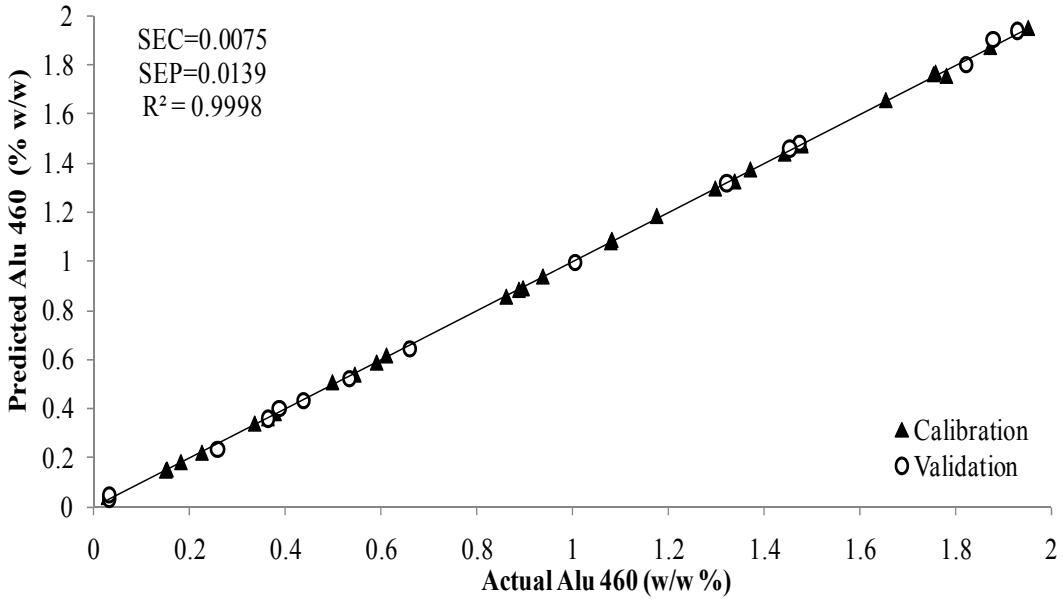

Figure 6.64. The actual versus predicted concentrations for Alu 460.

Figures below show the predicted concentrations of Alu 460 contaminant in real process samples. The concentrations predicted vary in a range of 0.03 to 0.28% (w/w %) for C1, C3, system samples (Figure 6.65), whereas FH1, FH2, FH3, and FH4 changes between 0.16 and 0.52% (w/w %) (Figure 6.66).

Although C2, C4, SH1 and SH2 process samples were also predicted, they were not given in the plots. The reason is that the predicted concentrations for those system samples are very low. The reason could be that the contamination in those system samples is at very low level so that it could not be detected.

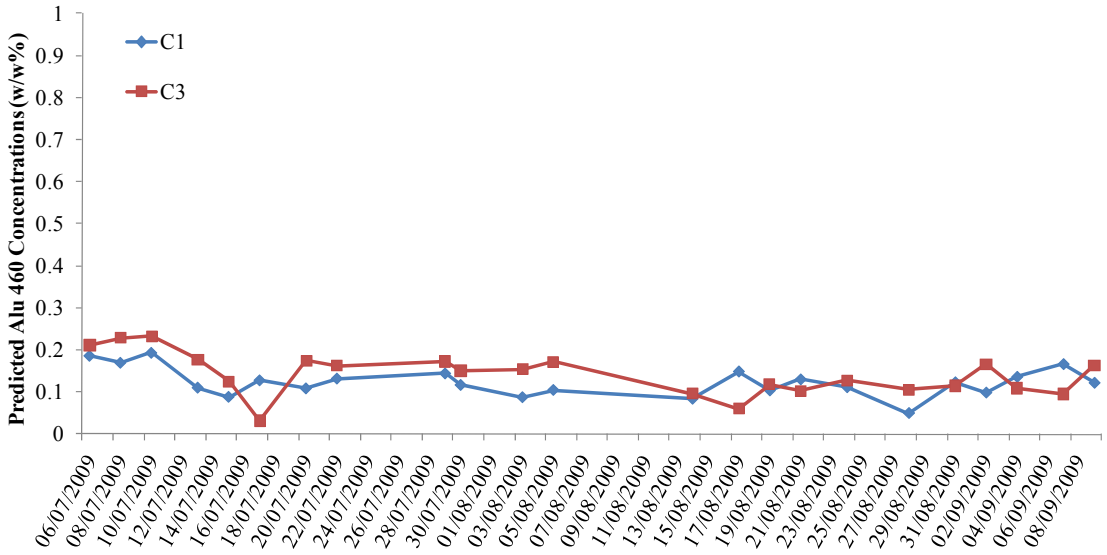

Figure 6.65. The line graphs of the predicted concentrations of Alu 460 contaminant in real process samples of C1, C3 systems collected in July, August and September 2009.

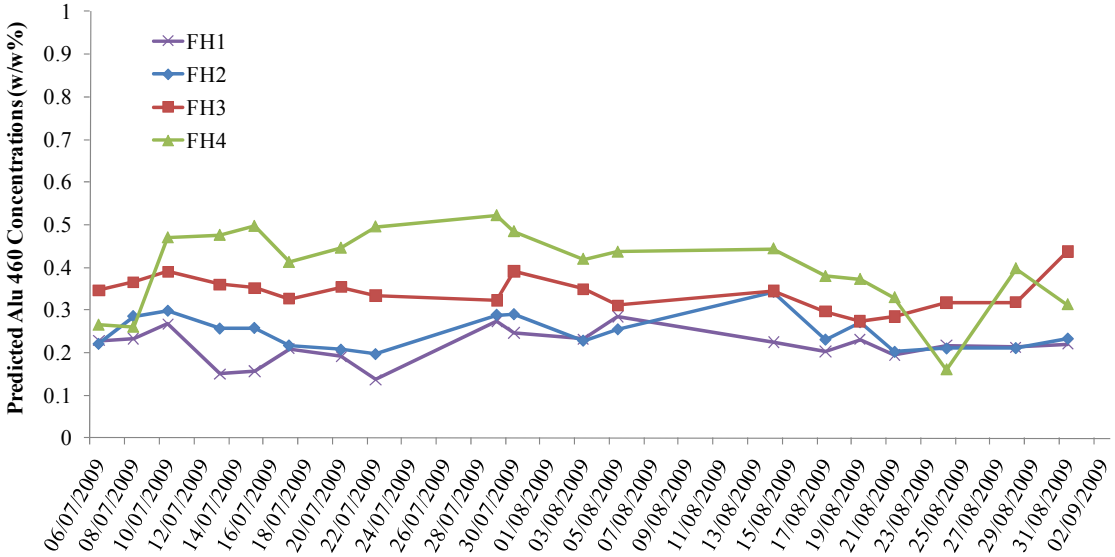

Figure 6.66. The line graphs of the predicted concentrations of Alu 460 contaminant in real process samples of FH1, FH2, FH3, and FH4 systems collected in July, August and September 2009.

6.2.2. Additive Analysis

The additives, Nafol and Cindolube results were also compared with the GILS-FTIR results. Since the spectra of real samples are very similar, it is not possible to use univariate calibration (Figure 6.67). Therefore, GILS was used for the construction of the calibration models for both Nafol and Cindolube. Those results obtained from the reference method GC, were compared with the GILS predicted results which uses FTIR data.

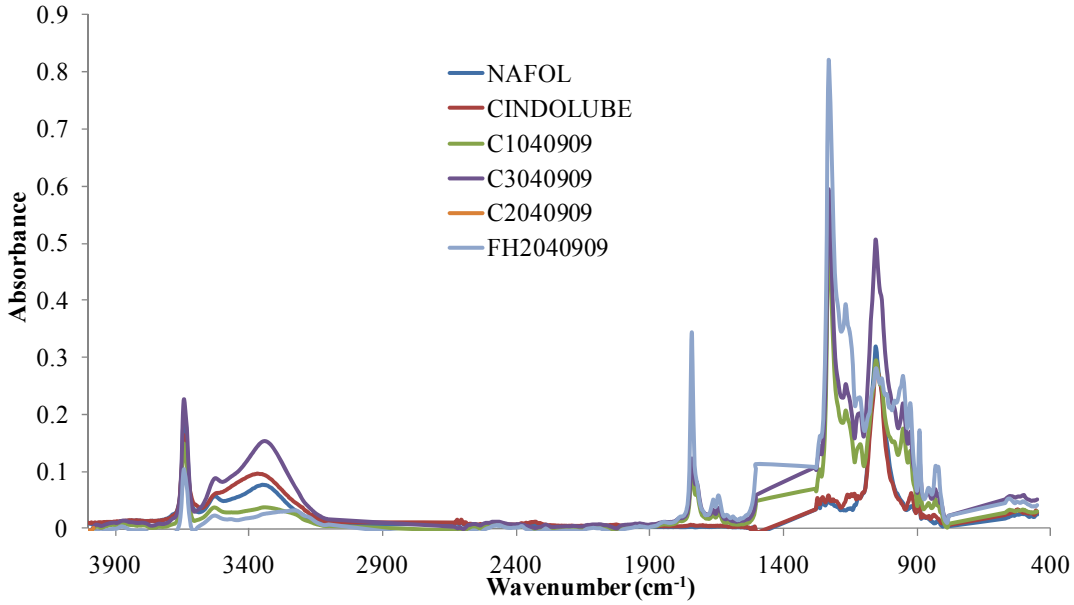

Figure 6.67. The spectra of Nafol and Cindolube components with real samples.

For the Nafol additive, the concentrations for the calibration and validation sets are given in Table 6.8. 50 out of 100 samples were assigned as the calibration set and the rest was used for the validation set. Following the construction of the calibration model, the Nafol content in real process samples were predicted.

Table 6.8. The concentrations of the calibration and validation sets for the Nafol additive.

Calibration Set for Nafol (w/w %)				Validation Set for Nafol (w/w %)			
1	0.69	**26**	0.53	**1**	0.66	**26**	0.52
2	0.67	**27**	0.58	**2**	0.66	**27**	0.83
3	0.64	**28**	0.82	**3**	0.67	**28**	0.83
4	0.70	**29**	0.65	**4**	0.74	**29**	0.58
5	0.72	**30**	0.61	**5**	0.73	**30**	0.72
6	0.73	**31**	0.60	**6**	0.79	**31**	0.59
7	0.60	**32**	0.53	**7**	0.61	**32**	0.54
8	0.80	**33**	0.53	**8**	0.82	**33**	0.52
9	0.97	**34**	0.51	**9**	0.93	**34**	0.52
10	1.06	**35**	0.45	**10**	1.09	**35**	0.45
11	1.14	**36**	0.45	**11**	1.14	**36**	0.45
12	1.02	**37**	0.44	**12**	1.18	**37**	0.55
13	1.03	**38**	0.56	**13**	1.14	**38**	0.80
14	1.12	**39**	0.65	**14**	1.20	**39**	0.64
15	1.27	**40**	0.66	**15**	1.20	**40**	0.65
16	0.70	**41**	0.65	**16**	0.74	**41**	0.63
17	0.72	**42**	0.63	**17**	0.63	**42**	0.68
18	0.60	**43**	0.62	**18**	0.64	**43**	0.61
19	0.58	**44**	0.75	**19**	0.56	**44**	0.59
20	0.54	**45**	0.59	**20**	0.47	**45**	0.60
21	0.60	**46**	0.53	**21**	0.61	**46**	0.84
22	0.62	**47**	0.48	**22**	0.82	**47**	0.49
23	0.88	**48**	0.61	**23**	0.54	**48**	0.58
24	0.73	**49**	0.56	**24**	0.54	**49**	0.56
25	0.52	**50**	0.55	**25**	0.53	**50**	0.80

Figure 6.68 shows the actual versus predicted plot for the model constructed. The plot shows that the model seems to be quite successful with an R^2 value of 0.9858. The SEC and SEP values which are 0.0223 and 0.0281% (w/w %), respectively, are also given in the graph.

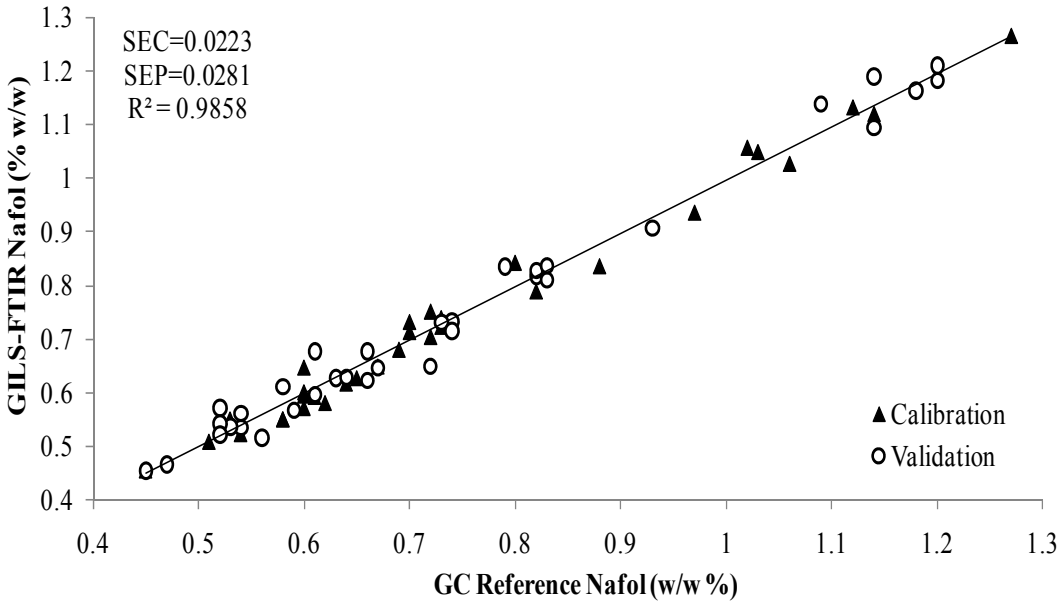

Figure 6.68. The actual versus predicted concentrations for Nafol.

The predicted Nafol concentrations vary in a range from 0.76% (w/w %) to 1.57% (w/w %) for C1, C3 and FH1 samples (Figure 6.69), where those values are between 0.52% (w/w %) and 0.93% (w/w %) for FH2, FH3 and FH4 system samples (Figure 6.70).

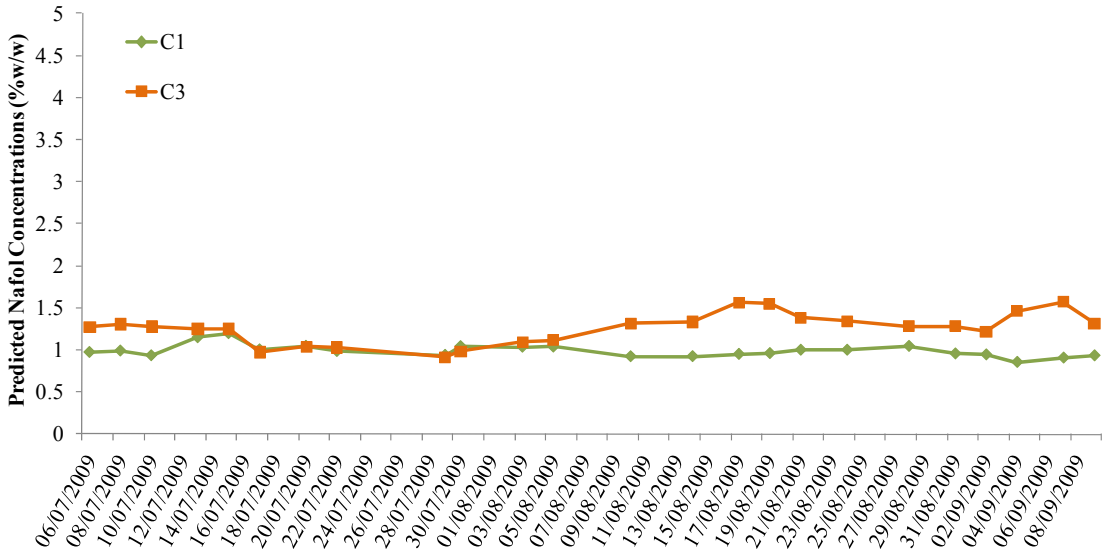

Figure 6.69. The line graphs of the predicted concentrations of Nafol additive in real process samples of C1, C3, FH1 systems collected in July, August and September 2009.

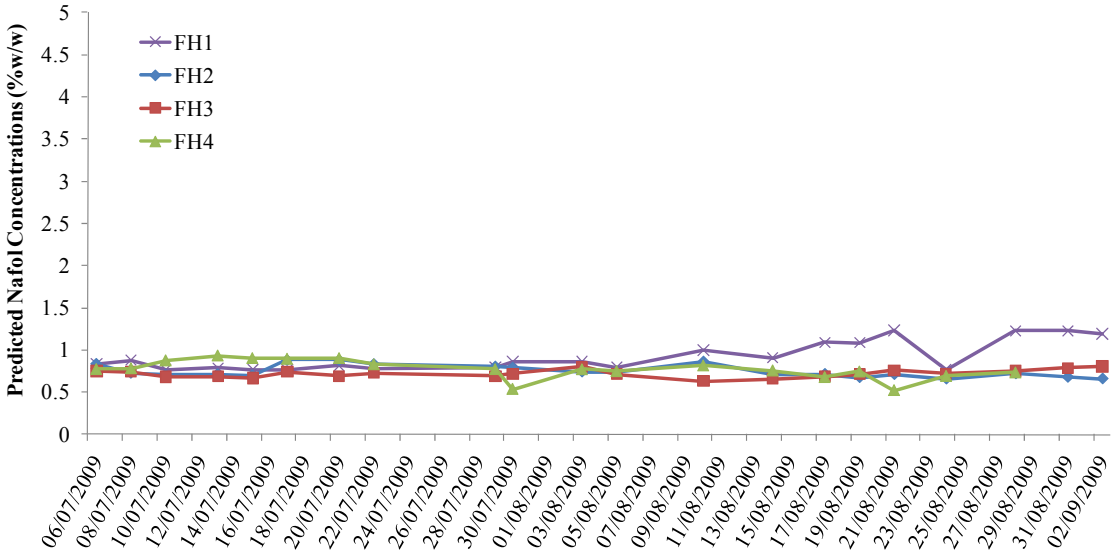

Figure 6.70. The line graphs of the predicted concentrations of Nafol additive in real process samples of FH2, FH3, and FH4 systems collected in July, August and September 2009.

Figures below show the line plots for the comparison of FTIR-GILS results with the reference results obtained from GC for Nafol additive (Figure 6.71, Figure 6.72 and Figure 6.73). The plots support the claims that the model is quite successful since the predicted results are in good agreement with the ones obtained from GC method.

The limits for the Nafol additive to maintain the permanent lubrication is in between 0.7-1.0% (w/w %). The results which are shown in those figures are not above this limit.

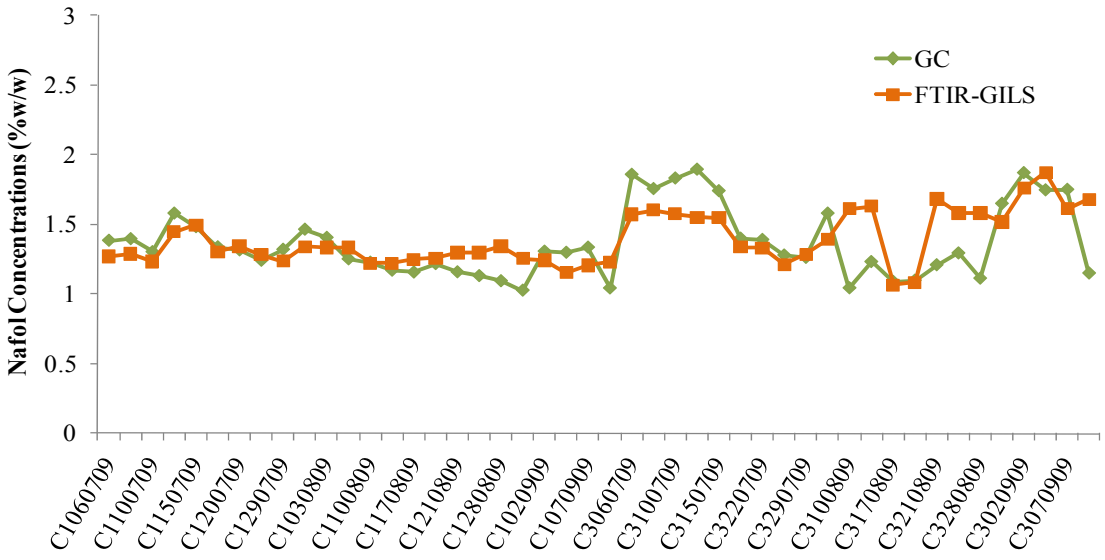

Figure 6.71. The comparison of FTIR-GILS predicted results with the GC-Reference results for the C1 and C3 real process samples collected in July, August, and September 2009.

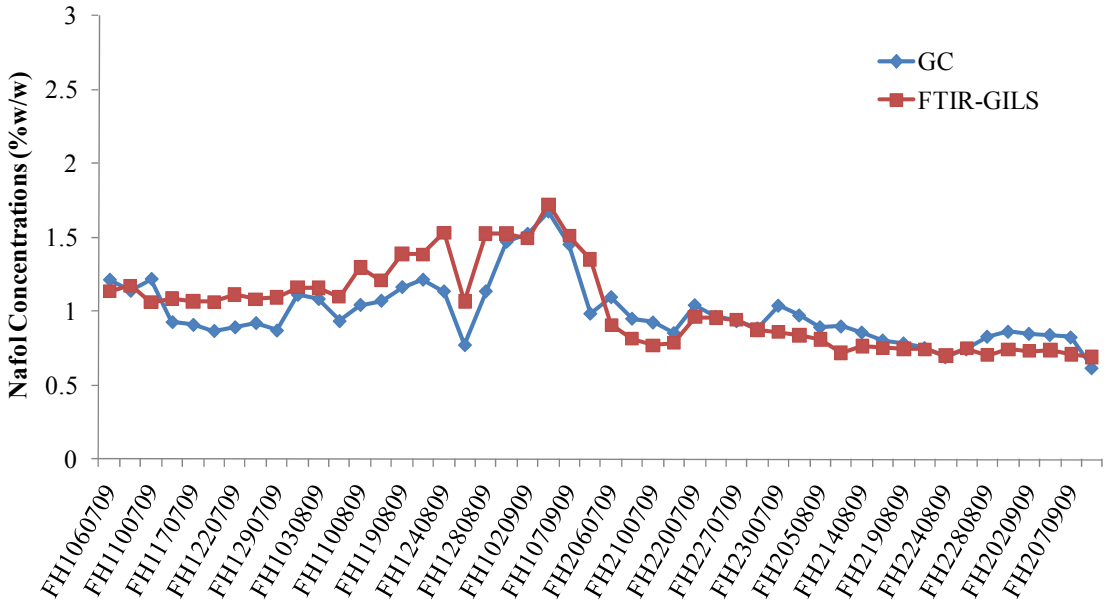

Figure 6.72. The comparison of FTIR-GILS predicted results with the GC-Reference results for the FH1 and FH2 real process samples collected in July, August, and September 2009.

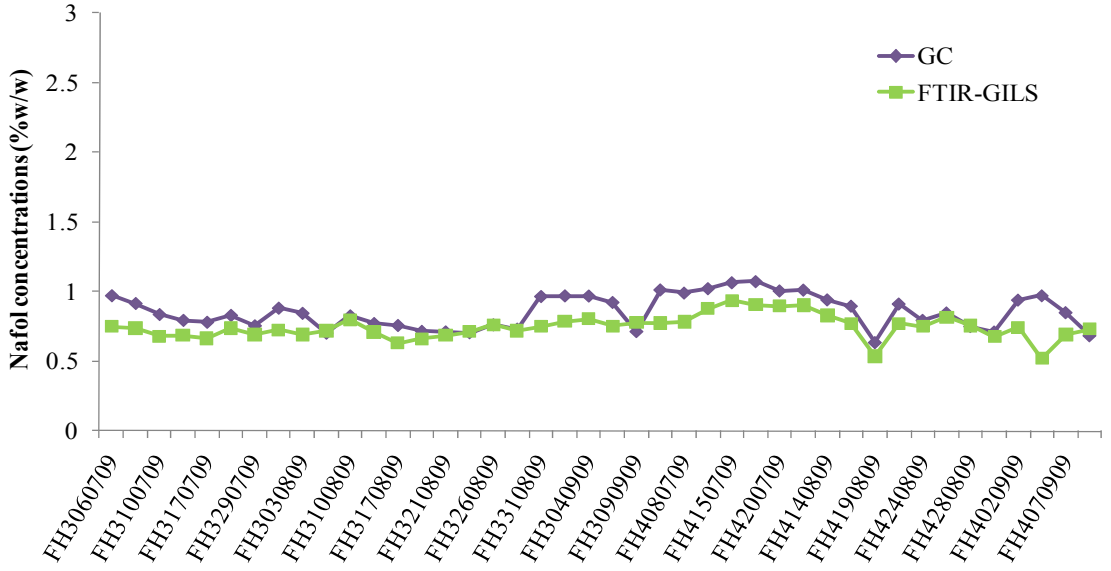

Figure 6.73. The comparison of FTIR-GILS predicted results with the GC-Reference results for the FH3 and FH4 real process samples collected in July, August, and September 2009

Table 6.9. The concentrations of the calibration and validation sets for the Cindolube additive.

	Calibration Set for Cindolube (w/w %)		Validation Set for Cindolube (w/w %)
1	5.15	**1**	5.05
2	5.09	**2**	5.28
3	5.52	**3**	5.40
4	5.74	**4**	5.79
5	5.28	**5**	5.40
6	5.37	**6**	5.40
7	5.58	**7**	5.43
8	5.64	**8**	5.46
9	5.60	**9**	5.80
10	4.36	**10**	5.52
11	6.39	**11**	6.16
12	5.69	**12**	6.07
13	6.21	**13**	6.32
14	6.00	**14**	6.23
15	6.07	**15**	6.00
16	6.00	**16**	6.27
17	5.96	**17**	6.15
18	6.23	**18**	6.30
19	6.50	**19**	6.50
20	6.51	**20**	6.50
21	4.05	**21**	5.81
22	4.63	**22**	5.10
23	5.47	**23**	5.06
24	5.36	**24**	5.44
25	5.60	**25**	5.70
26	6.01	**26**	5.89
27	5.92	**27**	5.93
28	6.21	**28**	5.96
29	5.80	**29**	5.55
30	5.79	**30**	5.60
31	5.96	**31**	5.69
32	5.90	**32**	5.86
33	6.18	**33**	5.80
34	5.76	**34**	5.77
35	5.60	**35**	5.72

The concentrations of the calibration and validation sets for the Cindolube additive are listed in Table 6.9.

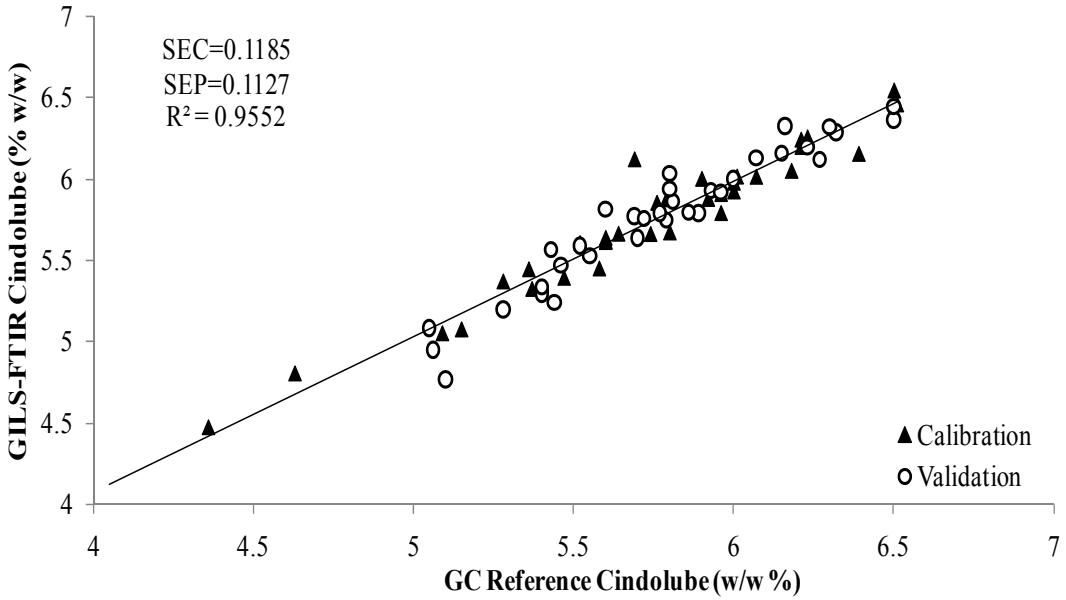

Figure 6.74. The actual versus predicted concentrations for Cindolube.

.

Figure 6.74 shows the actual versus predicted plot for the model constructed. The plot shows that the model seems to be quite successful with an R^2 value of 0.9552. In the graph, the SEC and SEP values are also given which are 0.1185 and 0.1127% (w/w %), respectively.

The predicted Cindolube concentrations vary in a range from 4.25% (w/w %) to 6.82% (w/w %) for C2, C4, SH1, and SH2 system samples. Those predicted concentrations were also represented on line graphs, respectively (Figure 6.75 and Figure 6.76).

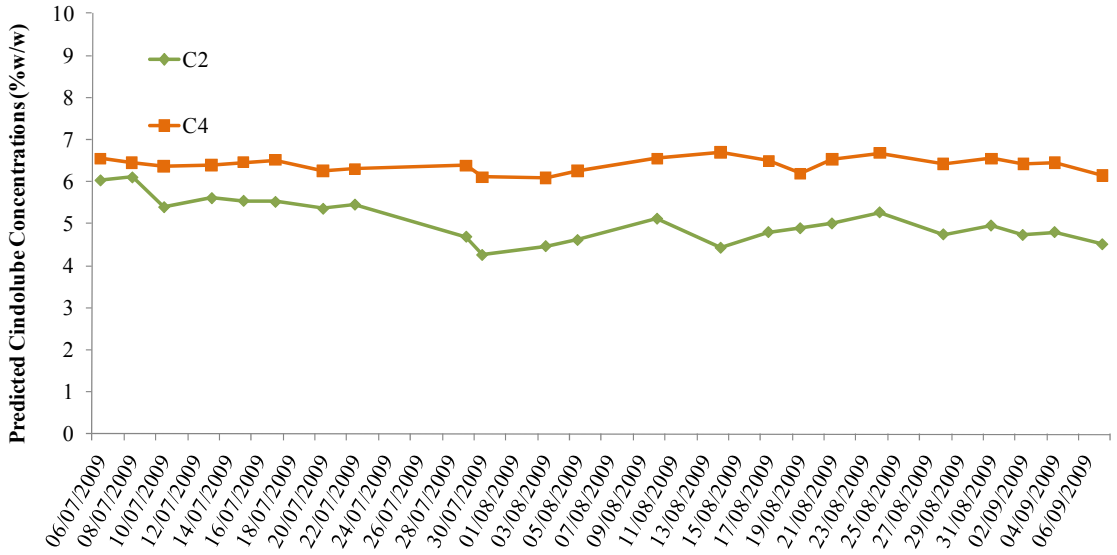

Figure 6.75. The line graphs of the predicted concentrations of Cindolube additive in real process samples of C2, C4 systems collected in July, August and September 2009.

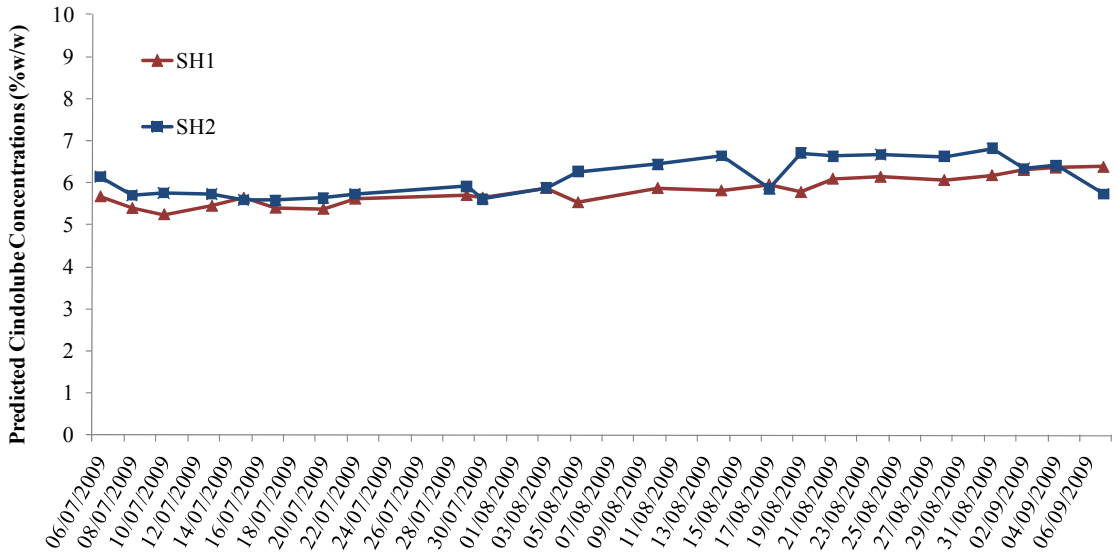

Figure 6.76. The line graphs of the predicted concentrations of Cindolube additive in real process samples of SH1 and SH2 systems collected in July, August and September 2009.

Following the prediction of Cindolube, the results were compared with the predicted results from the reference method, GC. Figure 6.77 and Figure 6.78 show the

line plots for the comparison of FTIR-GILS results with the reference results obtained from GC for Cindolube additive. The plots support the claims that the model is quite successful since the predicted results are in good agreement with the ones obtained from GC method.

The limits for the Cindolube additive to maintain the permanent lubrication is in between 5-7% (w/w %). The results which are shown in those figures are not above this limit.

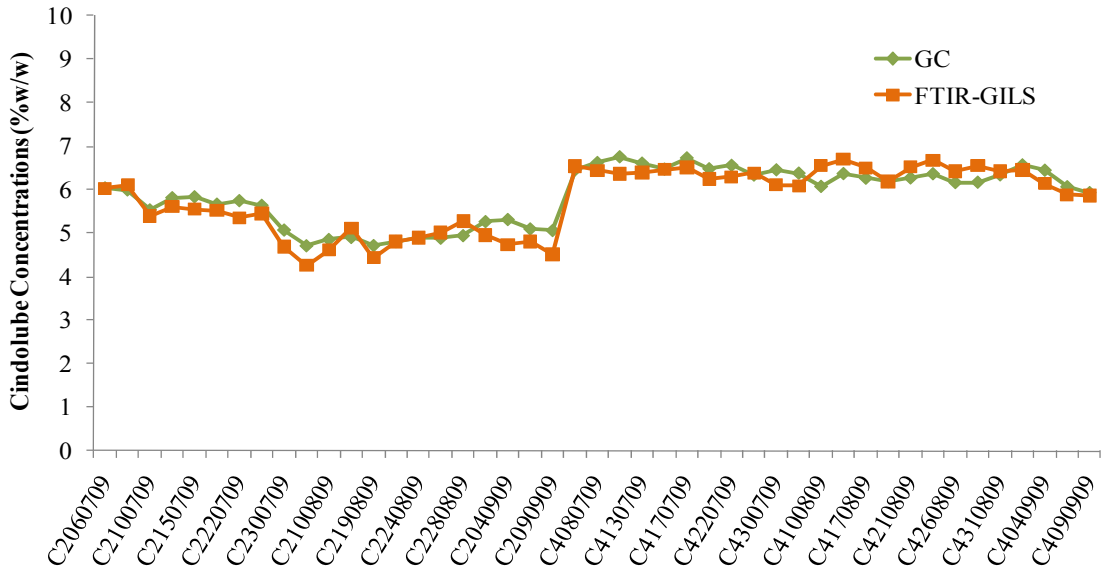

Figure 6.77. The comparison of FTIR-GILS predicted results with the GC-Reference results for the C2 and C4 real process samples collected in July, August, and September 2009.

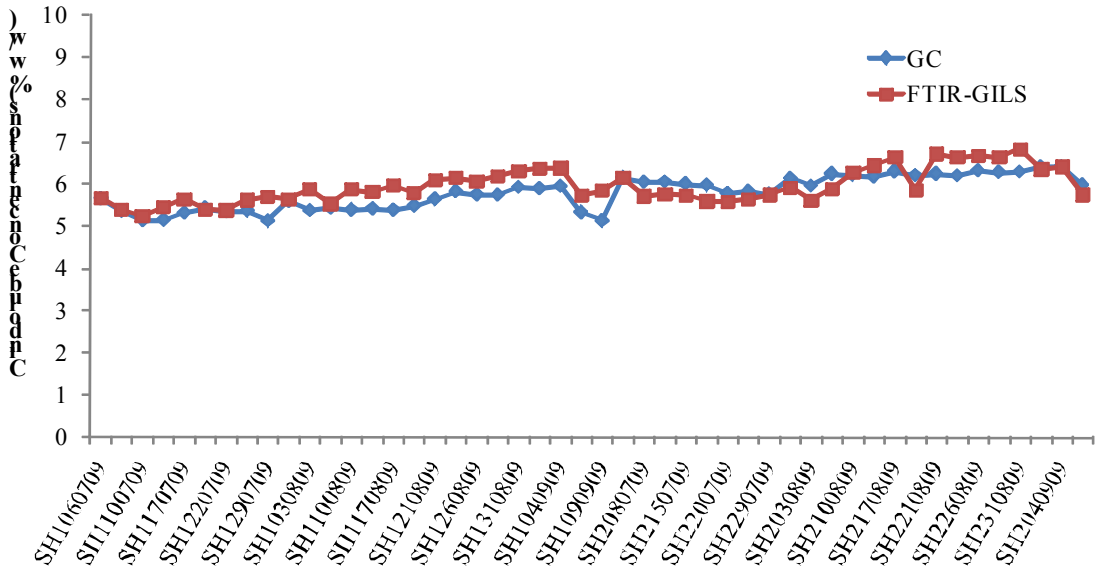

Figure 6.78. The comparison of FTIR-GILS predicted results with the GC-Reference results for the SH1 and SH2 real process samples collected in July, August, and September 2009.

Average Percent Recovery (APR) values are calculated for both the calibration and validations sets for each component (Equation (6.1)).

$$APR = \frac{\sum_{i=1}^{m}\left(\frac{\hat{c}_i}{c_i}\times 100\%\right)}{m} \tag{6.1}$$

Table 6.10 and Table 6.11 show the calculated APR values for calibration and validation sets of each component with their corresponding SEC and SEP values. In conclusion, having minimum SEC and SEP values and APR values very close to 100%, those components in interest are predicted quite successfully, and can be concluded that GILS is a promising multivariate calibration method for the prediction of concentrations in complex mixtures with its ability to extract the relevant information.

Table 6.10. The calculated APR values with the related SEC of each component regarding to *calibration* set for GC compared data sets and synthetic samples' data set.

GC COMPARED				
	NAFOL	**CINDOLUBE**	**TOTAL ALU**	**ALU 16**
SEC (w/w %)	0.0223	0.1185	0.0510	0.0248
APR	100.79	100.04	100.03	100.94

SYNTHETIC			
	ALU 46	**ALU 320**	**ALU 460**
SEC (w/w %)	0.0065	0.0135	0.0075
APR	99.71	100.55	101.02

Table 6.11. The calculated APR values with the related SEP of each component regarding to *validation* set for GC compared data sets and synthetic samples' data set

GC COMPARED				
	NAFOL	**CINDOLUBE**	**TOTAL ALU**	**ALU 16**
SEP (w/w %)	0.0281	0.1128	0.0819	0.0545
APR	100.48	99.78	100.82	98.81

SYNTHETIC			
	ALU 46	**ALU 320**	**ALU 460**
SEP (w/w %)	0.0080	0.0290	0.0139
APR	100.09	101.17	103.48

CHAPTER 7

CONCLUSIONS

The additives in base oil are used to improve rolling efficiency and quality of rolled products where as contaminants are undesired components that may be leaked from gear and hydraulic systems of the rolling mills to the base oil and cause serious staining problems on the rolled aluminum sheets and foils. Therefore, continuous monitoring of the composition of rolling oils is one of the most important issues in aluminum rolling industry.

This study focuses on the spectroscopic determination of the contaminants and additives in rolling mill oils in an aluminum plant (ASSAN Aluminum Corporation). The complex mixtures of the lubricating oils were analyzed by using FTIR. By using the spectra obtained from the spectroscopic analysis, calibration models were constructed for every component. The necessity of the knowledge about the composition and concentration informations forces the use of a reference method. For this reason GC is used in order to assign the reference values.

Since the samples are complex mixtures of those heavy oils, the univariate calibration is inefficient. Thus, the proposed solution in this thesis is that the construction of the calibration models for those additives and contaminants regarding to a reference method data and GILS programme in which the spectral data is used.

The study showed that infrared spectroscopy coupled with multivariate calibration can be used for continuous monitoring of additives and contaminants in aluminum rolling oil. By this way, analysis time is significantly reduced and simultaneous determination of all the components can be accomplished. The developed multivariate calibration models has been already incorporated into the royutine analysis protocols of ASSAN Alumium Corporation and currently are in use. With the shorter analysis times, the technical stuff of the plant now are able to monitor ptroduction lines and degree of contamination levels in a faster and cheaper manner.

REFERENCES

Answers.com. 2009. http://www.answers.com/topic/aluminum-sheet-plate-and-foil (accessed March, 2009).

ASSAN 2009. http://www.assan.com.tr (accessed March 2009).

Bernabei, M., Secl`ı, R., Bocchinfuso, G. 2000. Determination of Additives In Synthetic Base Oils For Gas Turbine Engines. *J. Microcolumn Separations*. 12(11):585-592.

Borin, A., Poppi, R. J. 2005. Application of Mid Infrared Spectroscopy and iPLS for The Quantification of Contaminants in Lubricating Oil. *Vibrational Spectroscopy* 37: 27–32.

Bucsi, W. G. 1995. Multivariate FTIR Analysis Of Aluminum Cold-Rolling Coolants. *Lubrication Engineering*. 51(2): 131-33.

Cobert Associates 2009 www.cobertassoc.com/gc_packed_columns.htm (accessed April, 2009).

Cong, P. and Li, T. 1994. Numeric genetic algorithm part I. theory, algorithm and simulated experiments. *Analytica Chimica Acta* 293:191-203.

eFunda 2009. http://www.efunda.com/processes/metal_processing/extrusion.cfm (accessed March, 2009).

European Aluminium Association 2009. http://www.eaa.net/en/about-aluminium/production-process/rolled-products (accessed March, 2009).

Extruded Profiles 2009. http://www.extrudedprofilesworld.com/extrusion-press.html (accessed March 2009)

Fontain, E. 1992. The problem of atom-to-atom mapping. An application of genetic algorithms. *Analytica Chimica Acta* 265:227-232.

Gale, W.F., Totemeier, T.C. 2004. *Smithells metal reference book*, eighth edition, Publisher: Elsevier ,Butterworth-Heinemann,Oxford.

Gilbert R. J., Goodacre, R., Woward, A. N., and Kell, D.B. 1997. Genetic programming: a novel method for the quantitative analysis of pyrolysis mass spectral data. *Analytical Chemistry 69*:4381-4389.

Guthrie, Virgil B. 2005. *Petroleum Products Handbook*, Publisher: Knovel.

Heenan, D.F, Januszkiewicz, K.R, Stratford, G. 1993. Chromatographic and Titrimetric Characterization Of Synthetic Esters Used In Aluminum Hot-Rolling Lubricants. *Lubrication Engineering*. 49(12):969-974.

Hibbert, D.B. 1993. Genetic algorithms in chemistry. *Chemometrics and Intelligent Laboratory Systems* 19:277-293.

Hirani, N., Chvedov, D., Jones, R. 2007. Characterization of organic monolayers on the surface of aluminum in the process of thermal treatment. *Thin Solid Films* 516:310–315.

Jennings, W., Mittlefehldt, E., and Stremple, P. 1997 *Analytical Gas Chromatography, second edition.* Elsevier Inc.

Kramer, R. 1998. *Chemometric Techniques for Quantitative Analysis*, Publisher: Marcel Dekker.

Leardi, R., Boggia, R., Terrile, M. 1992; Genetic Algorithms As A Strategy For Feature Selection. *Journal of Chemometrics*. 6:267–81.

Lucasius, C. B., Kateman, G. 1993. Understanding And Using Genetic Algorithms. Part 1. Concepts, Properties And Context. *Chemometrics and Inteligent Laboratory Systems*. 19:1–33.

Özdemir, D., Öztürk, B. 2004. Genetic Multivariate Calibration Methods For Near Infrared (NIR) Spectroscopic Determination Of Complex Mixtures. *Turkish Journal of Chemistry.* 28:497–514.

Özdemir, D., Mosley, R.M., and Williams, R.R. 1998a. Hybrid calibration models an alternative to calibration transfer. *Applied Spectroscopy* 52:599-603(5).

Özdemir, D., Mosley, R.M., and Williams, R.R. 1998b. Effect of wavelength drift on single- and multi-instrument calibration using genetic regression. *Applied Spectroscopy* 52: 1203-1209(7).

Özdemir, D. and Williams, R.R. 1999. Multi-instrument calibration with genetic regression in UV-visible spectroscopy. *Applied Spectroscopy* 53:210-217(8).

Paschoal, J., Barboza, F. D., Poppi, R. J. 2003. Analysis Of Contaminants In Lubricant Oil By Near Infrared Spectroscopy And Interval Partial Least-Squares. *Journal Of Near Infrared Spectroscopy*. 11(3): 211-18.

Quadrex Corporation 2009. http://www.quadrexcorp.com (accessed April, 2009).

Schomburg, G., 1990. *Gas Chromatography, A Practical Course*, Publisher: VCH Weinheim.

Sheffield Hallam University 2009. http://teaching.shu.ac.uk/hwb/chemistry/tutorials/chrom/gaschrm.htm (accessed April, 2009).

Skoog, D.A., Holler, F.J., Nieman, T.A. 1998. *Principles of instrumental analysis – fifth edition*. Philadelphia: Saunders College Publishing, Harcourt Brace College Publishers.

Smith, B.C. 1996. *Fundamentals of Fourier transform infrared spectroscopy*. New York: CRC Press.

Sprissler, B., Lockwood, F. E. 1985. Analysis Of Machinery Oil Contaminants In Aluminum Cold Rolling Oil By Reversed-Phase Liquid Chromatography. *Journal of Chromatography.* 319: 222-29.

Suranaree University of Technology 2009. www.sut.ac.th/Engineering/Metal/pdf/MetForm/04_Extrusion.pdf (accessed March, 2009).

The Aluminuim Association 2009. http://www.aluminum.org/Content/NavigationMenu/TheIndustry/SheetPlate/default (accessed March, 2009).

University of Massachusetts Amherst, College of Engineering 2009. www.ecs.umass.edu (accessed April, 2009).

Vahaoja, P., Narhi, J., Kuokkanen, T., Naatus, O., Jalonen, J. Lahdelma, S. 2005. An infrared spectroscopic method for quantitative analysis of fatty alcohols and fatty acid esters in machinery oil. *Analytical and Bioanalytical Chemistry*. 383: 305–311.

Wienke, D., Lucasius, C. B., Ehrlich, M., and Kateman, G. 1993. Multicriteria target vector optimization of analytical procedures using a genetic algorithm: part II. polyoptimization of the phothometric calibration graph of dry glucose sensors for quantitative clinical analysis. *Analytica Chimica Acta* 271:253-268.

Williams, D.H., Fleming, I. 1995. *Spectroscopic Methods in Organic Chemistry, fifth edition.* McGraw-Hill Education Publishers.

Wiseman, M., Ahsue, A. 1992; Monitoring Oil Degradation Using FTIR Analysis. *Lubrication Engineering*. 48(3): 236-41.